

# ***Generation IV Nuclear Energy Systems – The Gas-Cooled Fast Reactor (GFR) Report on Safety System Design for Decay Heat Removal***

*K. D. Weaver (INEEL)  
T. Y. C. Wei (ANL)  
E. E. Feldman (ANL)  
M. J. Driscoll (MIT)  
H. Ludewig (BNL)  
T. Marshall (INEEL)*

*September 2003*

*Idaho National Engineering and Environmental Laboratory  
Bechtel BWXT Idaho, LLC*



## Table of Contents

Table of Contents .....	2
Abstract .....	3
1. Introduction .....	3
2. Design Options for the Gas-Cooled Fast Reactor .....	4
3. Decay Heat .....	6
4. Passive, Semi-Passive, and Active Systems .....	10
4.1 Fully Passive Option .....	10
4.2 Prestressed Vessels .....	12
4.4.1 Reactor Physics Considerations .....	15
4.3 Mechanisms .....	16
4.3.1 Mass Transfer .....	16
4.3.2 Boundary Conduction/Radiation Cooldown and Thermal Inertia .....	17
4.3.3 In-Core Heat Sinks .....	17
4.3.4 Natural Convection .....	18
4.3.5 Flow Inertia/Semi-Passive Systems .....	19
4.4 Evaluations .....	20
4.4.1 Mass Transfer .....	20
4.4.2 Conduction/Radiation Cooldown to Boundary and Thermal Inertia .....	25
4.4.3 Core Heat Sinks .....	33
4.4.4 Natural Convection .....	38
4.4.5 Flow Inertia and Semi Passive Systems .....	43
6. Conclusions .....	52
7. Future Work .....	53
Appendices .....	53
A.1 Accident Sequences .....	53
A.1.1 Design basis conditions .....	54
A.1.2 Design extension conditions .....	55
A.1.3 Residual risk situations .....	56
A.2 RELAP5 Model Assumptions for Pebbled Bed Core Simulation .....	56
A.3 RELAP5-3D/ATHENA Models for Block Core .....	62
A.3.1 GFR Design Characteristics .....	62
A.3.2 RELAP Model .....	63
A.3.3 Loss of Coolant Accident .....	64
A.3.4 Conclusions .....	65
References .....	74

## **Abstract**

The gas-cooled fast reactor (GFR) was chosen as one of the Generation IV nuclear reactor systems to be developed based on its excellent potential for sustainability through reduction of the volume and radiotoxicity of both its own fuel and other spent nuclear fuel, and for extending/utilizing uranium resources orders of magnitude beyond what the current open fuel cycle can realize. In addition, energy conversion at high thermal efficiency is possible with the current designs being considered, thus increasing the economic benefit of the GFR. However, research and development challenges include the ability to use passive decay heat removal systems during accident conditions, survivability of fuels and in-core materials under extreme temperatures and radiation, and economical and efficient fuel cycle processes. This report addresses/discusses the decay heat removal options available to the GFR, and the current solutions. While it is possible to design a GFR with complete passive safety (i.e., reliance solely on conductive and radiative heat transfer for decay heat removal), it has been shown that the low power density results in unacceptable fuel cycle costs for the GFR. However, increasing power density results in higher decay heat rates, and the attendant temperature increase in the fuel and core. Use of active movers, or blowers/fans, is possible during accident conditions, which only requires 3% of nominal flow to remove the decay heat. Unfortunately, this requires reliance on active systems. In order to incorporate passive systems, innovative designs have been studied, and a mix of passive and active systems appears to meet the requirements for decay heat removal during accident conditions.

## **1. Introduction**

During the 1960s through 1980s, gas-cooled fast reactors were being considered and advocated as an alternative to the mainstream, worldwide program development of the liquid-metal fast breeder reactor. These designs used technologies based on metal clad pins containing solid solution fuel; these were essentially sodium core designs that replaced the sodium coolant with helium, where the cladding was roughened (or finned) to enhance heat transfer during normal/steady-state operation. However, it was recognized earlier on that gas coolants (in the low pressure range) had poor heat transfer properties and low thermal inertia as compared to liquid metal coolants, or even water. The consequence of depressurization combined with total loss of electric power (offsite and emergency) was melting of the core due to the decay heat, even though this extreme accident condition (in residual risk probability space) was highly improbable. This early realization led to the focus on, and extensive research and development of, reliable active decay heat removal systems. Steam driven turbines for powering circulators in shutdown heat removal systems, and emergency heat removal systems were initially considered. Probabilistic risk assessment studies convinced designers to modify these designs, which were replaced with electric powered blowers. As such, emergency power supply alternatives (e.g., diesel generators, compressed air, etc.) were investigated, as were extra trains, redundancy, single failure possibilities, and common mode failures. It is important to note that the roughened (or finned) cladding designs were also beneficial during depressurization events when forced convection was employed, but were not helpful for natural convection (passive decay heat removal) due to the increased friction and resulting pressure drop across the pin.

The gas-cooled fast reactor designs of the 1960s through 1980s (e.g., the GCFR of Gulf General Atomic, the GBR-4 of the European community, and the KFK/KWU designs in Germany), eventually utilized highly reliable active decay heat removal systems. However, the accident at TMI-2 occurred during this time period, which led to core disruption and melt. This accident had a profound impact on the nuclear community, and eventually led to consideration of passive mechanisms to remove the core decay heat, in conjunction with well-known active systems. It is important to note that liquid metal fast reactors investigated passive safety mechanisms as a complement to active systems, under the auspices of the IFR program, and reactor vessel cooling mechanisms as alternatives. Within thermal spectrum, gas-cooled reactor programs, an approach of utilizing passive decay heat removal has come to the forefront of design efforts; indeed, walk-away passive removal of core-generated heat has now become a part of the safety case. Unfortunately, the gas-cooled fast reactor programs were canceled before work could be performed on identifying or developing passive decay heat removal systems.

Within Generation IV, the use of passive safety systems has been strongly encouraged, which would eliminate complete reliance on purely active decay heat removal systems or, at the least, utilize an optimum combination of passive and active systems. As discussed earlier, the former gas-cooled fast reactor designs (i.e., metal clad pins) would not survive a depressurization accident (or loss of flow accident) due to the immediate temperature rise within the core; far exceeding the melting point of typical cladding. Use of refractory metals will greatly increase the melting point, but can also be strong neutrons absorbers. An obvious balance is needed between the safety and material requirements, not forgetting the competitive economics needed to satisfy the Generation IV goals. This report takes the opportunity to address the use passive safety mechanisms in a gas-cooled fast reactor, while trying to maintain a balance between the other Generation IV goals. The down-selected systems will be optimized in future work to match the best candidate fuels, materials, and reactor design.

## **2. Design Options for the Gas-Cooled Fast Reactor**

The following design options are being considered for the GFR:

- Reference: helium cooled, direct power conversion cycle at 5-7 MPa, and 850°C outlet temperature.
  - Alternate: helium cooled (5-7 MPa), indirect power conversion cycle using supercritical CO<sub>2</sub> on the secondary side at 20 MPa, and 550°C. (Allows for cooler primary outlet temperatures at ~ 600°C, thus reducing the materials requirements with respect to temperature. This also has a strong safety case with respect to decay heat removal systems.)
- Option: supercritical CO<sub>2</sub> cooled, direct power conversion cycle at 20 MPa, and 550°C outlet temperature.

In addition to these options, a base case can be used for comparison purposes, which would be the CO<sub>2</sub> cooled, indirect power conversion cycle reactor. The secondary side is variable at this point, which may be steam, supercritical pressure water, etc. This is essentially a fast spectrum Advanced Gas Reactor (developed by the United Kingdom), metal clad pin/solid solution fuel design, with modifications to increase efficiency. In addition to the coolant, variations in core

geometry also exist, where pin, block/plate, and pebble fuel designs are being considered. However, experience with this reactor can be used in comparison with the current GFR designs.

As stated above, the reference design for the GFR is a helium cooled, direct Brayton cycle energy conversion system. The other characteristics of an initial GFR reference design can be seen in Table 1 below.

Table 1. Initial reference GFR parameters.

<b>System Parameter</b>	<b>Reference Value</b>
<b>Power level</b>	<b>600 MWth</b>
<b>Net efficiency</b>	<b>48%</b>
<b>Coolant pressure</b>	<b>70 bar</b>
<b>Outlet coolant temperature</b>	<b>850 °C</b>
<b>Inlet coolant temperature</b>	<b>490 °C</b>
<b>Nominal flow &amp; velocity</b>	<b>330 kg/s &amp; 40 m/s</b>
<b>Core volume</b>	<b>11 m<sup>3</sup> (H/D ~1.7/2.9 m)</b>
<b>Core pressure drop</b>	<b>~0.4 bar</b>
<b>Volume fractions of Fuel/Gas/SiC</b>	<b>50/40/10 %</b>
<b>Average power density</b>	<b>55 MW/m<sup>3</sup></b>
<b>Reference fuel composition</b>	<b>UPuC/SiC (50/50 %)</b>
<b>Breeding/Burning performances</b>	<b>fissile breakeven</b>
<b>In core heavy metal inventory</b>	<b>30 tonnes</b>
<b>Fissile (TRU) enrichment</b>	<b>~20 wt%</b>
<b>Fuel management</b>	<b>multi-recycling</b>
<b>Fuel residence time</b>	<b>3 × 829 efpd</b>
<b>Discharge burnup ; damage</b>	<b>~5 at%; 60 dpa</b>
<b>Primary vessel diameter</b>	<b>&lt;7 m</b>

The alternate design is also a helium-cooled system, but utilizes an indirect Brayton cycle for power conversion. The secondary system of the alternate design utilizes supercritical CO<sub>2</sub> at 550°C and 20 MPa. This allows for more modest outlet temperatures in the primary circuit (~600°C), reducing the strict fuel, fuel matrix, and material requirements as compared to the direct cycle, while maintaining high thermal efficiency (~45%).

The optional design is a supercritical CO<sub>2</sub> cooled (550°C outlet and 20 MPa), direct cycle system. The main advantage of the optional design is the modest outlet temperature in the primary circuit, while maintaining high thermal efficiency (~45%). Again, the modest outlet temperature (comparable to sodium-cooled reactors) reduces the requirements on fuel, fuel matrix/cladding, and materials, and even allows for the use of more standard metal alloys within the core. This has the potential of significantly reducing the fuel matrix/cladding development costs as compared to the reference design, and reducing the overall capital costs due to the small size of the turbomachinery (and other system components).

The safety system design will be affected by the choice of primary coolant, whether a direct or indirect power conversion cycle is used, and the core geometry (i.e., block, plate, pebble, etc.). The trade-off between high conductivity and high temperature capabilities led to the choice of ceramics, including refractory ceramics. The reference fuel matrix for the Generation IV GFR is

SiC using a uranium-carbide dispersion fuel, based on a balance between conductivity and high temperature capability.

### 3. Decay Heat

The driving force that sets the size of active decay heat removal system, and the feasibility of proposed passive decay removal mechanisms, is the well-known decay heat generation curve. Figure 1 shows the typical curve for uranium fuel with infinite irradiation time. The important features are: 1) it starts off at ~6% of nominal power; 2) drops to ~ 3% power after an initial period; 4) is down to the 2% level after ~ 1 hour; and 4) then holds at ~1% for hours. Additional decay is on the order of days, months, and years. Figure 2 shows the integrated energy under the decay heat curve plotted as a function of time. Unless decay heat removal capability is provided, this energy has to be stored in the fuel, and, depending upon fuel heat capacity (thermal inertia), would lead to an ever-increasing fuel temperature curve. Also included on Figure 2 are plots where decay heat removal capability of different constant capacity is introduced. Typically, decay heat removal systems are designed for 1-2% decay heat. All the integrated decay heat energy during the initial period has to be absorbed in the fuel. This sets requirements on fuel heat capacity and fuel failure temperature limits. The parametric plots show time scale effects for different heat removal capability. The fuel temperature peaks at ~15 minutes for 2% decay heat removal capability, after which the decay heat generation rate decreases below the heat removal rate. Note that at 0.5% capability it takes days to reach the peak. Confinement systems would have to be designed for a duty period of days. If a secondary pressurization system approach is taken for passive decay heat removal, a design period of days may be very challenging. However, one of the key design variables could be adjusted so that the fuel and structure temperatures could be tolerated from the structural design point of view. The key design variable is the rated fuel power density. Certainly fuel heat capacity could also be adjusted depending upon the choice of materials selected since

$$\dot{T} = \frac{\ddot{q}}{\rho c} \quad (1)$$

where  $T$ =temperature  
 $\rho$  = material density  
 $c$  = material heat capacity  
 $\ddot{q}$  = fuel power density

Figure 3 shows the heat absorption capacity required for a given decay heat removal capability. However, as will be seen later, the selection of materials is limited. For the GFR, one of the major design goals for the reactor is the thermo-chemical production of hydrogen using process heat. Currently, the list of envisioned thermo-chemical reactions for reactor production of hydrogen are all high temperature reactions at  $\geq 800^\circ\text{C}$ . At these temperatures, and under the high fluence conditions of the GFR, the material limits are very challenging. The material options for GFR core and structures are very limited. Much more flexibility is available in the selection of power density. As can be seen from equation (1), power density affects time scales and Figure 2 shows the importance of time scale.

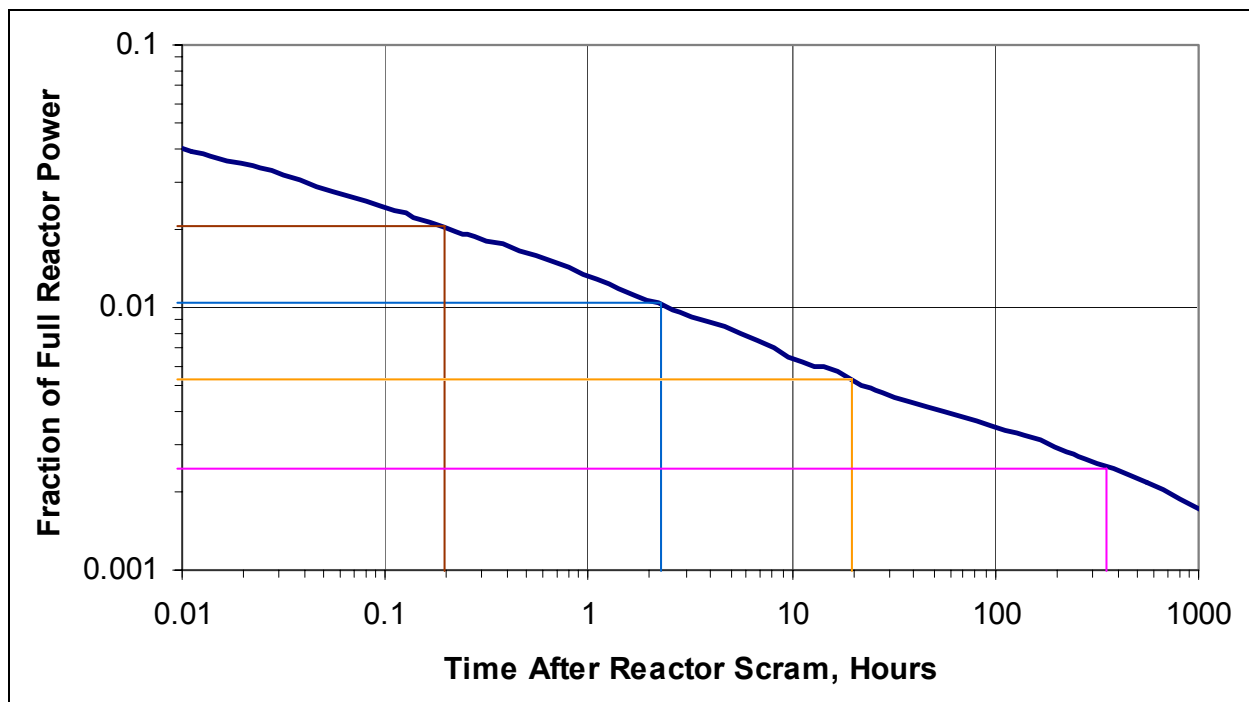


Figure 1. Decay Heat Curve for Uranium-Fueled Reactors

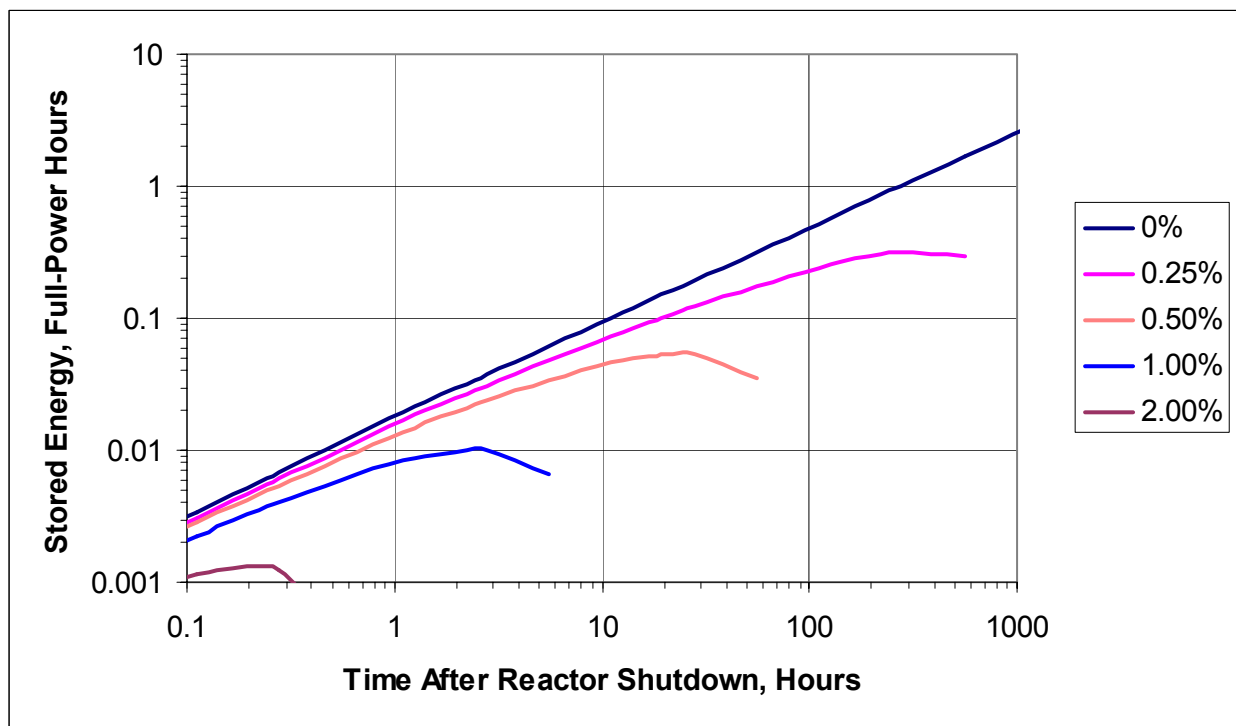


Figure 2. Stored Energy for Parametric Values of Decay Heat Removal Rate

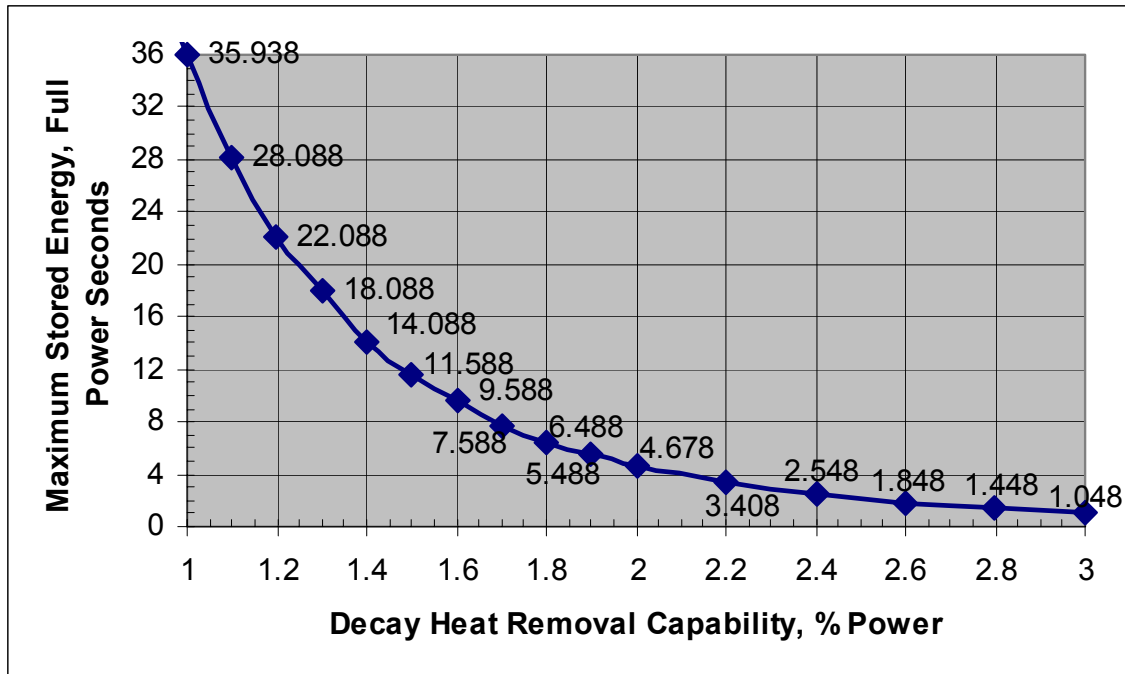


Figure 3. Maximum Stored Energy

Not only is the time scale important for Figure 2, but it also requires time to transport heat through conduction, radiation, or convection. These are all potential passive heat removal mechanisms. Subsequent sections will emphasize the importance of time scales in the discussion of potential passive decay heat removal mechanisms. Twenty-five years ago, the GA GCFR was rated at 250 W/cc fuel power density. Typical projected LMFBR numbers were even higher in the 300-500 W/cc range. EBR-2, the 60 MW sodium cooled fast reactor that was designed, built, and operated at ANL, had a rated power density of 700 W/cc. Sodium has excellent heat transfer characteristics, heat capacity properties, and natural convection capabilities even at low pressure. However, gas coolant requires pressurization, and, for reasonable design pressures, requires a lower core fuel power density than the sodium coolant. Note, however, LWRs run at  $\sim 100$  w/cc and water is acknowledged to be a better heat transfer medium than gas. Furthermore, thermal gas cooled reactors (HTGRs and PBMRs) operate at power densities of 5 w/cc which is low compared to the other reactor types<sup>a</sup>. For a given reactor power, thermal gas cooled reactors have the largest primary systems. The low power density is a key factor in the passive safety case of the HTGR/PBMR. The time scale for decay heat removal transients is much larger. Certainly the good thermal conductivity and heat capacity of graphite, coupled with the high disruption temperature, are important factors in the passive safety case; but the low power density is paramount. To derate the core by reducing the power density is a possibility for the GFR, but it invites economic disincentives. A low power density would increase core size and related primary system size, and therefore capital costs. But more importantly, from the viewpoint of fuel cycle costs and plant costs, a low core power density would have a significant impact.

<sup>a</sup> It is important to note, however, that the specific power (W/g) of thermal spectrum gas reactors is relatively high due to the low heavy metal density.



This is because core power density and specific power are related by

$$\dot{q} = \rho p_{sp} \quad (2)$$

where:

$p_{sp}$  = fuel specific power (watts/gm)

As shown in [4], fuel cycle costs are related to fuel specific power. Fuel cycle cost in mills per kilowatt hour (mills/kW-hr) normalized as of the start of irradiation is given by:

$$fcc = \left( \frac{C}{24 \cdot \eta \cdot B_d} \right) \left( \frac{XT}{1 - e^{-XT}} \right) \text{mills/kW-hr} \quad (3)$$

where:

$C$  = Cost per kilogram of fuel as of the start of irradiation

$\eta$  = Plant thermodynamic efficiency,

$B_d$  = Fuel discharge burnup,

$X$  = Discount rate

$T = \frac{B_d}{0.365 \cdot SP \cdot L}$ , duration of fuel residence in core in years

$L$  = Plant capacity factor,

$SP$  = Specific power

Since recycle costs have at this point significant uncertainty, the point to be made is illustrated by using a uranium start-up core for the GFR. It can be seen from equation (2) that the higher the rated SP, the harder the fuel is worked, and the higher the rate of energy extraction. This results in a better rate of return in terms of the time value of money invested in the fuel. Reference [4] indicates that for fuel cycle costs (in mill/kwh) comparable to those of current PWRs, SP needs to be  $> 25$  W/g. For the typical density of fuels and materials currently considered by the NERI and I-NERI GFR projects, this translates to a power density of  $\sim 70$ -100 W/cc. To summarize, fuel power density is an important parameter in the feasibility of proposed passive decay heat removal mechanisms. Reducing fuel power density would aid the safety case. However, economics (and in particular fuel cycle economics) sets the lower limits on the power density. A power density range of 70-100 W/cc appears to be acceptable.

## 4. Passive, Semi-Passive, and Active Systems

As regards design strategy to insure low core damage frequency, two distinct approaches have evolved:

Strategy 1:

- a. Three, 50% capable, shutdown cooling system (SCS) active loops.
- b. One, 100% capable, emergency cooling system (ECS) passive loop.
- c. A prestressed concrete vessel (PCR/V) guard vessel enclosing the reactor and power conversion unit so as to insure maintenance of high post-LOCA ambient pressure – to facilitate both natural and forced convection.

Strategy 2:

- a. Adoption of a PCR/V (or preferably PCIV: prestressed cast iron vessel) and an indirect cycle to reduce LOCA probability and rate of blowdown.
- b. Three, 50% capable, combined SCS/ECS auxiliary loops inside the reactor vessel. The SCS is active, while the ECS mode is semi-passive (as described subsequently).
- c. Use of rugged, reliable, compact Heatric<sup>TM</sup> printed circuit heat exchangers for both IHX and auxiliary loop service. Their small size allows emplacement inside the PCR/V/PCIV.

A description of the heat transfer components of these designs can be found in the sections that follow.

### 4.1 Fully Passive Option

As was discussed previously, it is possible to design a gas-cooled fast reactor that utilizes fully passive decay heat removal mechanisms (i.e., reliance on conduction, radiation, and natural convection). Previous work using the optional design, cooled by supercritical CO<sub>2</sub>, and utilizing a metal matrix core was studied [17]. Figures 4 and 5 shows the peak temperatures for this design. Note that the peak temperature in all cases is < 1200°C; well below the melting temperature of the fuel or matrix. If a ceramic-based core were to be used in this case, the margins would be even greater. In summary, this particular design has the same walk-away safety characteristics of its thermal spectrum counterparts, and operates at only a slightly higher power density (~ 8 W/cc). In addition, this design also exhibits the following characteristics:

- Solid fuel blocks – no core compaction scenario and associated reactivity increase and energy release
- High thermal storage and conductivity – passive decay heat removal in loss of coolant accident – LOCA concerns eliminated
- Can be designed with acceptable reactivity increase from coolant voiding
- Negative fuel temperature feedbacks – inherent shutdown in accidents leading to fuel temperature increase
- Small reactivity swing – transient overpower eliminated
- Excellent matrix fission product retention capability - less fission product release

Figure 6 illustrates the high fuel cycle costs as discussed in the previous section.

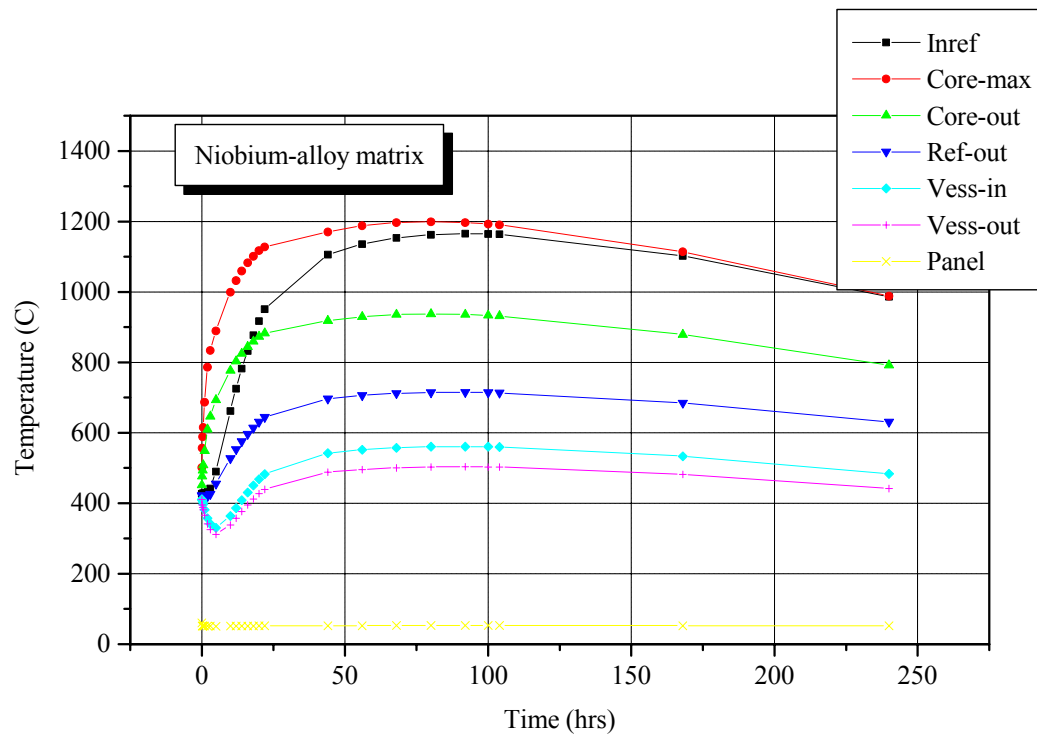


Figure 4. Temperature traces following LOCA

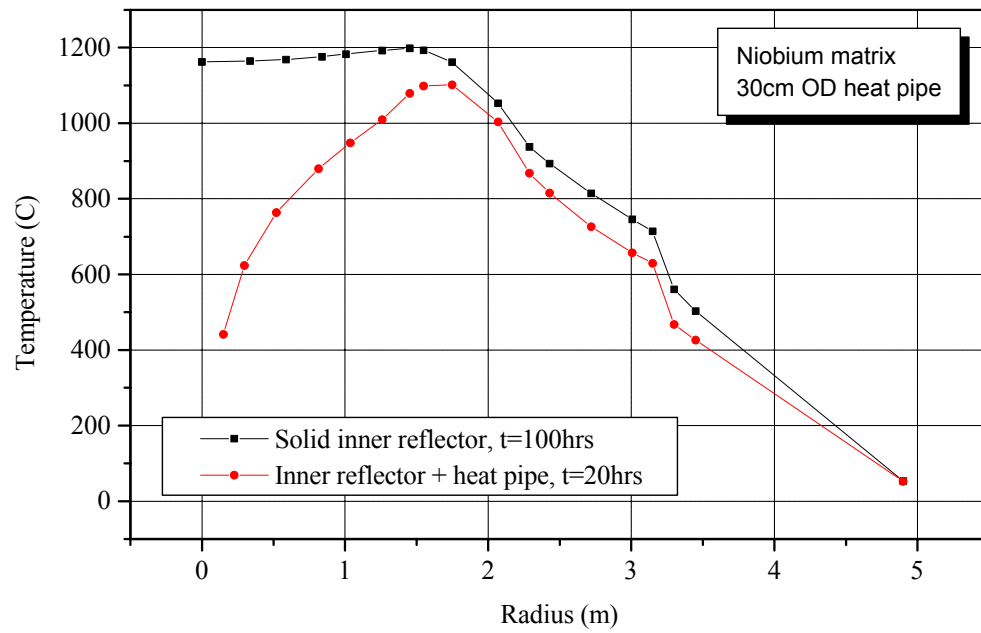


Figure 5. Temperature profile at time of peak core T

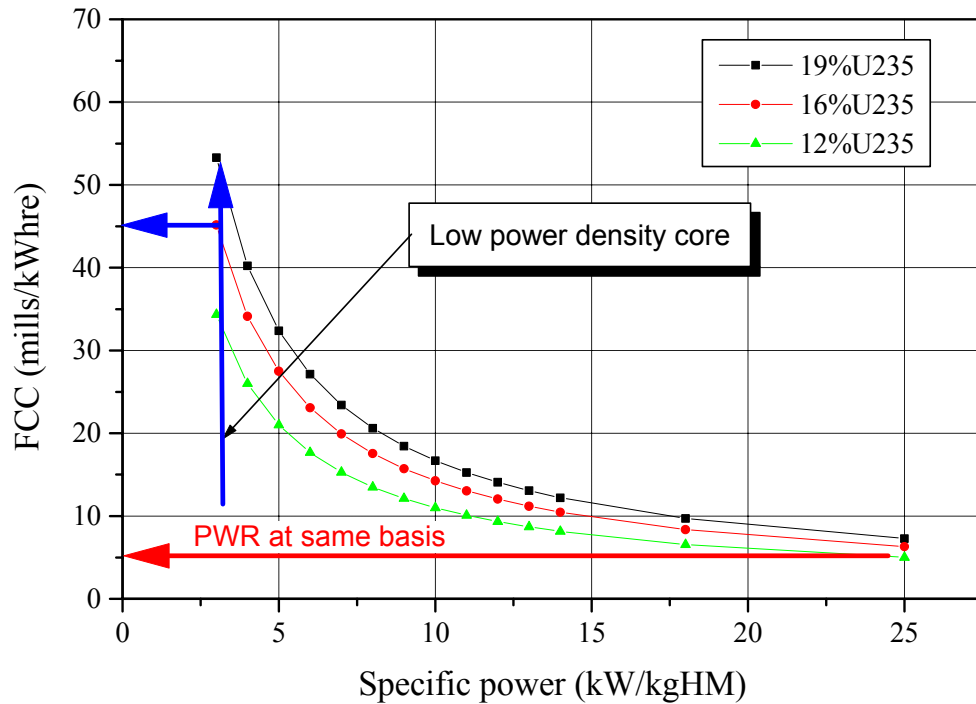


Figure 6. Fuel cycle cost versus specific power

Unfortunately, the first core fuel cycle costs in this design can be equal to the capital costs of the reactor. Clearly the economics of this design outweigh the safety case, even though true passive safety is achieved. However, the lessons learned from this exercise give insights as to the possible mechanisms that may be available for decay heat removal, and are discussed throughout this report.

## 4.2 Prestressed Vessels

Reference [11] reviews lessons-learned from the GCFR design projects of the 1970 time frame, and basically re-affirms many of the decisions made during that era. Thus our approach has been primarily to update and improve upon these prior efforts. Reference [4] describes a generic model developed and exercised for natural or forced convection core cooling loops in support of our performance assessment activities.

Accordingly, minimization of LOCA probability is given a high priority. We have concluded that this could best be done using a PCR/V or PCIV. Both direct and indirect power cycle versions are being evaluated. Specifically, the prestressed cast iron reactor vessel, considered from time-to-time in the past, and specified for the VHTR designed by Westinghouse Astronuclear, again in the 1970's, is our current reference design [12] and can be seen in Figure 7.

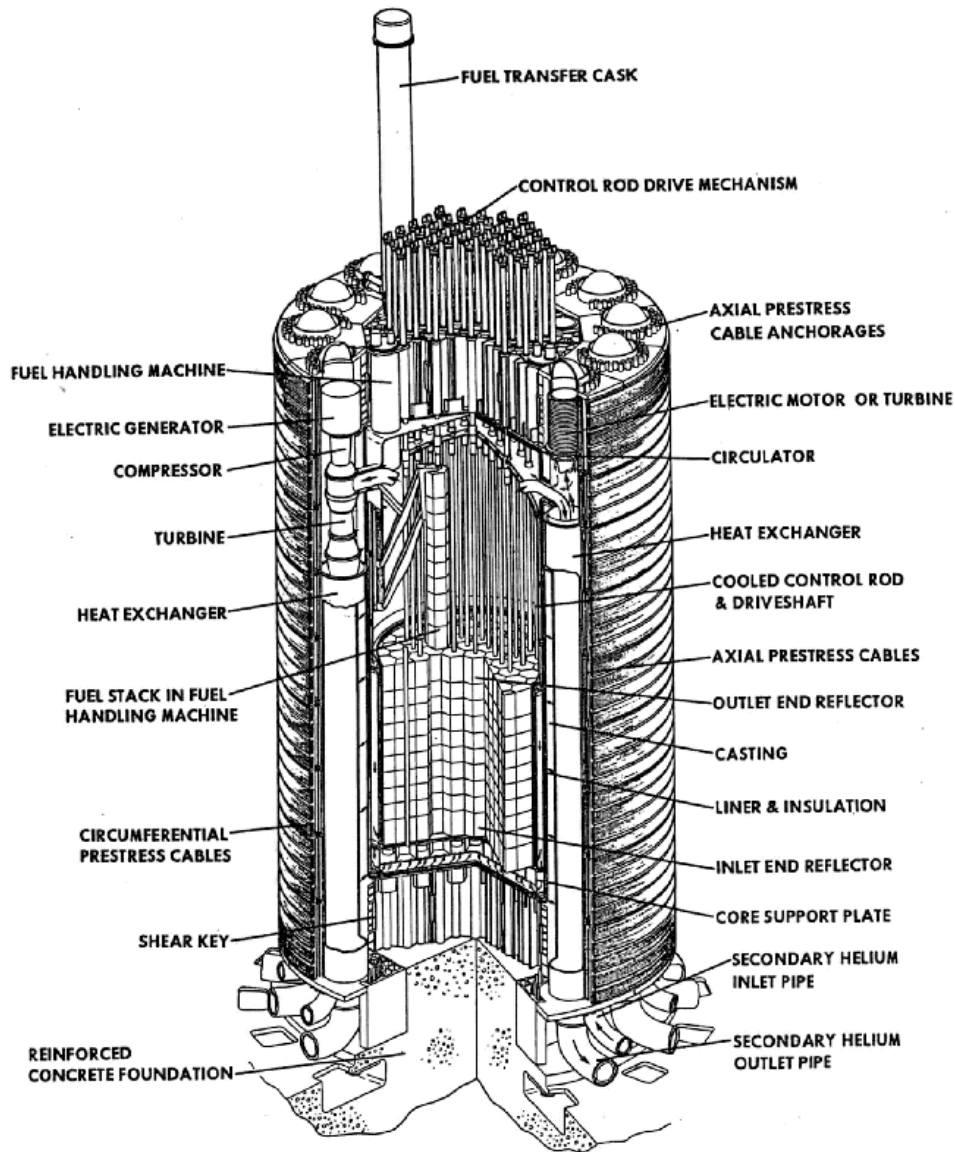


Figure 7. VHTR for Process Heat as Designed by WANL

This PCIV can accommodate an HTGR rated at 3000 MW<sub>th</sub>. It has a dozen circumferential cylindrical heat exchanger/machinery pods surrounding the core barrel, which house intermediate He/He heat exchangers, auxiliary cooling loops, and gas turbine power units. This layout is a good fit to current GFR needs, except that in the indirect version the power cycle — supercritical CO<sub>2</sub> Brayton units—will be located outside the PCIV. The configuration is also ideal for Heatric<sup>TM</sup> type heat exchangers, which are a recent (late 1980's) development.

The GA GCFR of the 1970's employed three auxiliary cooling loops. Based upon a PRA assessment, we have confirmed that the use of three 50% capable loops is to be preferred due to the limitation imposed by common mode failures. Figure 8 includes the beta factor ( $=0.1$ ) common cause consideration and the rare event approximation, thus illustrating a reasonable estimate of system failure probability for the respective component failure probabilities.

To further reduce system failure probability, passive gas accumulators that can power the gas turbines used to drive auxiliary loop gas blowers have been added, as shown in Figure 9. This approach was employed to increase the diversity of emergency power sources, since failure to provide service by diesel generators is typically the dominant event in LWR severe accident scenarios. During a LOCA the  $\text{CO}_2$  accumulators discharge through a valve normally held shut by primary loop pressure. The turbine exhausts into the primary system, thereby providing  $\text{CO}_2$  makeup replacing He; the former is much more effective under natural convection. In the event of station blackout without primary system depressurization, the  $\text{CO}_2$  accumulators discharge through a valve normally held shut by station electricity, to power a pneumatic motor on the compressor driveshaft; in this case the  $\text{CO}_2$  is vented to the atmosphere.

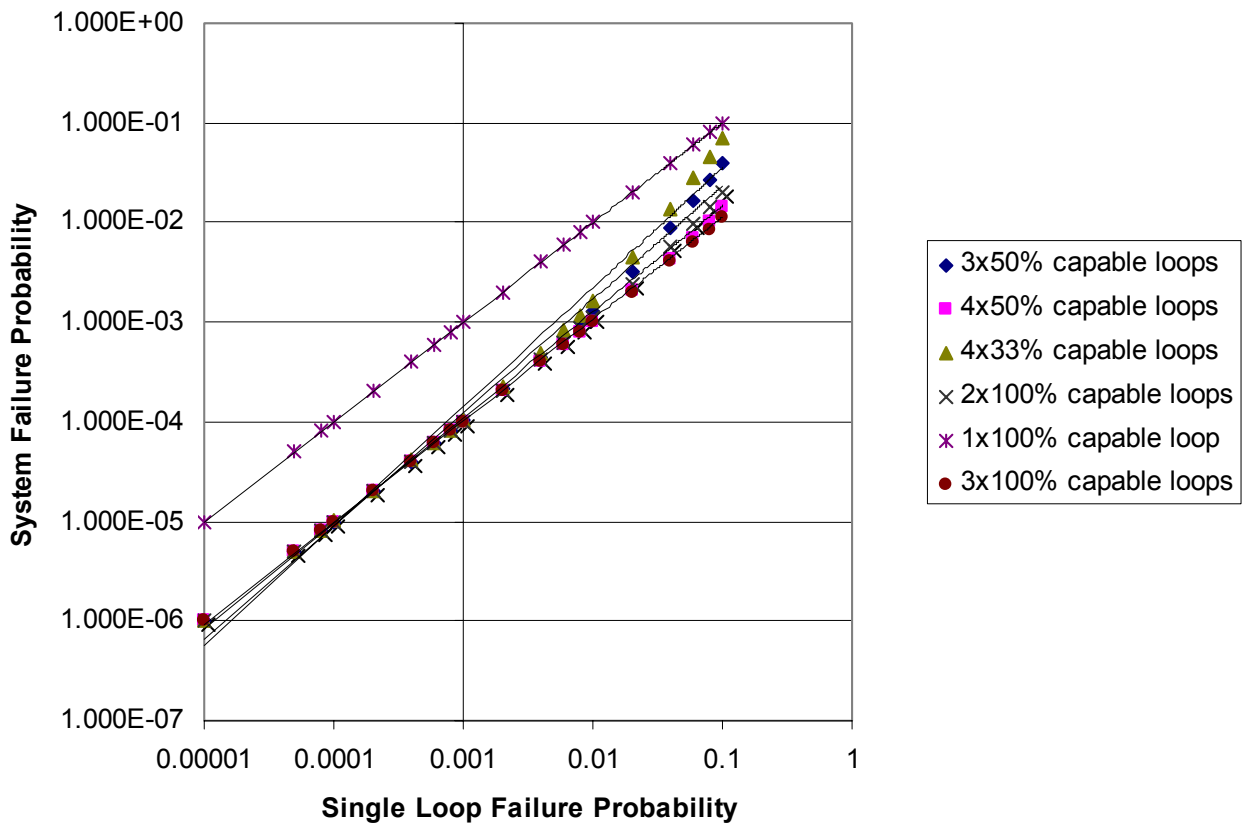


Figure 8. Comparison of Failure Probability for Auxiliary Cooling Loop Options (Common Cause Failures modeled with Beta factor = 0.1)

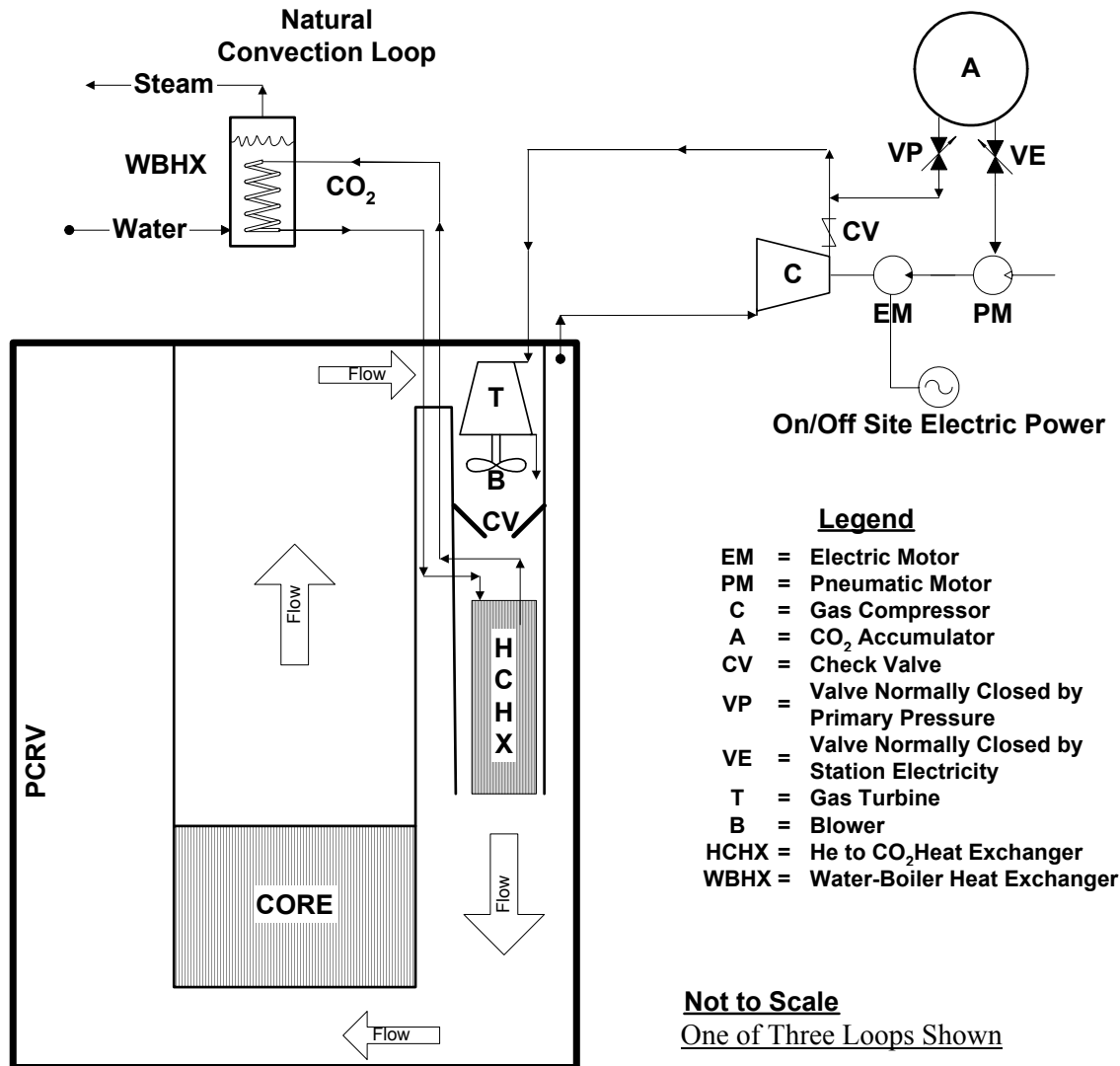


Figure 9. Pneumatically-powered Decay Heat Removal System for Gas-Cooled Fast Reactors

#### 4.4.1 Reactor Physics Considerations

Another issue of concern in GFR safety analysis is the presence of positive coolant void reactivity. In general it is positive for both He and CO<sub>2</sub>, and for particular combinations of composition, configuration and normal coolant pressure, can exceed one dollar. Accordingly we have investigated means for its mitigation, including modification of core and reflector composition, core shape (pancaking, streaming assemblies), and passive reactivity feedback devices.

The most promising approach appears to be use of a titanium reflector. Full particulars are reported in a Global 2003 paper [13].

We have also described three reactivity feedback devices in the transactions for the November 2003 ANS/ENS International Winter Meeting [14][15][16]. At present further development is being held in abeyance, pending a fuller exploration of the use of composition control.

### **4.3 Mechanisms**

Focusing on the core design, in particular on fuel forms, and the implications of alternatives for the passive removal of decay heat, it is evident that the pebble fuel has a unique possibility which the other major fuel forms (pin and block/plate) would have difficulty to emulate. In addition to heat transfer, there is the possibility of mass transfer. Below is a summary of the potential passive decay heat removal mechanisms.

1. Mass Transfer
  - Fuel dump system
2. Heat Transfer
  - Radiation/conduction cooldown
    - vessel boundary
    - core/internal heat sinks (cooled/uncooled)
    - primary system heat sinks (cooled/uncooled)
  - Natural convection
    - vessel boundary
    - core internal heat sinks (cooled/uncooled)
    - primary system heat sinks (cooled/uncooled)
  - Special devices
    - heat pipe
    - cold finger
3. Inertia
  - increasing fuel form thermal inertia
  - increasing flow coastdown times

#### **4.3.1 Mass Transfer**

In the case of the mass transfer option, the idea would be to remove fuel rapidly from the core perhaps even outside the primary system, where alternative means of cooling without the need for active systems can be utilized to prevent fuel damage. Advocates of the pebble bed thermal gas cooled reactor have continued to stress the ease of fueling and defueling the reactor with this particular spherical fuel form. Continuous on-line refueling with this option is taken to be the norm for the PBMR. This particular characteristic for steady state operation could also be possibly used to advantage under accident situations. Removal of the fuel pebbles from the core within the time scale of the accident to system locations where the conditions are more amenable to control is an attractive option. Pebble evacuation systems or bed dump systems need to be designed for the depressurization accident with the total loss of electric power such that the decay heat will not degrade the pebble significantly during the transient and the final pebble collection area needs to have passively coolable and subcritical geometry.



#### **4.3.2 Boundary Conduction/Radiation Cooldown and Thermal Inertia**

The radiation and conduction heat transfer modes are a different case from mass transfer. Pebble beds have both radiation and conduction heat transfer with radiation being the more important. The spherical form in packed beds is a good form for radiation as there are radiation pathways to the exterior boundary from within the interior of the bed. Complete shadowing is very difficult to achieve in this geometry for the range of pebble sizes of interest. But ultimately there needs to be a heat sink. In the case of the thermal gas cooled reactor, heat radiation/conduction core generated decay heat to the vessel boundary (“conduction cooldown mode”) has been a major part of the safety case. This is both for the prismatic fuel design as well as for the pebble/bed fuel design. Conceptually, this is also therefore a heat sink/decay heat pathway for the pebble bed fast gas cooled reactor. But as noted previously, there is a major difference between the power density of a thermal gas cooled reactor and the power density of a GFR.

Conduction/radiation of the core decay heat to the vessel wall boundary is a function of power density, material properties and geometry. If conduction cooldown is not possible due to too large a target power density or geometrical constraints on surface-to-volume ratio, then distributed core internal heat sinks would be a potential alternative. For the pin-based reactor there is no conduction component to this pathway unless some type of a web type spacer design is envisioned but that would increase the steady-state coolant pressure drop through the core. Furthermore unless there are “few fat pins” as opposed to “many thin pins” there will be a large number of radiation interface between the center of the core and the vessel boundary. This could lead to large temperature drops. In the case of the block core, the radiation interfaces are the gaps between the blocks. These clearances are necessary for the mechanics of refueling. Larger blocks could help the passive conduction of heat to the boundary but the weight would increase the requirements on the refueling machines. Interblock gaps are a necessity. High conductivity block matrix material would be advantageous to this mode of passive decay heat removal. High thermal inertia block matrix material would also be advantageous. Both these attributes would be useful for the pebble matrix material and the fuel pin pellets. Though in the case of the pellet, typically the decay heat level is low enough that it is the radiation temperature drops between the pins that dominate. In addition to material properties, geometry matters. In particular the surface-to-volume is the important parameter. This affects the aspect ratio of the core and ultimately of the primary vessel. The PBMR and the GT-MHTGR thermal reactors are both tall thin reactors to promote the conduction of the core decay heat to the vessel boundary and thereby the conduction cooldown off the vessel wall. This geometry however also promotes neutron leakage from the core and impacts the neutron balance adversely. For a fast reactor where the neutron leakage is typically much larger than the thermal reactor, this would unfortunately be a large effect.

#### **4.3.3 In-Core Heat Sinks**

Given the unfavorable trends it is still possible to consider conduction cooldown as a potential passive decay heat removal mechanism if the ultimate heat sink is not the vessel boundary but a series of distributed core internal heat sinks. These heat sinks could be uncooled thermal inertia sinks or cooled through secondary natural convection pathways. For the uncooled option it can be seen from Figure 3 and the discussion, that a significant amount of thermal capacity could be

required to absorb the excess heat until the decay heat production decays to the heat removal rate possible through the vessel boundary. For the cooled options, the passive heat removal in these internal core heat sink locations could be natural convection cooled heat exchangers or special devices such as heat pipes. In all cases the cooled option requires the provision of connections through the primary system boundary to the ultimate external heat sink. There is also the use of the vessel wall as an intermediate heat sink with external cooling of the wall. However even in this case, the same difficulty exists of connecting all these internal core heat sinks to the ultimate heat sink. A complex piping system for this internal heat transport problem within the vessel may have to be designed. This system would have to be accommodated by control rod drives internals and the refueling mode of operation. Failure of this system should not depressurize the primary coolant system otherwise it would not meet the single failure criteria. The choice of coolant on the secondary side is also an important factor. Moisture in the GFR core has historically been regarded as a positive reactivity effect and there are certainly combinations of fuel materials and coolant selection that should be avoided for compatibility reasons. As far as conduction/radiation of the core generated decay heat to those in-core locations the same phenomena governing the conduction/radiation cooldown to the vessel wall would govern here. The pin core with its multiple radiation interfaces would be at a disadvantage. The gaps in the block core could be minimized depending upon design. The pebble bed core could have challenging temperature conditions for the heatsink boundary material as contact would be made with the pebbles.

#### **4.3.4 Natural Convection**

Just as mass transfer is acknowledged as a special feature of the pebble bed fuel form and configuration, it is also acknowledged that in general the pebble bed form is not the optimum form for natural convection. The pressure drops inherent to the pebble bed configuration are not conducive for natural circulation. There is certainly more flexibility in the design of other fuel element forms to optimize for natural convection. However, even if pin based or block plate based cores are selected for the natural convection heat transfer mode, helium is a poor heat transfer medium at one atmosphere pressure. The level of the acceptable accident pressure whether a separate heavy gas injection needs to be arranged, and the means to maintaining a residual backpressure are all design questions that need to be resolved. The question of the residual backpressure required to maintain an acceptable level of natural convection to transport the decay heat away from the core is tied closely to the selection of the coolant gas. The light gas helium is acknowledged to be a natural convection medium that requires very tall chimneys and large elevation heads. Heavy gases such as  $\text{CO}_2$  are acknowledged to be better. A lower backpressure is required for the same heat removal rates. Conversely shorter chimneys can be used. However, since helium has been selected as the primary coolant, heavy gas injection into the primary system would be required to replace the helium with the heavy gas. The issue of mixing, bypass and timescale all need to be addressed. Furthermore fuels such as carbides are chemically reactive with gases such as  $\text{CO}_2$ . The list of economic possibilities is limited. Presuming that an appropriate gas for the natural convection mode has been selected, a heat sink needs to be provided to couple to the core. Heat sinks external to the primary system would require a guaranteed convection path through the primary boundary during depressurization accidents. Quick opening valves in the boundary would be required. This would have the drawback of being a potential system depressurization initiation. There are certainly inherent

heat sinks such as shield/reflector regions, upper internals and the vessel metal, but unless provision is made for passive cooling of the vessel wall, there would be need for a dedicated emergency heat exchanger that is designed for natural convection cooling on the secondary side. Credit should be taken for the inherent heat sinks, both thermal inertia and natural convection cooling off the vessel walls in the cavity/silo as the phenomena will occur. But confirmation of this type of heat loss mechanism would require substantial CFD analyses and experimental confirmation of natural convection cell patterns. Maintenance of a backup pressure during primary system break/leak induced depressurization events would require a secondary guard containment or vessel surrounding the preliminary boundary. The challenge in designing and building this guard containment would depend upon the backup pressure level selected and the layout of the primary system and balance-of-plant. The questions of direct vs. indirect cycle, hydrogen production vs. electricity generation and others such as these would do have a large impact on the design of the guard containment.

#### **4.3.5 Flow Inertia/Semi-Passive Systems**

In the section on the discussion of conduction/radiation to internal cooled core heat sinks (heat pipes/cold fingers) the role of accumulators was briefly mentioned. Accumulators have been proposed in the NERI/I-NERI projects to handle the early decay heat transient (3%-6% power). There is an essential difference between the use of accumulators proposed for the GFR and LWR accumulators. The function of accumulators in LWRs is to keep the core covered and cooled through reflood, refill and rewet. Essentially, it is the water mass inventory that is important to the boil off. This is not the case here. The role of the accumulator here is to produce a residual coolant flow through the core to maintain cooling. This is basically the hydraulic equivalent of the pump motor flywheel to build on flow inertia and produce a longer coastdown. A flow, however small, of the order of few% is sufficient. This can be maintained by a low power circulator (couple hundred kilowatts) as mentioned in the NERI/I-NERI projects [4,5]. However this would be considered an active system in PRA space. It has moving parts and requires a power source. An accumulator with a rupture disc for instance may be considered to be semi-passive or passive depending upon the regulatory authority.

But the I-NERI project [6] has shown a considerable storage capacity even at cryogenic conditions would be required. Moreover there is the potential issue of ECCS bypass. Depending upon break location and size, accumulator injected flow may bypass the core and proceed directly to discharge through the break. One novel possibility of solving the bypass problem for the GFR is to design for a ductless pin-based core and inject directly into the core at key locations internal to the core. The means for delivery would be the control rod system. In the case of the Browns Ferry fire, the TVA BWR, a core melt accident was prevented by injection control rod leakage flow through the rod hydraulic system and directly into the core to augment the core coolant inventory. The I-NERI GFR design is proceeding along the lines of a bottom entry pneumatic driven control rod drive system. There is therefore the possibility of utilizing this drive system as a dual function reactivity control system and a passive decay heat removal system for heavy gas injection. This concept is not likely to be feasible in block/plate or pebble based cores. The best option would be a ductless pin-based core similar to the PWR.

But this concept may not be the most efficient use of the compressed gas in the accumulator. It could be more efficient to use the compressed gas to drive an auxiliary circulator. Very low core

flow, once the initial decay heat transient has been mitigated, is needed to remove the residual decay heat. In addition if an indirect power cycle reactor plant is used, the secondary side could be S- CO<sub>2</sub>, which would be a significant inventory of compressed gas. This would be an advantage of selecting an indirect cycle plant over the direct cycle one. Further extrapolation of this semi-passive/semi-active approach would lead to autonomous systems where the reactor decay heat power could be used to drive an auxiliary circulator through an emergency heat engine system. These concepts would require a PRA assessment to confirm the reliability of the approach. There would be a need for active elements. An active circulator would drive the core flow. The heat engine would be an active component. To return to a more passive approach the possibility of utilizing a gas-gas ejector could be considered. This could be similar to the BWR jet pump that is a liquid-liquid ejector.

#### **4.4 Evaluations**

The thermal gas cooled reactor development work of the last twenty years for both the HTGR and PBMR types have set the boundary of the safety case for decay heat removal accidents. For protected depressurization events with combined total loss of electric power, passive decay removal mechanisms can prevent core melting conditions even though fuel failure is anticipated in the case of break areas of less than 100 sq. inches. Comparable safety cases have also been developed in the last twenty years for fast reactors using the sodium coolant option. The NERI and I-NERI GFR project supported by DOE has explored the possibility of achieving a similar safety case for the GFR. Additional calculations performed during the initial phase of this Gen IV project have produced complementary information. The main focus of these efforts has been on the effect of core fuel form and configuration on the feasibility of these passive decay heat removal mechanism for the GFR. The major alternatives for fuel forms are:

- 1        Metal clad pins with fuel pellets.
- 2        Block or plates with dispersion or coated particle fuel

The DOE supported NERI project, [2,5] and I-NERI project [3,8] have produced results for a small modular pebble bed GFR (300 MWt), and a larger modular reactor (600 MWt) with either a pin-type or block-type GFR core design. Additional RELAP5/ATHENA simulations have been performed in the Gen IV effort for a 600 MWt pebble bed design GFR to augment the NERI and I-NERI evaluations. Based on the sum total of these lessons learned, a number of conclusions can be drawn for each of the potential mechanisms identified in Table 1.

##### **4.4.1 Mass Transfer**

The removal of the pebble fuel out off a pebble bed core during an accident by the dump system to a passively coolable location has been divided by the NERI/I-NERI projects into two stages (1) initial transport of the pebbles to the collection tanks (2) the controlled cooldown of the collection tanks. The I-NERI project work [6] has concluded that for a reasonable power density range of 50 W/cc the time scale needed for transporting the pebble is on the order of tens of seconds, which is very much shorter than that for the thermal reactor system that is on the order of hours. Work still needs to be done on the design of the transport ducts in particular, the temperature response of the structures but given the smaller number of pebbles and the potential velocities achievable, the transport of the pebbles may be feasible. A larger issue is the design of

the collection tanks. There may need to be a large number of tanks (tens) with limited dimensions restricted by both criticality criteria and passive conduction/radiation heat transfer criteria on heat removal to the tank boundary. Sacrificial collector material may need to be used. The NERI project [5] has shown that if water boiling is allowed then a natural convection preflux condensation system could be designed with a reasonable size cooling tower. However, if borated water is needed for reactivity control, then the issue of the boundary passive cooling will have to be re-evaluated. Those conclusions are supported by the following summary of the various analyses performed to date. Figure 10 shows previous German work on a pebble dump system for the German pebble bed reactor designs. A GFR pebble bed during system would be similar but the manual dump would be replaced with a temperature sensitive or pressure sensitive dump valve. Figure 11 show the typical timescale for the adiabatic heat up of the pebbles in a 50w/cc pebble-bed core. The results show that about a minute is available before fuel damage becomes of concern. Table 2 show results based on velocity correlations presented in the German work for core dump times for a range of parameter values. It appears that a 50-60 cm bottom orifice would be needed to dump the entire core within the one-minute thermal time scale. Given that the pebble bed core diameter is ~3 meter, this size bottom orifice may be feasible and the I-NERI project is continuing to investigate the engineering design issues.

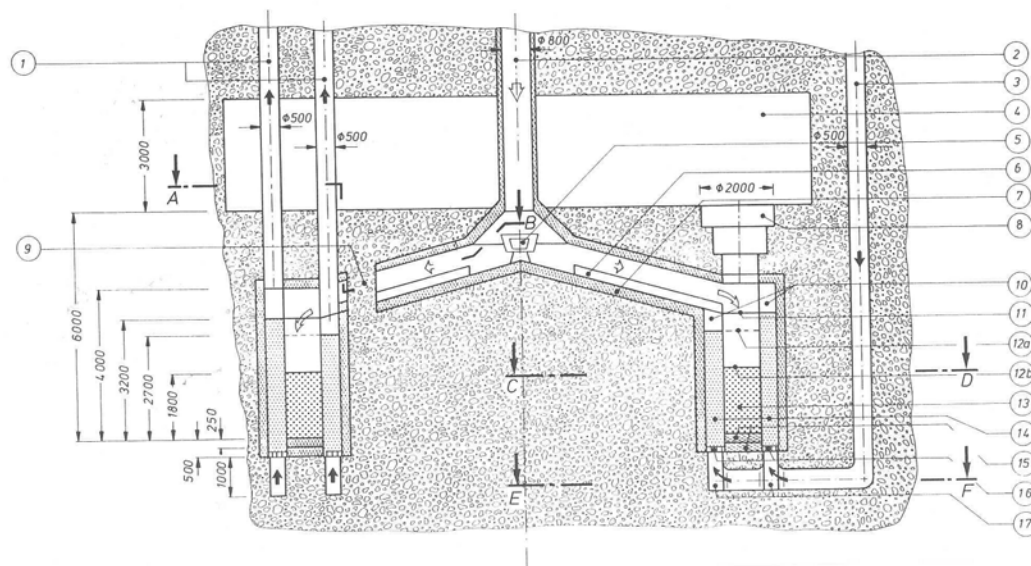


Figure 10. Longitudinal Section through Core Evacuation System [6]

1. Hot air outlet ducts (cooling system)
2. Pebble evacuation duct
3. Cold air inlet duct (cooling system)
4. Pebble management area
5. Catch/distribution funnel
6. Guide vane
7. Fire brick insulation
8. Access cover
9. Foundation
10. Hot air plenum

11. Fire brick wall
- 12a. Maximum height of pebble bed (2 filled locations)
- 12b. Maximum height of pebble bed (3 filled locations)
13. Pebble bed
14. Cast iron pebble bed
15. Floor and insulation
16. Inlet frit
17. Inlet air plenum and distributor

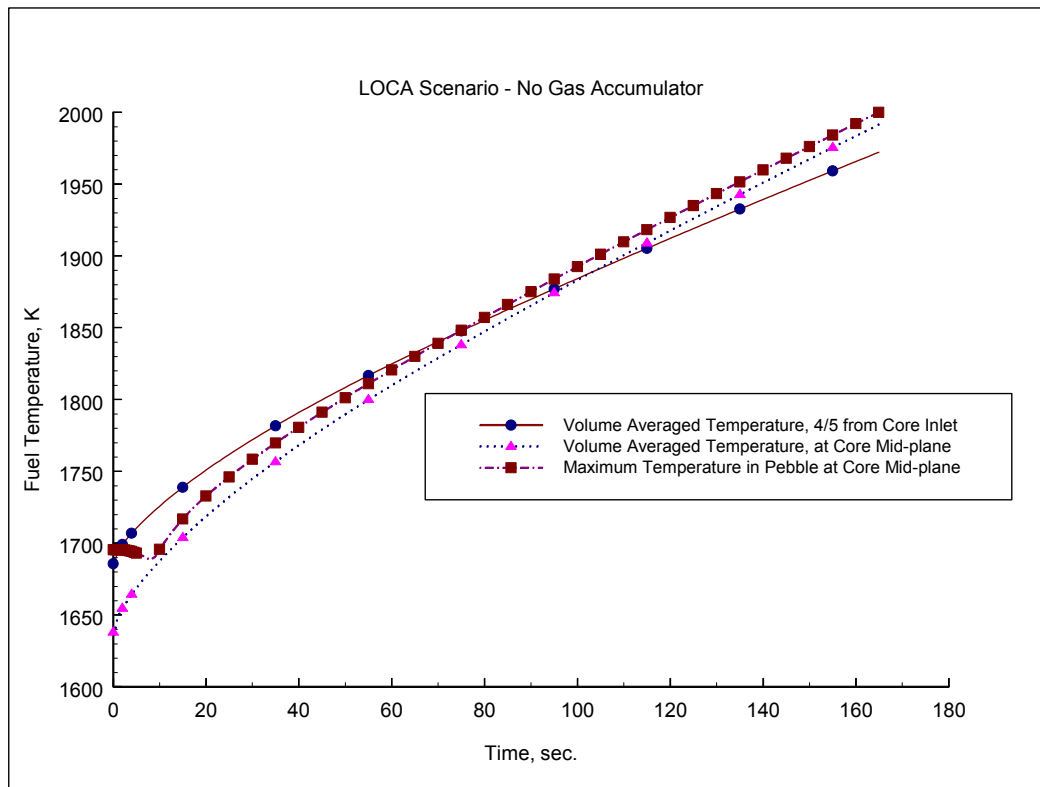


Figure 11. Variation of Fuel Temperature with Time in 5-cm Pebbles – No Gas Accumulator.  
[6]

<b>Table 2. Core Evacuation Time for Representative Pebble Densities and Sizes [6]</b>				
Orifice diameter (cm)	Pebble diameter (cm)	Pebble density (gm/cc)	D/d	Evacuation time (s)
60	3	6.5	20	27.6
50	3	6.5	17	46.5
40	3	6.5	13	88.2
20	3	6.5	6.5	681.2
60	3.5	6.8	17	29.1
50	3.5	6.8	14	49.1
40	3.5	6.8	11	93.8
20	3.5	6.8	5.5	735.5
60	4.0	7.1	15	30.6
50	4.0	7.1	12.5	51.8
40	4.0	7.1	10	99.2
20	4.0	7.1	5	817.0

#### Pebble bed concept long-term decay heat removal

In view of the above conclusions this work has concentrated on ultimate safe storage configurations of the pebbles, which have to satisfy the following two requirements:

- 1) The configuration must be sub-critical assuming fresh fuel (presumably the most reactive). A value of the multiplication factor of 0.95 will be assumed to be sufficiently sub-critical.
- 2) The decay heat remaining in the fuel pebbles must be conducted out of the storage configuration and into a long-term heat removal system. The maximum temperature of the pebbles must be below the maximum allowed accident temperature ( $\sim 1600^{\circ}\text{C}$ )

Both the above two requirements are more difficult to meet for gas cooled fast reactor fuel than for the gas cooled thermal reactor concept for which this concept was developed. The pebble fissile loading in the case of the fast reactor is significantly higher than for the thermal reactor, and thus the possibility of creating a critical assembly in the storage bins is a lot higher for the fast reactor fuel. Since the operating power density in the case of the fast reactor is much higher than in the thermal reactor concept, the decay heat is proportionately higher, and thus the long-term heat removal by conduction through the pebble bed and natural convection using air is not practical.

Temperature history estimates of pebble fuel following a depressurization accident were made using the RELAP code, which included the PCU volume, and a realistic break area of  $100\text{ in}^2$ . The pebble temperature as a function of time following the start of the accident is shown on Figure 12. It is seen that initially the temperature drops to a minimum of  $\sim 670^{\circ}\text{C}$  after  $\sim 200\text{ s}$ , and then increases adiabatically for  $\sim 1000\text{ s}$  before it reaches the unacceptable limit. Thus, it is necessary that any self-sustaining scheme for removing the decay heat startup and reach steady state operation in  $1000\text{ s}$ . In the current case this implies that the core evacuation and transition

to long-term heat removal take place in this time frame. The core evacuation will take place in 90 s – 120 s, thus ~ 800 s are available to transition to steady state heat removal. In view of the above heat removal limitations, a scheme is proposed in which the eventual configuration of the pebbles consists of a randomly packed bed infiltrated by a suitable eutectic. The eutectic must have a density below that of the pebbles (in order that the pebbles sink into the molten eutectic), a sufficiently high thermal conductivity to remove the decay heat to the container surface, a melting point temperature well below the unacceptable limit, and a boiling point above the unacceptable temperature limit. Several candidate eutectics exist that satisfy at least two of the above criteria, but only an aluminum-magnesium (Al-Mg) alloy (equally mixed) satisfies all the conditions. It has a density of ~ 2.7 gm/cc (well below the pebble density), melting point (~ 450° C), a boiling point above 2000° C, and high conductivity (~ 100 W/m-K). Assuming that the initial pebble temperature contacting the surface of the eutectic is 670° C, and progressively higher temperatures, it was assumed that the process at the interface between the particles and the solid eutectic is similar to that of ablation, in that the melt phase is removed from the surface as it forms. In the ablation case this process is clear, and in the current case the molten material is assumed to infiltrates into the spaces between the pebbles behind the layer in contact with the solid eutectic. Thus fresh eutectic is continually melted and flows up into the pebble bed. The molten eutectic is the primary heat removal medium to the container walls. It can be shown that the rate of melt front progression is proportional to the heat flux, and inversely proportional to the density, heat of fusion, and the heat required to raise the solid eutectic to the melt temperature. Preliminary estimates of the melt front progresses at 1.0 mm/s – 2.5 mm/s, depending on assumptions made regarding the initial eutectic temperature, and the heat flux. At this rate a column of pebbles 50 cm high would sink into the eutectic in ~ 500 s or less. This value is well within the time limit discussed above, and should ensure that it is possible to cover the pebbles with an appropriate molten eutectic before the unacceptably high temperatures are reached. Assuming that the columns are 50 cm high and have a radius of 20 cm, it would be necessary to divide the initial core volume into 96 cylindrical containers. These containers are arranged in a hexagonal lattice with a pitch of 45 cm. The containers are made of borated stainless steel with a wall thickness of 0.5 cm. The spaces between the containers is assumed to be filled with light water, which is assumed to be boiling in the steady state long-term heat removal phase.



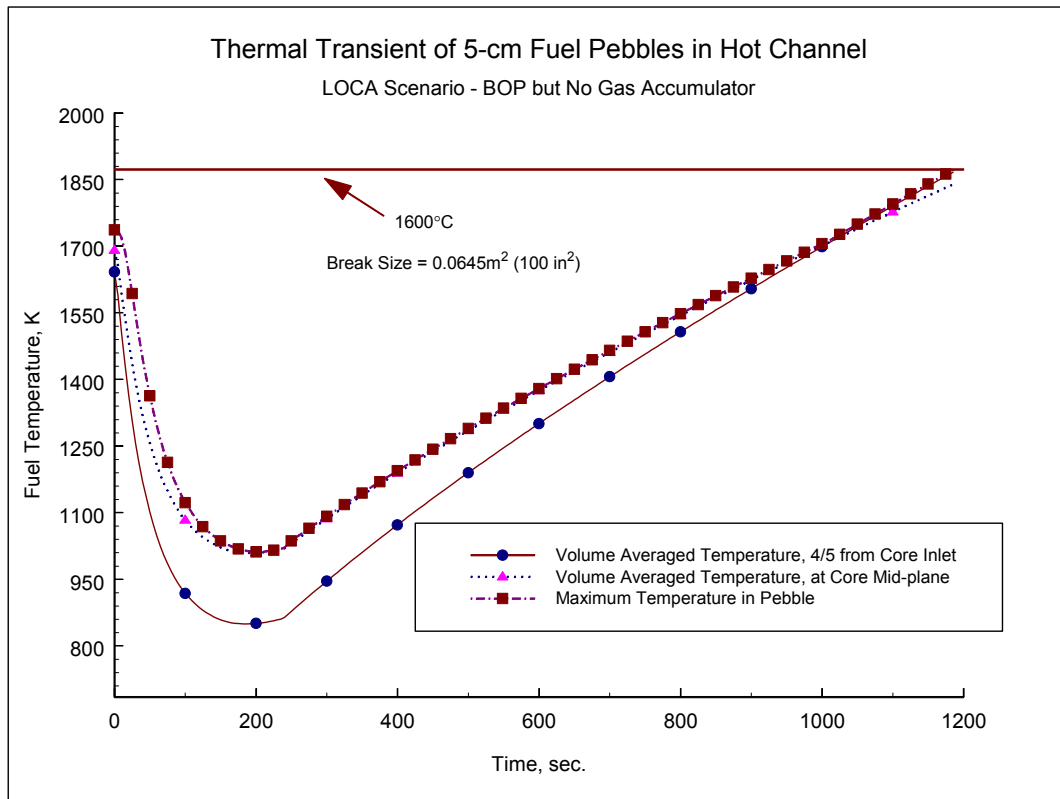


Figure 12. Pebble fuel temperature as a function of time following a depressurization accident

Preliminary estimates of the multiplication factor using the MCNP Monte Carlo code and both the CEA and ANL TRU fissile material vectors indicated that in both cases the initial configuration would indeed be super-critical. Thus boron was added to the stainless steel wall to de-couple the water from the fissile material in the pebbles. The boron was assumed to be natural boron, and ~ 8000 appm are necessary to ensure that the multiplication factor is below the target value of 0.95. Finally, assuming that the heat transfer at the container surface is by boiling then the maximum centerline temperature of the pebble-eutectic mixture is ~ 800° C, and the inner surface temperature of the container is ~ 350° C. This is a modest operating temperature for stainless steel, and it should be able to withstand any imposed mechanical and pressure induced loads.

#### 4.4.2 Conduction/Radiation Cooldown to Boundary and Thermal Inertia

The major design parameter for accommodating decay heat passively for all three fuel types is core fuel power density. Certainly major fuel power derating from the traditional GCFR values of 250w/cc from 25 years ago would be a major positive factor in improving the feasibility of the proposed passive decay heat removal mechanisms. However for all these fuel forms, current fuel cycle economic factors for a uranium startup core would set a minimum power density range on the order of 70-100 w/c<sup>3</sup>. This is still a major reduction from the historical range. With core fuel power density of 70-100 w/c<sup>3</sup>, the thermal gas reactor “conduction cooldown” mode of passive heat transfer of core generated heat through conduction and/or radiation inter and intra fuel

elements to the vessel boundary is not possible for the GFR. This is irregardless of fuel form, block/plate, pin or pebble. With the limited conductivity of the potential core fuel and structural materials, even 1 to 2% decay heat would lead to core disruption conditions. With the high temperature requirements of the Gen IV GFR (~850°C coolant outlet) and the fuel flux/fluence conditions the set of potential materials is small. However, even if graphite with its neutron spectrum softening disadvantage, utilized in the thermal gas reactor cores was used, success would not be attained. The crux of the matter is the low (~ 5w/cc) power density of the thermal gas reactor. To lower the density of the fuel by adding diluents, equation (2) shows that it could lower the power density and still retain the high specific power requirements. This would also be attractive from the viewpoint of adding thermal inertia. However a fast reactor core requires significantly higher fuel densities/loading to maintain criticality over a high burnup fuel cycle (~ 30% volume function of 10 gm/cc ceramic fuel with 20% fissile). Moreover the thermal properties of potential diluents are in the same range of the fuel. Adding diluents is not a potential solution for the GFR given the state of future core material development work. Adding thermal inertia to absorb decay power in sensible heat until ~0.1% decay power is reached, is not feasible.

### Evaluation

Those conclusions are supported by the following summary of the various analyses performed to date. Figure 13 shows that the steady state thermal conduction solution for a two dimensional cylinder with uniform heat generation and constant temperature boundary condition, can be correlated as a non-dimensional grouping.

$$\eta = \frac{P}{\kappa \ell \Delta T} = f\left(\frac{D}{\ell}\right) \quad (4)$$

where:

P = power

D = diameter

$\kappa$  = conductivity

$\ell$  = length

$\Delta T$  = temperature rise

Figure 13 is a numerical fit of the analytical series solution provided in [2].

Asymptotically as  $\frac{D}{\ell} \rightarrow 0$  the solution approaches that for a thin rod while in the other limit

$\frac{D}{\ell} \rightarrow \infty$  it approaches that for a thin plate. Figure 13 can be translated into Figure 14 where core length (height) is plotted as a function of aspect ratio for a given  $\eta$  value [3]. Table 3 shows a range of  $\eta$  values of interest for a 600 MWt reactor core.

Table 3. Values of  $\eta l$

$\square T^{\circ}\text{C}\backslash\text{Kw/m-c}$	15	300	P = 6MWt (1% of nominal)
500	800	40	
1000	400	20	
2000	200	10	

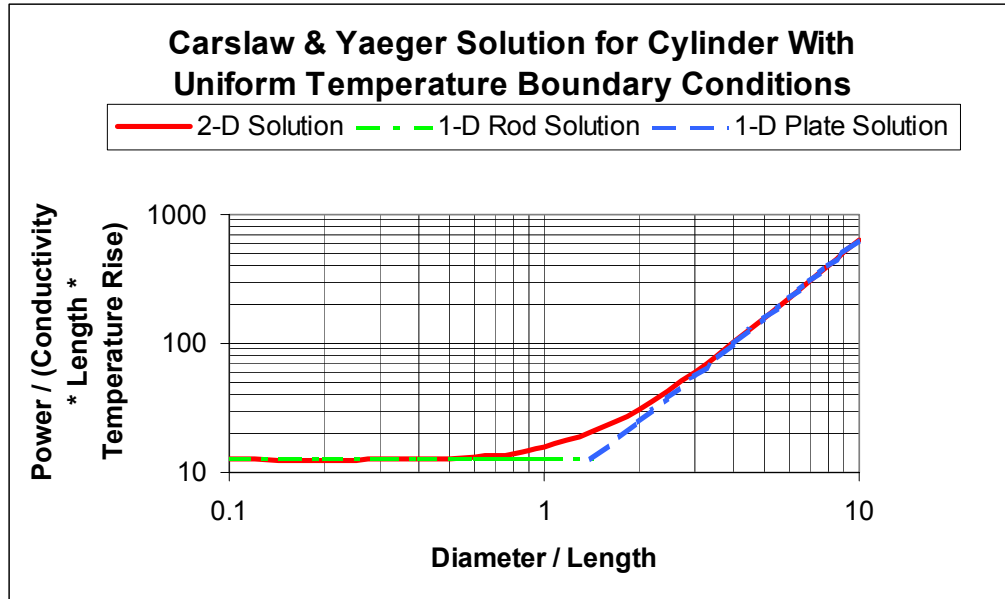


Figure 13. Two-Dimensional Solution for a Cylinder with a Uniform Heat Generation Rate and Constant Temperature Boundary Conditions. [2]

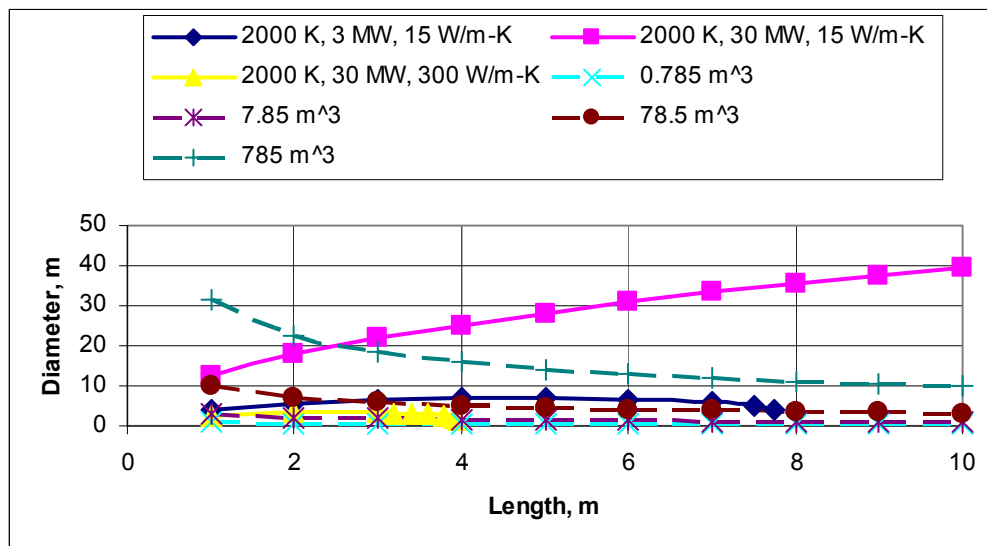


Figure 14. Core Length Versus Aspect Ratio for a Given Power/(Conductivity Delta-T) [3]

The values are tabulated as a function of the temperature rise through the cylindrical core for two values of conductivity. The conductivity of stainless steel is  $\sim 15 \text{ W/m}^\circ\text{C}$  while that of copper is  $\sim 300 \text{ W/m}^\circ\text{C}$ . The core materials currently being considered for the GFR have conductivities in the range  $15\text{-}30 \text{ W/m}^\circ\text{C}$ . It can be seen from Figure 14 that for  $200 < \eta\ell < 800$  and for historical fast reactor aspect ratio of  $\sim 1$  (0.5 to 2.0) core dimensions are large (5 to 10 meters). This would translate to power densities of  $\sim 1 \text{ W/cc}$  which is very much smaller than the GCFR value of 25 years ago of  $\sim 250 \text{ W/cc}$ . To achieve these historical values of power densities would require some very skewed core shapes with aspect ratios at the extremes (0.1 or 10). This would lead to very large neutron flux leakage and very short burnup cycles or very large fissile content. Furthermore the limiting temperature on materials could be particle coating integrity limits on the order of  $1600^\circ\text{C}$  and there are additional temperature drops (mostly radiative drops) between the core edges and the vessel wall. Unless substantially higher conductivity core materials can be developed, passive removal of decay heat ( $> 1\%$  nominal power) through pure conduction cooldown alone to the vessel boundary will not be feasible for economic operations of the GFR. This is not a thermal gas cooled reactor where, as discussed previously, a power density of  $5 \text{ W/cc}$  is economically acceptable.

But conduction alone is not the sole mechanism for transporting core decay heat to the wall boundary through the fuel elements. For fuel forms such as the pin or the pebble, as opposed to monolithic blocks, radiation heat transfer is a major component of the fuel element-to-fuel element heat transfer. To compare the relative effectiveness of conductivity relative to radiation in transferring heat from fuel element to fuel element to the vessel wall boundary, reference should be made to Tables 4-5 and Figures 15-16 [2]. A single fuel pin (0.285" diameter) and rated at  $6 \text{ kW/ft}$  as from 25 years ago, is placed at the center of a 26ft diameter cylinder. The Tables and Figures show the temperature rise from the boundary to the pin for a solid opaque cylinder (conduction) and for a transparent material with zero conductivity (radiation). Clearly materials with the conductivity of copper are far superior, but even with the conductivity of steel it is not until the temperature range is between  $1000 - 1200^\circ\text{C}$  that radiation heat transfer becomes better than conduction heat transfer. Furthermore, in the case of radiation heat transfer, the central fuel pins are shadowed from the vessel wall boundary by many other rows of fuel pins. The NERI project [3] has shown that for the GCFR fuel bundle design of 25 years ago ( $250 \text{ W/cc}$ ) with a hexagonal assembly of 271 ceramic fuel pins configured into ten rows, even at a decay heat level  $0.33\%$  of rated power there is a temperature difference of  $1200^\circ\text{C}$  between the center pin ( $2050^\circ\text{C}$ ) and the hex duct ( $316^\circ\text{C}$ ).

Table 6 shows the effective pin bundle conductivity for fuel pin conductivities changed to those of steel ( $15 \text{ W/m}^\circ\text{C}$ ). It can be seen that ten rows of pins with the corresponding radiation interfaces is very challenging for radiative heat transfer. Even if the hex assemblies were made of solid block fuel there would still be radiation interfaces due to the clearance gaps between the blocks designed for refueling. For the GCFR assembly design of 25 years ago, Table 7 shows results [3] for a  $50 \text{ W/cc}$  core rated at  $600 \text{ MWt}$ . This translates to 13 rows of 469 block-type fuel assemblies radiating heat through the gaps between the blocks made with infinite conductivity material to the vessel, which is held at  $316^\circ\text{C}$ . This shows that even with perfectly conducting block fuel, the fuel clearance gaps will make it very difficult to conduct/radiate decay heat through the fuel elements to the vessel wall boundary without damaging the fuel.

Table 4. Temperature Rise for Radiant Heat Transfer [2]

Temperature of Enclosure Surface, C	Temperature Rise for 60 W/ft	Temperature Rise for 30 W/ft
316 (600 F)	133.9	76.9
400	100.4	55.4
600	52.5	27.4
800	29.6	15.1
1000	18.1	9.1
1200	11.8	5.9
1400	8.1	4.1
2800	1.31	0.65

Table 5. Temperature Rise for Conductive Heat Transfer [2]

Thermal Conductivity, W/m-K	Temperature Rise for 60 W/ft	Temperature Rise for 30 W/ft
15	14.6	7.3
300	0.731	0.366

Table 6. Pin Bundle Effective Conductivity

Boundary T°C	k w/m-c
316	2.07
1600	7.54
2000	9.86

Table 7: Block Core with Gaps Peak Fuel Temperature	
% Decay Power	Fuel T <sub>peak</sub> °C
2.5	2955
5.0	3594

Table 8. Thermal Properties of Candidate Pebble Materials [5]

Material	Thermal Conductivity at 1000°C W/m-K	Density, kg/m <sup>3</sup> ρ	Specific heat capacity at 1500°C, J/kg-K (C <sub>p</sub> )	Product of ρ x C <sub>p</sub> , J/m <sup>3</sup> -k x 10 <sup>-6</sup>	Melting Point or Dissociation Temperature, C
Silicon Carbide	35.7	3160	1336	4.22	~2000
Titanium Nitride	22	6400	595	3.81	3230
Zirconium Carbide	22	6510	250	1.63	3530
Uranium Oxide	3.6/3.2	10960/9660	339	3.72/3.27	2730 (2805)
Uranium Carbide	20/17.5	13630/12970	272	3.71/3.53	2400 (2525)
Uranium Nitride	24.6	14320/13510	272	3.90/3.67	2600 (2850)
Graphite	~30	1700	~2000	3.4	3650

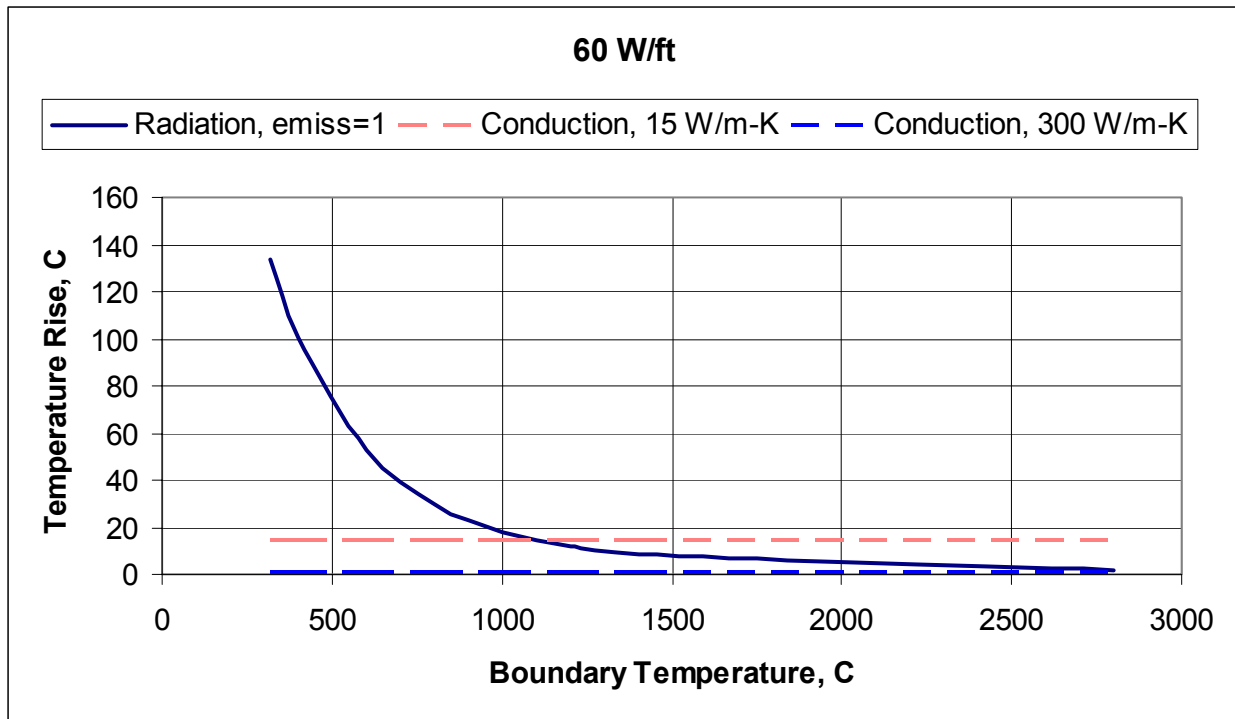


Figure 15. Radiation Versus Conduction for a Pin Power of 60 W/ft. (The lower dashed curve corresponds to conduction at 300 W/m-K.). [2]

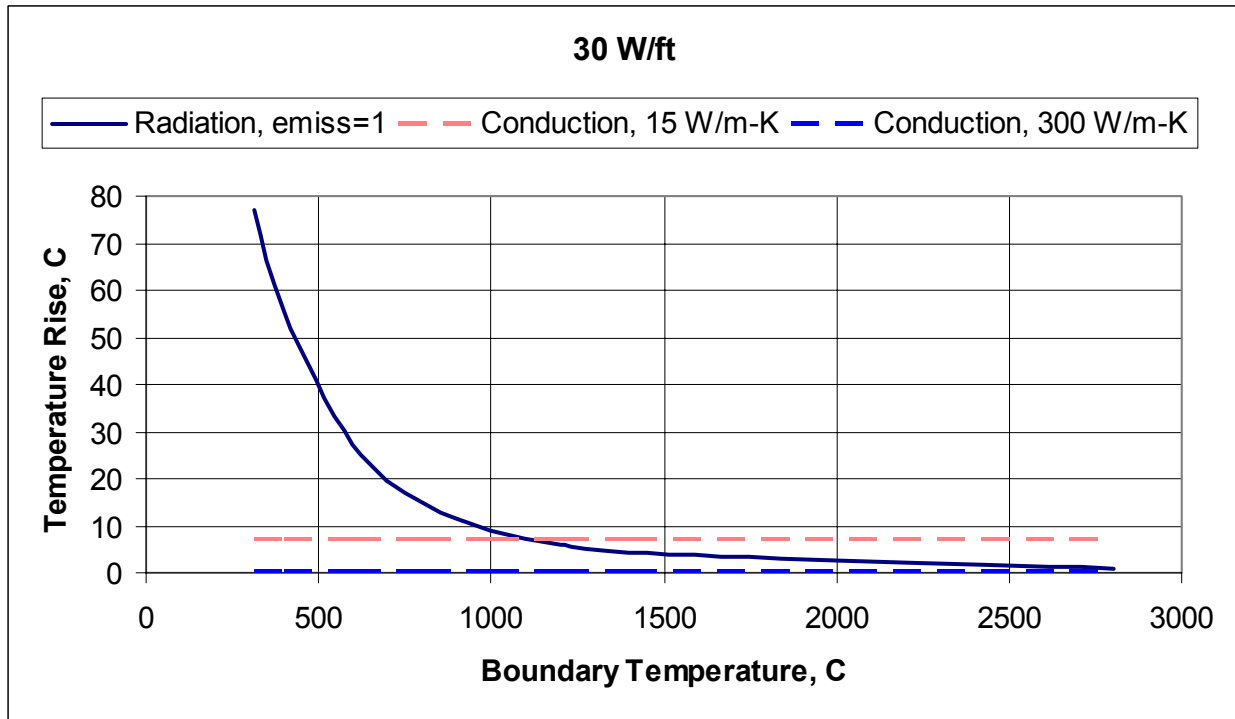


Figure 16. Radiation Versus Conduction for a Pin Power of 30 W/ft. (The lower dashed curve corresponds to conduction at 300 W/m-K. [2])

As discussed previously, the possibility exists to absorb excess decay heat by increasing the core thermal inertia, stretch out the time scale and reach a lower decay heat level before the conduction cooldown phase with boundary heat losses is required. Table 8 shows the thermal properties of candidate GFR core material being considered. It can be seen that the volumetric heat capacity, which is important to the thermal criteria, is largely in the range of 3-4 j/m<sup>3</sup>-K. While there are variations, there is no quantum improvement. However, even in the case of the thermal conductivity the value is principally in the range 20-30 w/m°K, with the exception of uranium oxide fuel, replacing fuel with matrix material can lead to improvements but it is not a quantum one. Table 9 shows the results for a series of one-dimensional transient conduction calculations performed for the one-dimensional slice through a reactor, which is shown in Figure 17 [3,5]. This is a pebble-bed core reactor. Table 10 shows follow-on calculations [5]. The pebble design is a two region (tootsie-pop) pebble when the inner region is an unfueled region. This decreases the temperature peaking in the pebble and leads to the possibility of using different thermal inertia material in the center of the pebble and perhaps also taking credit for the latent heat of the inner region. For the results presented in Table 9, both inner and outer region material utilize the properties of steel. Furthermore, in another effort to boost heat capacity, a number of the calculation in Table 9 are for an annular core design where the central core region is filled with unfueled pebbles. This once again is an effort to increase the thermal inertia. The reactor vessel boundary condition is both radiation and convection to an environment at 149°C (300°F). Table 9 shows that even for a small reactor of 300 MWt power, it would be difficult to meet a fuel temperature criteria of 1600°C for power densities greater than 15w/cc. In the follow-on cases shown on Table 10, all the cases are variations on case 19 where the only change

is the choice of pebble material. It can be seen that the candidate list of materials from Table 8 does not lead to a quantum improvement. This evaluation of the NERI/I-NERI project results provides the basis for the conclusion stated at the beginning of the section. In summary for the range of GFR power densities, conduction/radiation cooldown to the vessel boundary is not the optimum passive decay heat removal mechanism for this reactor type.

Table 9. One-Dimensional Cases [3]

Case Name	Inner Radius of Core, m	Core Volumetric Heat Generation Rate, W/cc	300 MWt Core Height, m	300 MWt Core Pressure Drop, psi	Max, Core Transient Temp., C	Max. Transient Reactor Vessel Temp., C
case 11	0	2.790	10.0	17.6	1517	372
case 13	0	5.580	5.0	8.8	1991	486
case 14	1.3081	5.580	10.0	65.5	1169	386
case 15	1.3081	11.16	5.0	32.7	1645	495
case 16	1/3081	16.74	3.3	21.8	1874	589
case 17	1.2	15.00	3.2	15.9	1982	603
case 18*	1.2	15.00	3.2	15.9	1835	615
case 19	1.4	15.00	4.4	38.4	1575	521
case 20**	1.4	15.00	4.4	38.4	1844	495 (after initial phase)
case 21	1.3081	15.00	2.7	17.8	1754	556

\*The reflector and the neutron shielding are made of nickel instead of 304 stainless steel.

\*\*The region from the outer surface of the reflector to the inner surface of the reactor vessel is filled with unfueled pebbles through which the inlet coolant flows during normal reactor operation. Also, the initial steady-state condition has been modified.

Table 10. Additional Vessel Conduction Decay Heat Removal Cases [5]

Case Name	Pebble Type	Core Maximum Temperature, C	Vessel Maximum Temperature, C
19	Steel (Tootsie Pop) with Latent Heat	1575	521
26	Steel (Tootsie Pop) without Latent Heat	1628	532
23	Silicon Carbide	1661	540
24	Zirconium Carbide	1774	564
22	Tungsten (with Tungsten Reflector)	1682	561



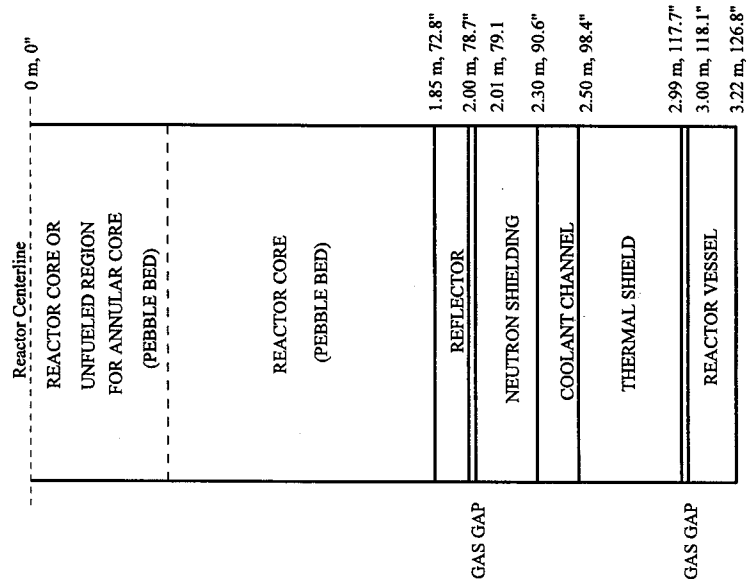


Figure 17. Radial Slice Through Core of Pebble-Bed Fast Reactor. [3]

#### 4.4.3 Core Heat Sinks

Inertia is insufficient and for the passive heat transfer option to be successful, there is the possibility of heat sinks internal to the core. These could be heat pipes or the cold finger concept (bayonet heat exchange) introduced in the NERI/I-NERI projects [8]. Fuel forms would make a difference here. Pin-based and plate-based cores can be ruled out, as there are too many radiation interfaces. Block cores would be the optimum if no interblock gaps were required. However for defueling this is not an option so pebble bed cores can be equally considered from the viewpoint of heat transfer. The NERI/I-NERI projects have shown that in the range 25-50 w/cc for 1 to 2% of decay power the number density of the heat pipes/cold fingers would be about that of the control rod positions. The cold fingers exploit this feature and the NERI/I-NERI projects have proposed designs where the finger has both reactivity control and passive heat removal functions. As of this date, there is no such dual design for a heat pipe. Furthermore transport of the decay heat from the heat pipe to the ultimate heat sink requires another fluid transport system, whereas for the cold finger a pressurized all-CO<sub>2</sub> system has been proposed. But with both concepts, refueling for the block core has to be bottom entry. For a passive system the heated coolant in the heat pipes and the cold fingers rise to the top of the reactor core. All the piping connections are made at the top, which makes top refueling for the block-based core very challenging. However this is not the case for the pebble bed core. Conceptually the pebble can be rolled in from the top of the reactor in to the lattice of heat pipes/cold fingers. This is a major design and materials problem but in principle may be solvable by a long term R&D program. This option would therefore be a high-risk/long term research and development possibility and in the end would be still on the low end of the desired core power density range. Moreover, the short term decay heat transient from ~6% to 3% power may require additional passive heat removal systems. The current round of RELAP5/ATHENA calculations is inconclusive in that regard. More detailed simulation is required of potential

supplementary passive heat loss mechanisms such as conduction/radiation from the core to the core barrel, to the upper internal and other structures that are all potential thermal sinks. If these phenomena are insufficient there may be the need for accumulators, which then leads to the discussion later on the balance between active and passive systems.

### Evaluation

These conclusions are supported by the following summary of the various analyses performed to date. Analyses have been performed of the heat-pipe option with the block core design and the cold finger option with the pebble bed core design. Since similar results have been obtained with the heat pipe/block core combination, this summary will focus on the results obtained with the cold finger/pebble-bed option. Figure 18 shows the cold finger concept [8]. Essentially the cold finger provides two key core functions in one location; (1) reactivity control and (2) passive decay heat removal. Core control rods have to be provided cooling irregardless of design, so the concept encloses the control rod with its thimble in a separate pressure tube housing isolated from the main primary system core coolant flow. Within the pressure tube there is an insulator tube that surrounds the thimble and provides the means for the control rod coolant flow with a U-turn at the bottom. The redirected upward flow then cools the pressure tube from the inside. During the accident sequence the core decay heat would be conducted/radiated through the fuel elements towards the internal core heat sinks, the cold fingers, instead of only toward the vessel wall boundary. Figure 19 shows the complete configuration. By design, the cold fingers would be inserted at the traditional control rod locations and connected to a natural convection pressurized CO<sub>2</sub> system. The ultimate heat sink would ultimately have to be a fully passive dry cooling power for example. Table 11 shows design results for two types of pebble design, a 50/50 metallic pebble and a solid graphite pebble. The 50/50 pebble would be the tootsie pop design discussed in section where half the pebble is fueled and the other half unfueled. The metallic designation is merely to indicate that the thermal properties used are largely typical of metals whereas the solid graphite pebble, which has no unfueled region, has thermal properties typical of graphite and the family of silicon carbides. The Table shows that ~24 cold fingers would be sufficient for a 600MWt core design rated at ~50w/cc to keep fuel temperature limits below the damage criteria of 1600°C. This is encouraging since typically for this size core ~24 control rods would be needed to limit individual rod worth's to 10 cents or less.

However, the decay removal rate is only 1% power. There may not be sufficient margin without additional devices such as accumulators extended coastdown and additional credit taken for vessel wall heat losses and heat transfer to other primary vessel heat sinks. More detailed analyses and accumulators asides, there is a materials issue which needs developmental R&D. These in-core locations are high fast flux and high temperature regions. Heat producing pebbles contact the cold finger pressure tubes and the contact temperature could be higher. Furthermore as the core is loaded, fuel pebbles will impinge upon these passive tubes.

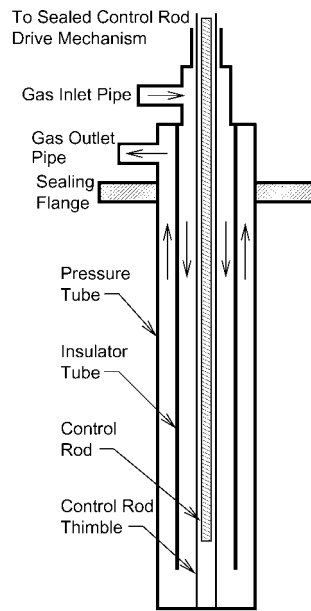


Figure 18. Cold Finger Design. [8]

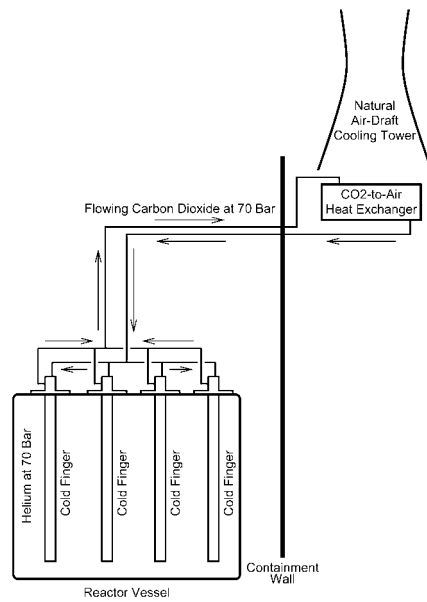


Figure 19. Cold Finger Concept. [8]

Table 11. Key Core and Cold Finger Parameters for the Two Design Choices [8]

Quantity	Parameter	
design choice	1	2
pebble diameter, cm	5.0	4.0
pebble material/design	50/50 metallic	solid graph.
core length, m	2.00	1.85
actual core diameter, m	3.00	3.12
rated reactor power, MWt	600	
decay power level, %	1.00	
elevation difference (chimney height), m	10	
fuel region heat generation rate, W/cc	50	
control rod thimble O. D., cm	5.0	
carbon dioxide coolant inlet temperature, C	50	
pressure tube thermal conductivity, W/m-K	15.0	
number of cold fingers	24	24
insulator tube I. D., cm	18.5	20.0
insulator tube O. D., cm	19.5	21.0
pressure tube, I. D., cm	22.0	23.0
pressure tube O. D., cm	23.6	24.7
effective fuel region O. D., cm	61.2	63.6
fuel region thermal conductivity, W/m-K	10.9	11.9
cold finger carbon-dioxide flow rate, kg/s	3.58	3.10
carbon-dioxide coolant outlet temp., C	127.0	138.5
pressure tube I. D. temperature, C	336.5	340.7
pressure tube O. D. temperature, C	430.4	442.1
maximum fuel temperature, C	1560.1	1551.5

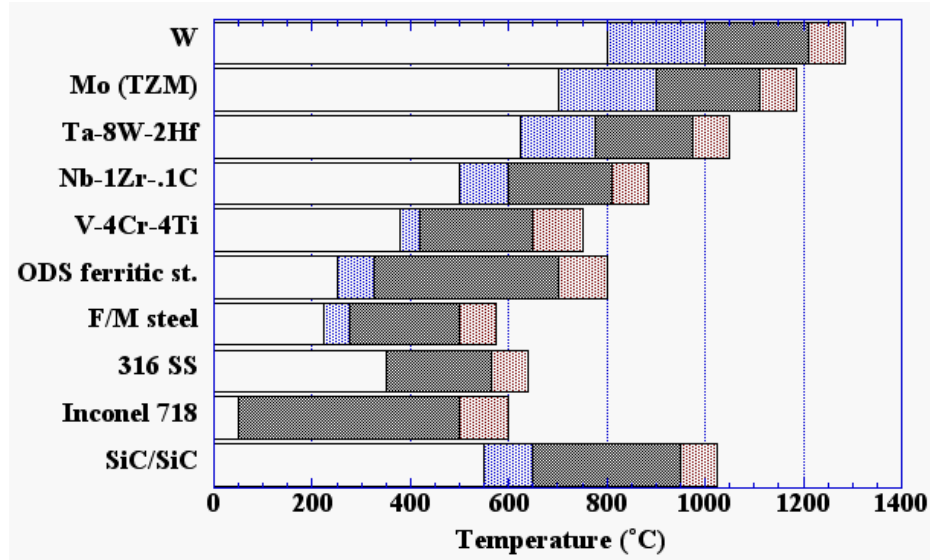


Figure 20. Estimated Operating Temperature Limits for Structural Alloys in Fission Reactors: 10-50 dpa. [9]

Table 12. Comparison of Properties of Commercial SiC-Based Fibers and Bulk SiC [10]

	cg-Nicalon	Hi-Nicalon	Hi-Nicalon type S	Dow Sylramic	Bulk SiC
Diameter ( $\mu\text{m}$ )	14	12-14	12	10	----
Tensile strength (GPa)	2.0-3.0	2.8-3.4	2.6-2.7	2.8-3.4	~0.1
Elastic modulus (GPa)	170-220	270	420	390-400	460
Density ( $\text{g}/\text{cm}^3$ )	2.55	2.74	2.98-3.10	3.0-3.10	3.25
Coefficient of thermal expansion ( $10^{-6}/\text{K}$ )	3.2	3.5	---	5.4	4.0
Thermal conductivity at 20° C ( $\text{W}/\text{m}\cdot\text{K}$ )	1.5	4	1.8	40-45	100-350
Oxygen content (wt. %)	11.7	0.5	0.2	0.8	0.0
C/Si atomic ratio	1.31	1.39	1.05	1.0	1.0

So not only high-temperature and high fast-flux resistant materials will have to be utilized but also with high mechanical impingement structural resistance. Figure 20 shows the estimated operating temperature limits for a set of candidate metals, an important subset of which are the refractory metals [9]. However the refractory metals have poor neutronic properties (large

absorption cores section). Table 12 shows properties of the current leading options, various forms of SiC [9]. In summary, the current design results show that while cold fingers are an option, it would be difficult to reach the power density range of 100 w/cc without additional passive safety mechanisms and there will be a challenging materials development effort.

#### **4.4.4 Natural Convection**

Conduction and radiation aside, the third possible heat transfer mode is convection which in the passive form is natural convection. It has historically been known that gas coolant provides a poor heat transfer medium with low thermal inertia at low pressure ( $\sim 1$  atmosphere) but historically it has been shown by design calculation that even for the historical high power density cores ( $\sim 250$  w/cc) natural convection can successfully remove core decay heat at pressurized conditions (70 bar) for acceptable primary system elevation differences. Even the short-term decay transient from 6% - 3% power can be accommodated. The NERI/I-NERI projects have shown that natural convection is best suited for the block/plate and pin fuel forms [2,10]. The pebble-bed fuel form would be the most challenging form for this option. Pebble beds have inherently high resistance to core flow, which are difficult to overcome through design. It is best to focus on block/plate and pin cores for the natural convection option. For this option to work, a guard confinement or double containment/vessel would be required. The approach is to only permit depressurization of the primary system through design means for a secondary backup pressure. The choice of the backup pressure is a major design choice. The lower the pressure the worse the natural convection heat removal capability but the less challenging the design and construction issues for the guard containment. The current optimum choice would be a block core design with a guard containment sized for 20 bar accident pressure.

#### Evaluation

These conclusions are supported by the following summary of the various analyses performed to date. The analyses have been a combination of steady state primary system calculations and RELAP-5/ATHENA primary system transient calculations performed by the Gen IV effort. Figure 21 shows the natural convection loop model of the primary systems used to provide the steady state results included here. The core, chimney, emergency heat exchanger (EHX) and cold leg hydraulic losses are explicitly represented in the primary system simulation. But, since the secondary side of the EHX is not modeling the EHX primary coolant outlet temperature is fixed. Based on a secondary-side pressurized CO<sub>2</sub> cooled natural convection loop and other design calculations [4] the EHX coolant outlet temperature is fixed at 250°C. It should be noted that the EHX tube designs were also taken from [4] for each simulation case. Figures 22-24 show the effects of primary system coolant choice, core outlet temperatures and decay power level on the primary coolant pressure required to maintain the steady state core heat removal capability. Results are shown for a core design of each of the three major potential fuel forms, pebbles, pins and blocks. The block-core design is for the reference 600 MWt reactor proposed by CEA [7] on the I-NERI project. It has been optimized for both 100% steady conditions as well as for natural convection accident conditions. The power density is rated at  $\sim 100$  w/cc. The block coolant channel sizes have been optimized for fabrication specifications. Any larger coolant volume fractions would probably lead to a plate-type core instead of a block-type core. Figure 22 is evidence that CO<sub>2</sub> leads to lower secondary (guard) containment pressure requirements than Helium. Even at 3% decay power, the 5-7 bars are within current PWR

containment technology. However, if heavy gas injection and mixing is an issue, then in the worst case Helium at 900°C, a guard containment pressure of ~25 bars is required. This pressure level is probably better accommodated by PCRV technology. 900°C is probably still acceptable for structural temperature whereas 1100°C is definitely not. Figure 23 shows the corresponding results for the pin-core design also at 100w/cc. This pin core is the back-up design proposed by CEA [7] for the 600MWt reactor. As with the block core it has been optimized for both the 100% steady conditions and the natural convection accident conditions. The resulting guard containment pressure required for the natural convection removal of the decay heat are quite comparable between the two core designs. Once again CO<sub>2</sub> is definitely better. Figure 24 shows the results for the pebble core design [8]. Given the essentially dictated pebble packing fraction of 40% coolant volume, the flexibility to optimize the pebble bed core for natural convection is limited. The results shown in the figure are for a 600MWt core rated at 50 w/cc and optimized by the I-NERI project. The results show that this pebble-bed core is definitely the worst performer in terms of the required guard containment fission. A pressure of 50 bars is required for Helium at 900°C.

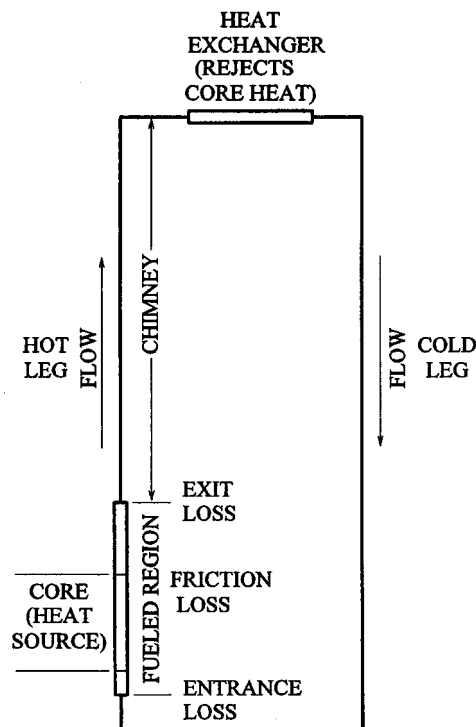


Figure 21. Natural Convection Loop

Figure 22. Block Core Natural Convection Pressure

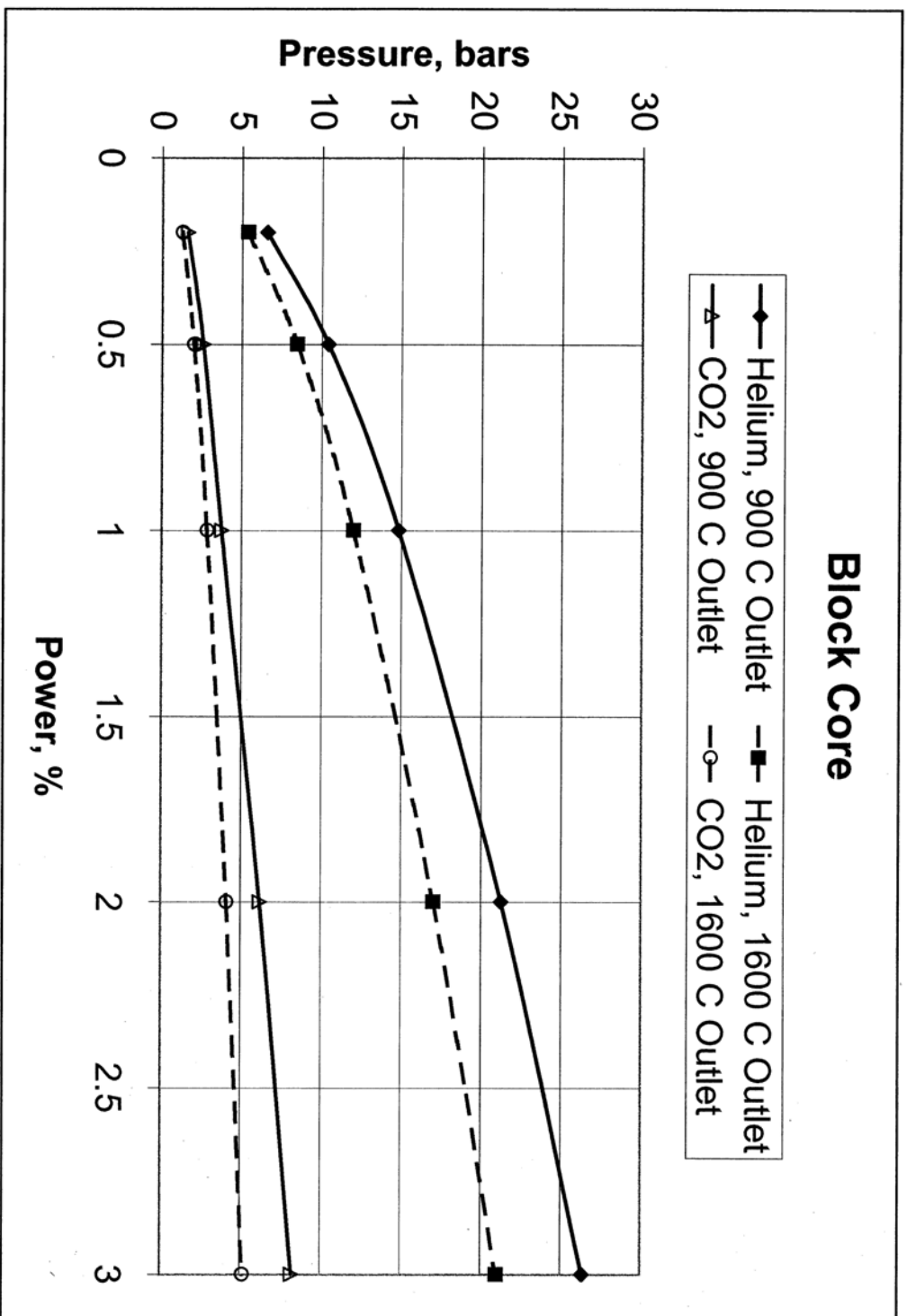




Figure 23. Pin Core Natural Convection Pressure

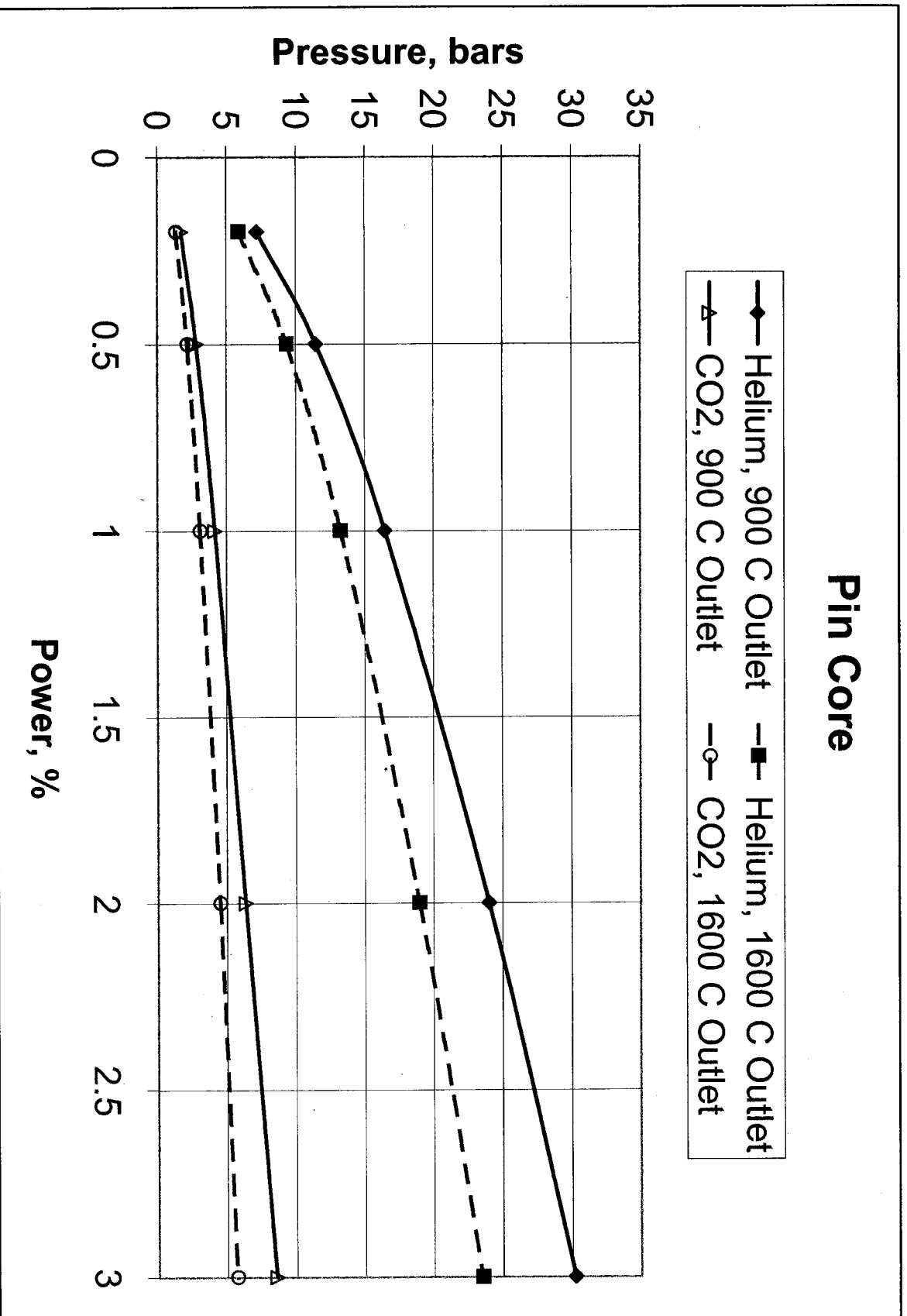
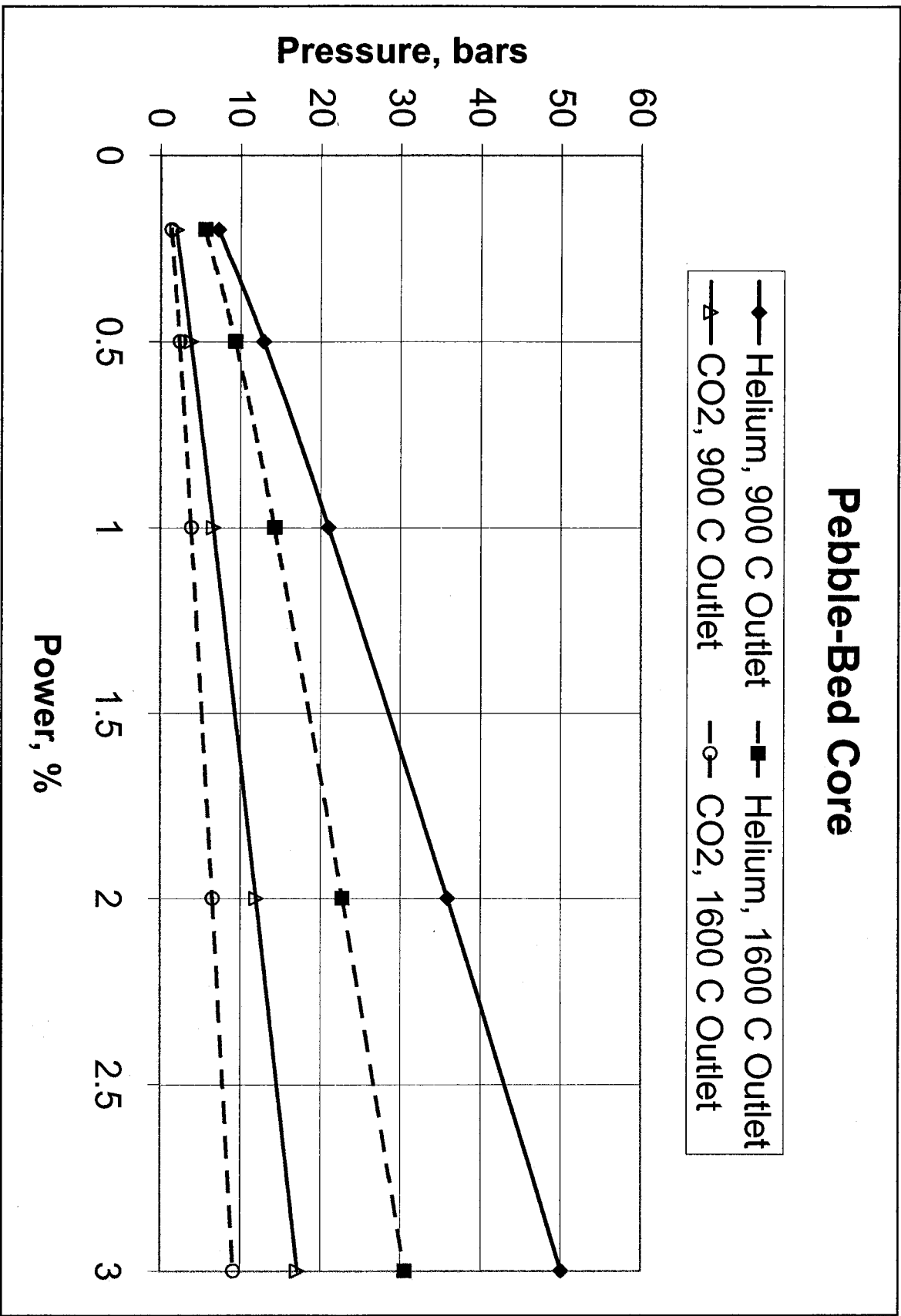


Figure 24. Pebble Bed Natural Convection Pressure



Since these results are all for steady state conditions a set of RELAP-5/ATHENA transient calculations were performed for the pebble bed core design using the plant nodalization model shown in Figure 25. This is a scoping type model and focuses on the natural convection loop between the core and the EHX. Since the PCU is only significant as an inventory of gas, it is modeled as two volumes. The turbo-machinery flow coastdown is a boundary condition forced by the source/sink volumes. As with the steady state analyses the EHX secondary side is not modeled in detail. However, the transient heat flux and thermal inertia of the EHX tubes are included. The temperature boundary condition is set on the CO<sub>2</sub> side of the EHX. Two sets of parametrics on the final guard containment pressure have been performed. In both sets, the turbo machinery coastdown flow is stepped down to zero instantaneously upon the reactor scram and the EHX boundary temperature is set at 300°C. The RELAP-5 calculations had a peaking factor of 1.3. In the first set the EHX length is set at 0.25 meters and in the second set the EHX length is set at 1 meter. Figures 26-29 show the fuel temperature at two locations, the fourth core node and the fifth core node of a five node core. The peak fuel temperature moves from the fourth core node to the fifth core node as the transient proceeds. The fifth core node is located at the core outlet. Figures 26-27 are for the EHX lengths of 0.25m. The figures show that the fuel temperature damage criteria of 1600°C is closely exceeded by the 20 bar final guard containment pressure design while the 45 bar final pressure results have significant margin. Figures 28-29 are for the EHX length of 1 meter. These results show that for the 20 bar final guard containment pressure the fuel temperatures widely exceed the 1600°C fuel temperature criteria while the 45 bar final pressure results do not. In summary these results show that the current optimum design for this safety approach should be the block core design with a guard containment sized for a final accident pressure of ~30 bars.

#### **4.4.5 Flow Inertia and Semi Passive Systems**

The NERI [3] project was only funded to evaluate potential core designs and core design modifications which would assist in the introduction of passive decay heat removal mechanisms. Primary design and BOP design was not considered. Therefore, the issue of turbo machinery and compressor/generator inertia on flow coastdown and its impact on the decay heat removal transient was not evaluated in the NERI project. The I-NERI project has been constructing CATHARE and RELAP-5/ATHENA primary system plus direct cycle BOP plant models. However this is still at an initial stage. The Gen IV effort at ANL is also constructing and has constructed a 600MWt pebble bed reactor primary system model and the details are available in Appendix A. But this effort is still interacting with INEEL on RELAP-5/ATHENA turbomachinery models. At this stage the flow coastdown implications of the turbomachinery inertia is still open.

However the I-NERI effort [6] has extensively studied the potential role of accumulators on mitigating the effects of the selected depressurization accident sequence. Thermal-hydraulically, CO<sub>2</sub> has superior performance over Nitrogen and Helium. Inventory storage design should also be less challenging. However even with cryogenic storage, ~300m<sup>3</sup> capacity would be required for storage to cool the 600MWt pebble bed core down to 1.0% decay heat level. There are engineering challenges on thermal stresses given the potential large difference in temperature. Strong consideration should be given to semiactive/semipassive systems to maintain ~few% residual flow capability at atmospheric conditions. In particular, autonomous systems which

utilize the reactor decay heat as the power source to drive circulation should be evaluated in PRA studies. Compressed air driven circulators should also be considered.

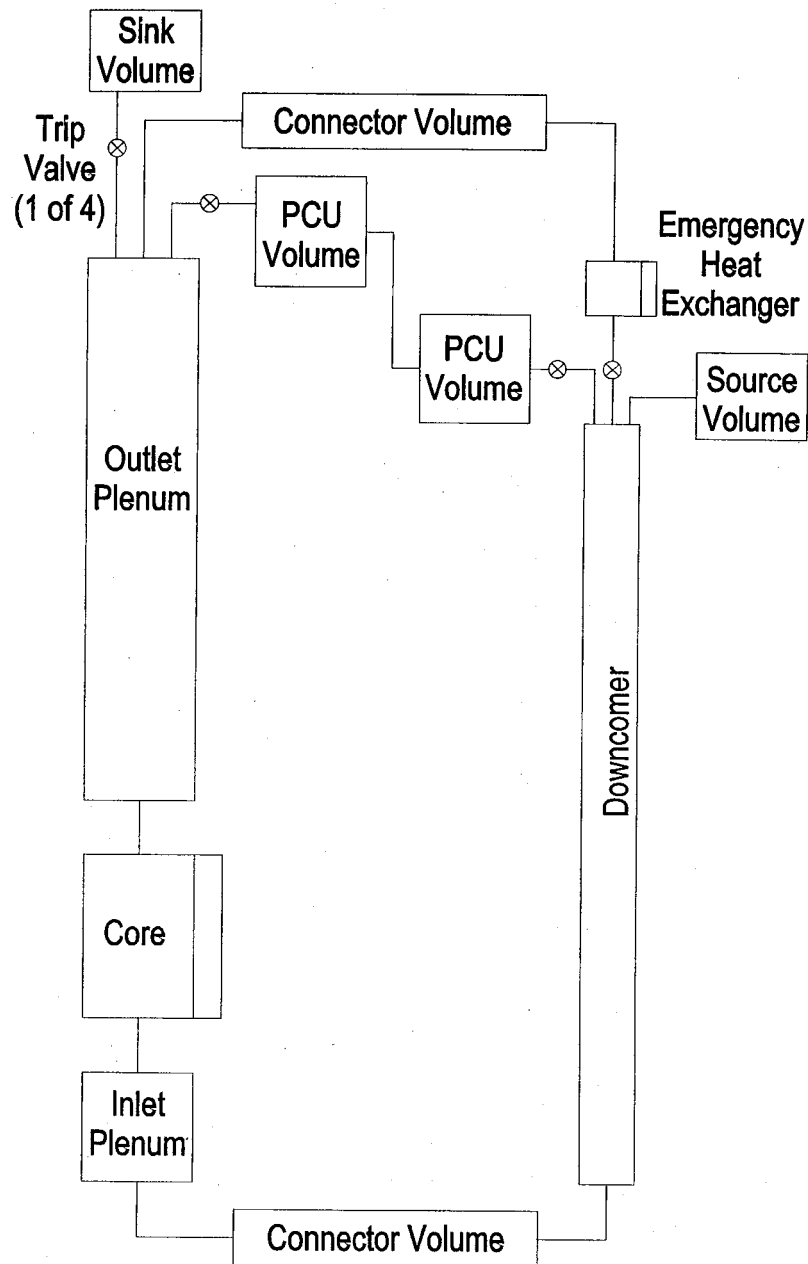


Figure 25. RELAP-5/ATHENA Pebble Bed Reactor Model Nodalization

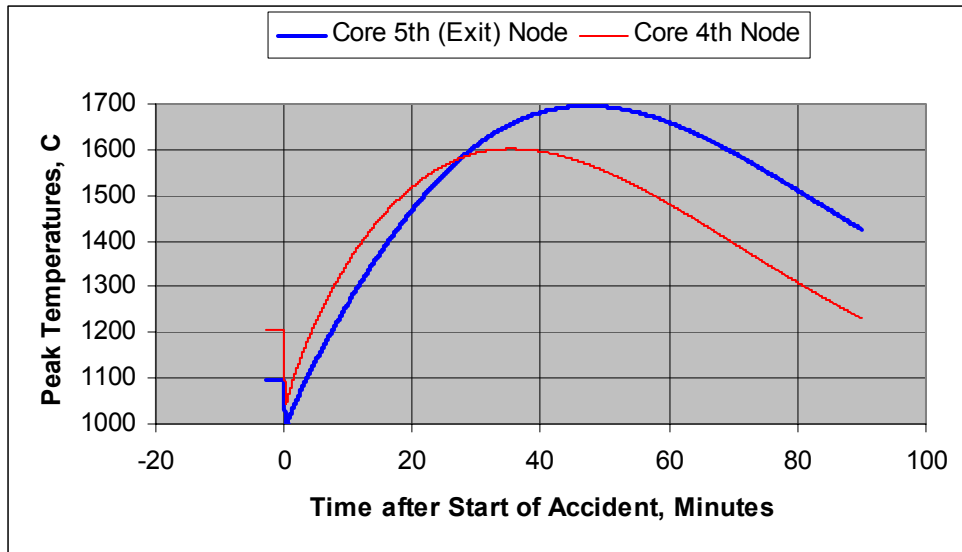


Figure 26. 2.0 MPa Guard Containment Fuel Temperature for 0.25m EHX.

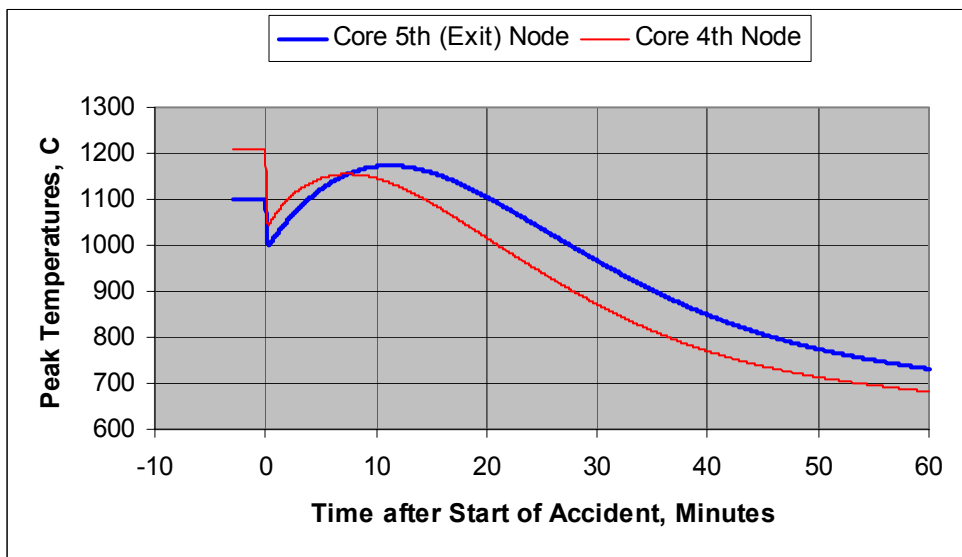


Figure 27. 4.5 MPa Guard Containment Fuel Temperatures for 0.25m EHX.

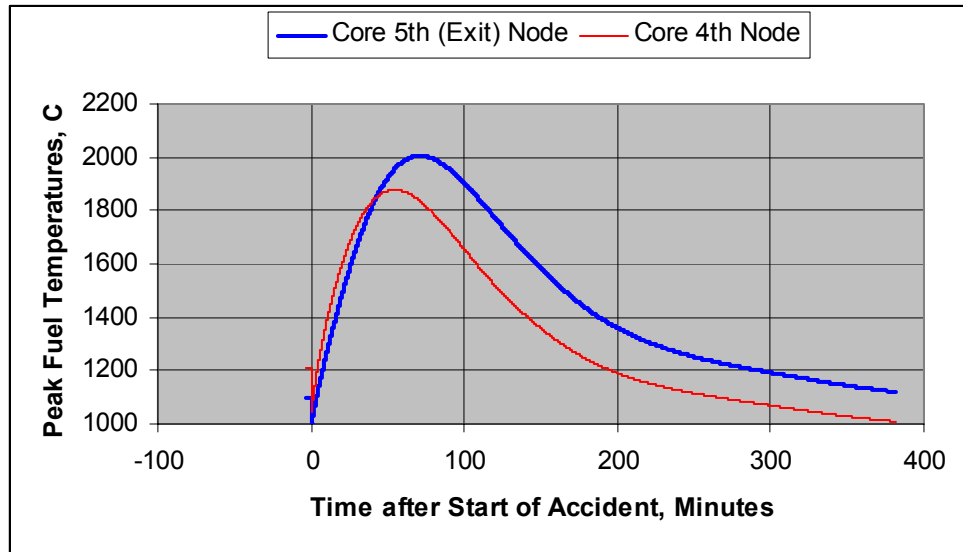


Figure 28. 2.0 MPa Guard Containment Fuel Temperatures for 1m EHX.

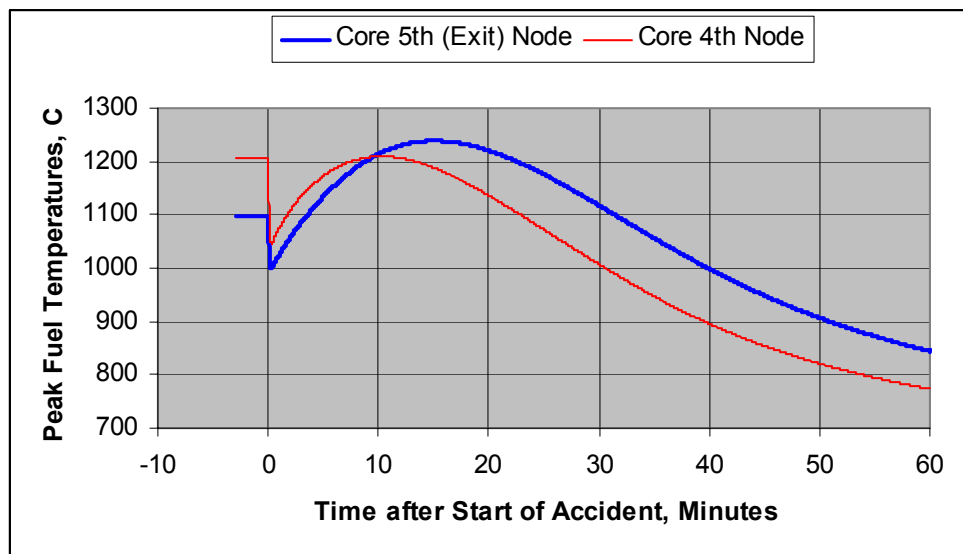


Figure 29. 4.5 MPa Guard Containment Fuel Temperatures for 1m EHX.

### Evaluation

These conclusions are supported by the following summary of the various analyses performed to date. These analyses have been performed by the I-NERI project [6]. Table 14 shows the relevant results. For a measure of the time it should be noted that the decay heat time scale is best summarized in Table 13.

Table 13. Decay Heat Timescale

Decay Heat %	Time Seconds
3	200
2	700
1	4000
0.5	40000

To reach 1% decay heat would require an accumulator flow time duration of 4000 seconds. An accumulator flow duration of  $10^3$  seconds would only reach 2% decay power. Table 14 shows that the most promising accumulator gas from a thermal-hydraulic point of view is CO<sub>2</sub>. But even with CO<sub>2</sub>, 50 volume units of CO<sub>2</sub> would be required to reach 1% decay power. Each volume unit is  $\sim 10^2 \text{ m}^3$ . If cryogenic storage is used this can be reduced to  $\sim 3.4$  volume units of liquid. The equivalent N<sub>2</sub> cryogenic storage volume is  $\sim 2.4$  volume units of liquid. There are engineering design challenges particularly with respect to large temperature differences. Figure 30 shows the phenomena. Essentially it is as discussed previously, a question of matching flow rate to the decay power history.

Table 14: Summary of Results Assuming Different Accumulator Gases [6]

Gas	Volume*	Area**	Initiation Pressure <sup>+</sup> (MPa)	Time to Reach 1600C (S)
Helium	20	10	3.5	707.6
Helium	50	10	3.5	1687.0
Helium	50	10	2.3	1687.0
Helium	50	10	1.75	1687.0
Helium	70	10	3.5	2373.0
Nitrogen	50	10	3.5	3199.0
Nitrogen	50	15	3.5	2734.0
CO <sub>2</sub>	30	10	3.5	2865.0
CO <sub>2</sub>	50	10	3.5	5035.0
CO <sub>2</sub>	70	10	3.5	7343.0
CO <sub>2</sub>	100	10	3.5	11010.0

\* Multiples of one volume unit ( $111 \text{ m}^3$ )

\*\* Multiples of one area unit (1-inch diameter pipe area)

+ System pressure = 7.0 MPa

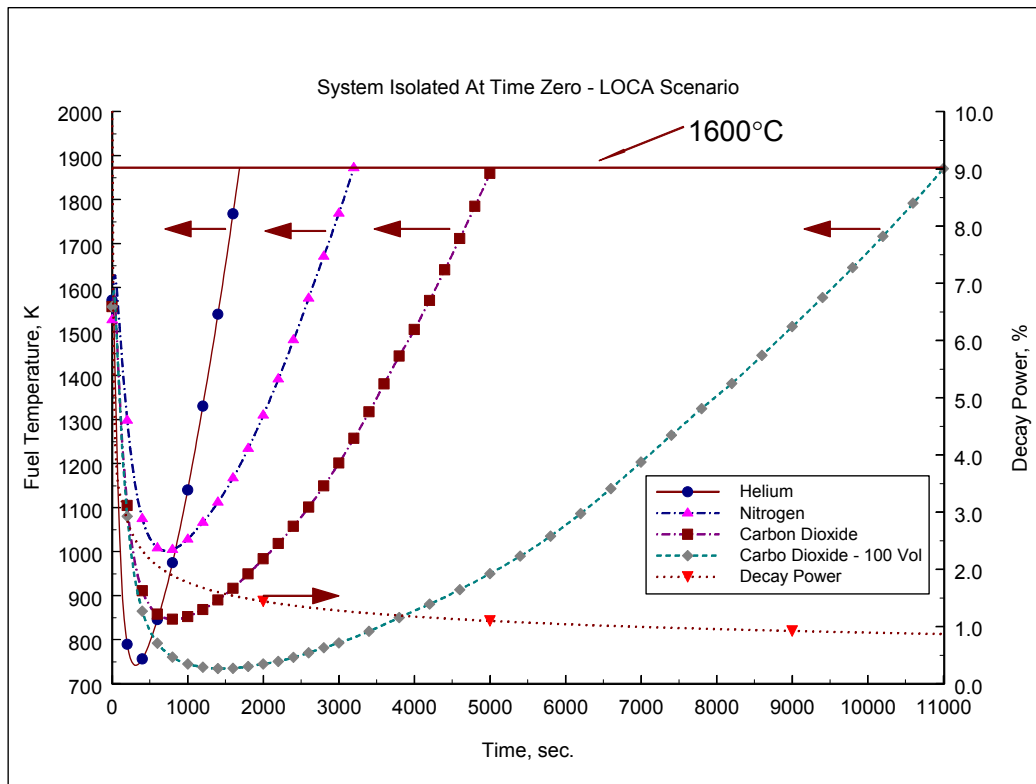


Figure 30. Variation of Fuel Temperature and Decay Power with Time (Various Gases) [6]

Work done in the NERI project on extending flow coastdown and shown in Figure 31 illustrates this behavior. As soon as there is a power/flow mismatch the fuel temperatures start to rise significantly. Only a few percent of core residual flow is required to maintain acceptable fuel temperatures. Ref. [5] showed that depending upon the range of conditions only 10-40 KW blower power is required for one atmosphere helium to remove 2% (12MW) decay heat without violating material damage criteria. If a reliable enough active system can be designed this low power requirement is very attractive. But the drawbacks of an active system are the probabilities of failure however small these may be, as opposed to a completely passive safety mechanism where there is no probability of failure occurring. There is an intermediate between the completely active system and the completely passive system, a certain hybrid combination of semiactive/semipassive system. An autonomous system is such a hybrid semiactive/semipassive system. An autonomous system would utilize the core decay heat as the power source to drive the low power circulator to maintain the required residual core flow rate. A primary system heat exchanger would be required to transfer the decay heat to an auxiliary heat engine which would product the low electric power required. The system would be on all the time and would not require start up or shut down. Figures 32-34 show some possibilities.



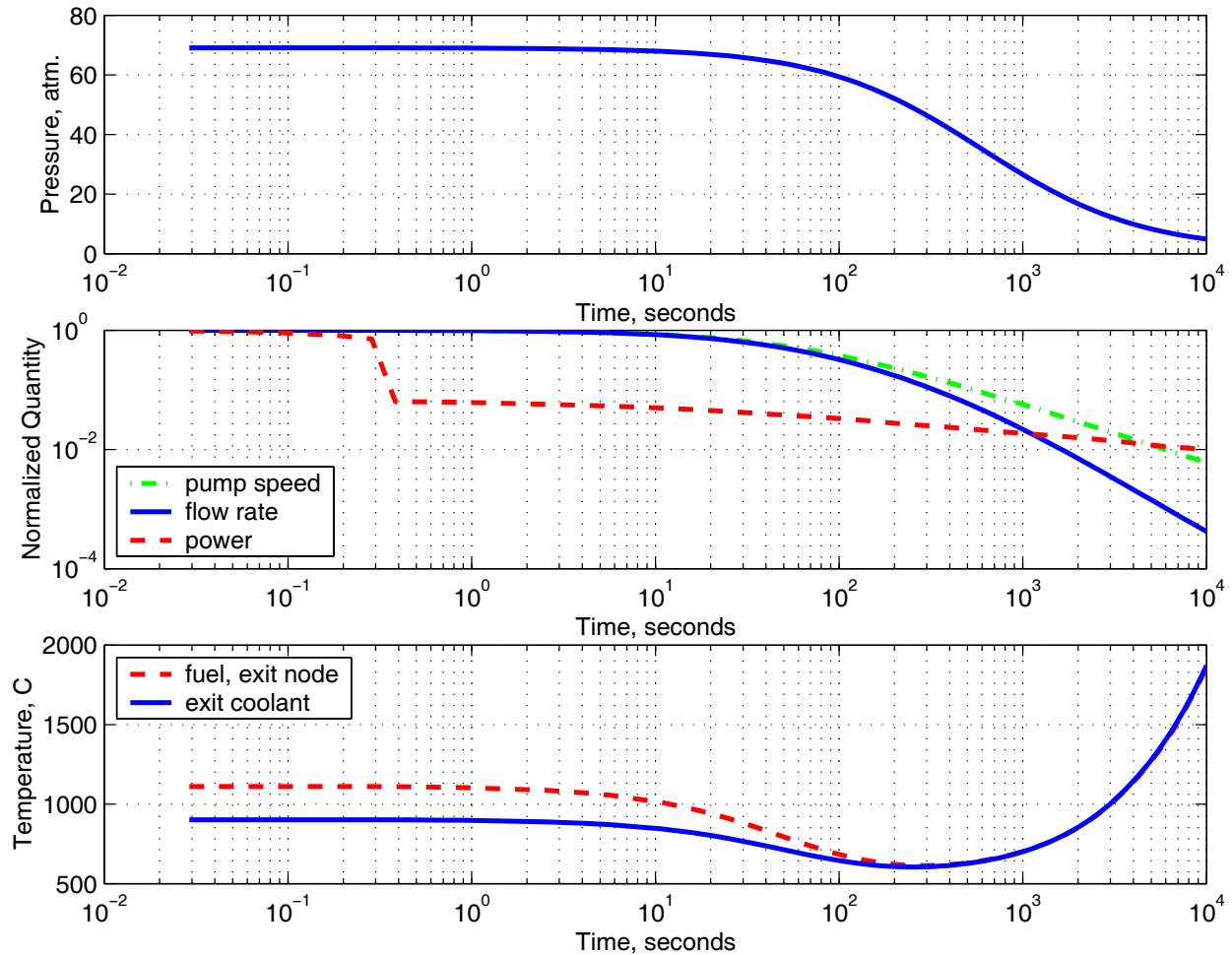


Figure 31. Dynamic Behavior Resulting from Assumed Flow and Pressure Coastdowns During a Depressurization Accident with Scram [5]

Figure 32 [10] shows a schematic diagram for a direct-cycle plant with an autonomous shutdown decay heat removal system (inside the dotted perimeter) in parallel with the main power conversion unit. If the main power conversion unit (on the left side of the figure) were not present and all of the primary flow went to the autonomous system, the plant layout would essentially be that of reactor plant with an indirect cycle, i.e., there is an intermediate heat exchanger between the reactor and the power cycle part of the plant, or heat engine, and this heat engine rejects heat to the atmosphere and produces electric power, via a generator (not shown). The autonomous system is designed to run all of the time, except when the decay power is extremely low. The electricity generated by this system is separate from the main (site) power grid and is therefore available even when the plant becomes disconnected from the main power grid.

Figure 33 [10] shows a schematic diagram for an indirect-cycle plant with an autonomous decay heat removal system in parallel with the main power conversion unit. The autonomous heat

removal system in Figure 33 is the same as the in Figure 32. The rest of the system layout is that of a typical indirect cycle plant except for the check valve that is included along the main primary flow path between the power conversion unit and the reactor. This check valve is needed to prevent backward flow through the main heat exchanger, i.e., the one on the left side of the reactor in the figure, when the power to the main primary compressor is lost and the autonomous system is driving coolant through the reactor core. This bypass flow would allow much of the primary flow to bypass the reactor. There could be some difficulties in obtaining a design with the proper flow balance between the main power conversion unit loop and the primary flow in the autonomous loop.

Figure 34 [10] shows a schematic diagram for an indirect-cycle plant with the main power conversion unit and the autonomous decay heat removal system in series in the primary loop. This arrangement does not require any check valves. Electric power to drive the primary flow comes for both the main power conversion unit and the autonomous one. If the power from the main power conversion unit is lost, then electric power produced by the autonomous system continues to maintain sufficient primary flow to remove decay heat.

The choices for heat engines for the autonomous system are a gas turbine (Brayton cycle), a steam turbine (Rankine cycle), Stirling engine (Stirling cycle), solid state devices, such as thermal photovoltaic, thermal electric, and thermionic ones, thermosiphon rankine engine, and ThermoAcoustic Heat Engine (TASHE). The choices for electric storage devices include electric storage battery, fuel cell, and flywheel.

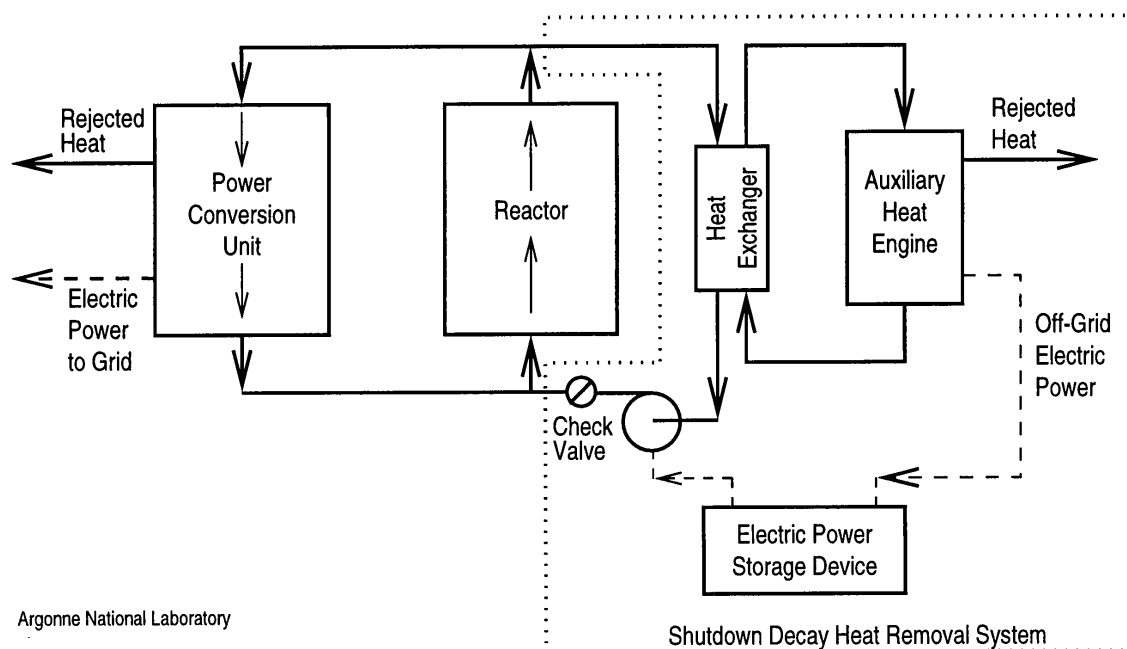


Figure 32. Direct-Cycle Layout with an Autonomous Shutdown Decay Heat Removal System [10]

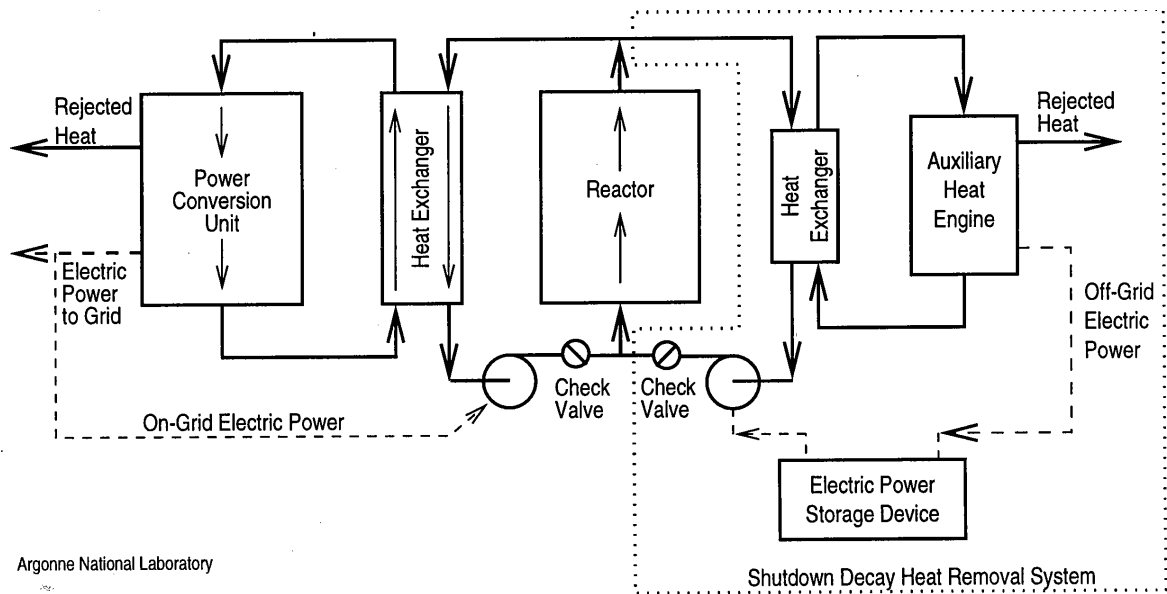


Figure 33. Indirect-Cycle Layout with an Autonomous Shutdown Decay Heat Removal System in Parallel [10]

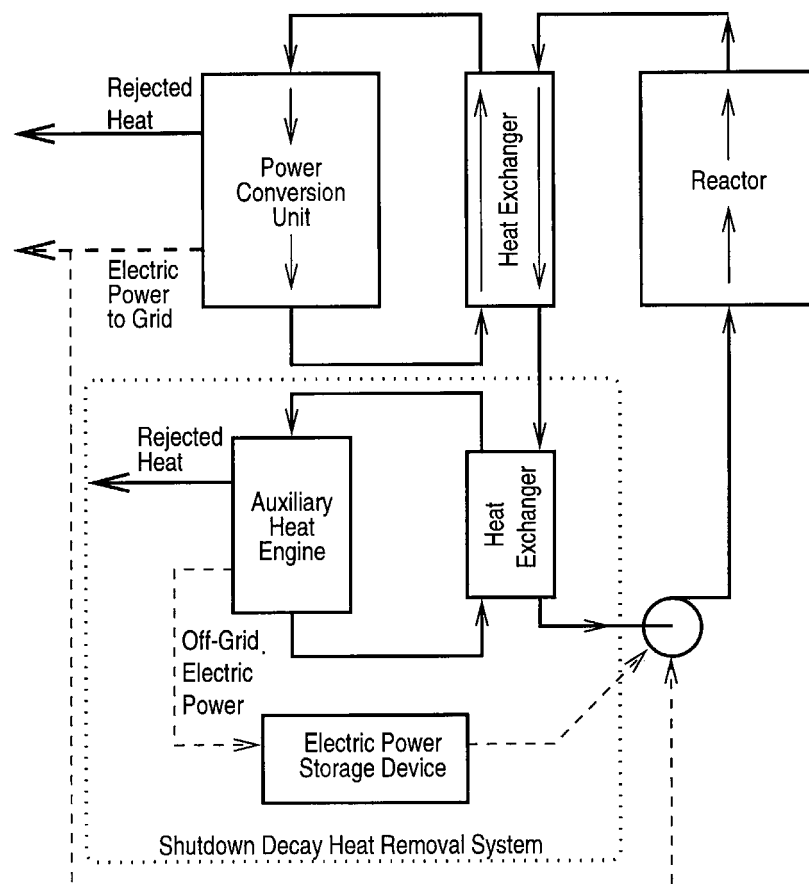


Figure 34. Indirect-Cycle Layout with an Autonomous Shutdown Decay Heat Removal System in Series [10]

In summary, the I-NERI and NERI results show the importance of providing the capability for some forced core residual flow of a few %. Accumulators may not be the most efficient approach as compared to semi-passive/semi-active systems. Semi-passive/semi-active systems such as autonomous systems or compressed gas driven circulators should be further considered in PRA studies.

## 6. Conclusions

At this point in the development of the GFR, innovative and novel concepts have been proposed for introducing passive safety mechanisms into the design, attempting to provide the GFR with walk-away safety for decay heat removal during accidents with depressurization and total loss of electric power. A significant amount of exploration work has been performed by the combined DOE sponsored NERI, I-NERI (France – US) and Gen IV projects in the assessment and evaluation of these concepts. From a technological risk viewpoint, and R&D planning, a number of options have been identified: 1) thermal inertia, conduction, and radiation; 2) in-core heat exchangers; 3) forced circulation; 4) natural circulation; and 5) heavy gas injection. Challenges and advantages of each are given below.

1. While the combined effects of heat storage (thermal inertia), in-core conduction, and vessel radiation are sufficient for thermal spectrum gas reactor decay heat removal, sole use of these mechanisms are not effective for decay heat removal in the GFR. The exception would be the use of mass transfer in the case of the pebble bed core design, where the ultimate resting configuration of the pebbles would allow for effective decay heat removal using the above effects. However, this is dependent on the rate of transfer.
2. In-core heat exchangers (heat pipes, cold fingers) are potentially very effective systems, but will carry a substantial neutronic penalty due to streaming. In addition, technological difficulties (including the question of location of the ultimate heat sink and its impact on vessel/containment penetrations), reliability, and other safety impacts need to be explored in greater detail.
3. Forced circulation is very efficient: 3% of nominal flow will enable core cooling while fulfilling fuel temperature criteria. Circulators of a very limited power ( $\sim 100$  KW) will meet the temperature requirements, but are typically seen as active systems.
4. Natural convection of helium is sufficient with a top mounted HX at nominal pressure. However, it requires a significant backpressure (which is a function of power density, HX elevation, core  $\Delta P$ , etc.) in the case of depressurization.
5. Heavy gas injection provides significant enhancement of natural circulation when compared with helium. However, there may be a considerable temperature increase of the injected gas, depending on the specific design of the system.

Given these options, the following decay heat removal strategies will be pursued by the GFR:

- Completely active systems (circulators, heat exchanger, valve). These systems would be classified as “safety”, redundant, and diversified. PRA/reliability analyses will be key for these systems.

- Heavy gas injection, followed by natural circulation. Key to this strategy is the design of the primary circuit and containment building to allow for sufficient backpressure for a specified time.
- Well-balanced mix of passive, semi-passive, and active systems. This is the ultimate goal for this reactor concept, and is similar to current advanced LWR design paths. This would include the combination of the best options (e.g., use of the injectable heavy gas to operate a blower, cold fingers combined with natural circulation, etc.).

In addition, design provisions favoring conduction paths, energy storage, etc., will continue to be investigated.

## **7. Future Work**

More detailed types of thermal-hydraulic analyses and design work will be performed. These evaluations will combine phenomena, such as internal heat sinks, heat transfer to and losses from the external boundary, turbomachinery coastdown, and natural convection. This integrated analysis will be done to justify the removal of conservatisms, and give best estimate results for trade studies comparisons/system optimizations.

Maintaining a backpressure within the containment (or proximate containment/PCR/PCIV) is paramount to the proposed decay heat removal schemes, and a more detailed analysis will be performed during the optimization phase of the work.

Work on the pebble bed long-term decay heat removal system will continue with an emphasis on assessing the requirements on the pebble transport system from the core to the ultimate long-term storage configuration. An integrated analysis will be carried out.

## **Appendices**

### **A.1 Accident Sequences**

The sizing of decay heat removal systems and the question of whether or not passive heat removal mechanisms can play a useful role is in a large part determined by the definition of the design basis. Most accident sequences can be accommodated by the provision of reliable/highly reliable system design of which active decay heat removal systems are the key to long-term recovery and stable cool down. Depressurization accidents with activation of reactivity scram systems can be accommodated when the main circulators and the active decay heat sinks are still available. Active shut down cooling system with auxiliary circulators and auxiliary heat removal trains are normally designed to be aligned when the decay heat is down ~ 2% of normal power and the main systems are normally brought down. However this does all require a reliable power source for the mover. If off-site power is lost, then vital buses are switched to the emergency power of which diesel generators are a prime example. Depressurization initiators with loss of off-site power and a loss of a shutdown train (single failure criteria) have all been accommodated in the design basis of the earlier GCFRs. However within the last twenty years with the occurrence of events such as TMI-2 and Chernobyl, and the whole role of beyond-design-basis and severe accidents with core melt down, the safety envelope has gradually reached the limits.

Within the space of the last ten years the thermal gas cooled reactors have defined the safety boundaries. Both the HTGR and the PBMR have claimed walk-away safety. With the failure of reactivity scram systems, failure of active heat removal systems including the decay heat removal systems, total loss of electric power both off-site and emergency, and for depressurization events the position is that no core meltdown would occur. Fuel failure could occur but these would be limited site release of fission products to the public. Efforts are concurrently being made to remove the need for emergency zone evacuation. Certainly the thermal gas reactor community has had to defend the issue of break size with the regulatory authorities and have had to introduce innovative design features such as cross-vessels, instead of cross-ducts but not with standing, it is a significant achievement and sets a target of comparison. However the fast reactor community also made similar progress on the sodium alternative, and the IFR program and the associated LMR program did also reach a comparable safety case before the programs were terminated. Given this background, it would appear appropriate for the Gen IV GFR to have such a safety goal too. From the viewpoint of decay heat removal accidents this would mean that protected depressurization initiators with total loss of electric power would not result in core meltdown. In other words, a station blackout combined with a depressurization would not lead to a severe accident. This is a major challenge and it should be understood that this postulated beyond-design basis accident is a very low probability event in residual risk space.

This can be realized from the following discussion, taken from the I-NERI Project report [1], of the classical definition of design basis and beyond basis which outlines the traditional understanding of the delineation of the accident groups within probability space.

### **A.1.1 Design basis conditions**

Initiating faults to be considered within the design basis cover the whole range of faults from those which are likely to occur several times within the life of the plant to those whose occurrence is highly unlikely but for which the consequences must be evaluated and if necessary design measures taken to restrict them. Postulated faults are assumed to occur within the design basis and are called design basis initiating faults. They may arise due to component failure, operator errors, internal or external hazards. Their consequences affect the plant behavior. The design basis initiating faults studied are selected as the worst conditions representative of families of faults. These are design basis events (DBEs).

Starting from a plant operating initial condition, a design basis condition is the changing plant condition which arise as a result of a design basis initiating fault combined with the conventional aggravating situations and the mitigating actions that are taken. The normal operating conditions of the plant are also included in the design basis conditions. The initiating faults to be considered in the design basis are assigned to three categories in addition to the normal operating conditions. The frequency of the initiating faults is used as the guideline for their classification. The design basis conditions are therefore grouped into four categories on the basis of the expected occurrence frequency of the corresponding initiating faults.

#### Normal operating conditions

These are planned and required plant conditions. They include special conditions such as tests during commissioning and start-up, part load, shutdown states, handling states, partial

unavailability for inspection, test, maintenance and repair. The decommissioning conditions are not included in the safety analysis of the operating plant. They will be specifically analyzed at an appropriate time. Nevertheless, considerations concerning the decommissioning have to be made.

The goal of the safety analysis of normal operating conditions is to verify that their consequences on the staff and the public are ALARA and in any case lower than the corresponding release criteria.

#### Category 2 operating conditions

These are operating conditions not planned but expected to occur one or more times during the life of the plant (mean occurrence frequency of the initiating event estimated to be greater than  $10^{-2}$  per year). The plant shall be able to return to power in a short period after fault rectification. The goal of the safety analysis of category 2 operating conditions is to verify that their consequences on the staff and the public are ALARA and in any case lower than the corresponding release criteria.

#### Category 3 operating conditions

These are operating conditions not expected to occur during the life of the plant, but after which plant restart is required (mean occurrence frequency of the initiating event between  $10^{-4}$  per year and  $10^{-2}$  per year). The goal of the safety analysis of category 3 operating conditions is to verify that their consequences on the public are lower than the corresponding release targets.

#### Category 4 operating conditions

These are operating conditions after which plant restart is not required. The consequences of the operating conditions must not exceed category 4 limits with a mean value of its frequency higher than  $10^{-6}$  per year. The goal of the safety analysis of category 4 operating conditions is to verify that their consequences on the public are lower than the corresponding release targets.

Internal and external hazards also have to be taken into account. Depending upon frequency, these hazards can fall into one of the above three categories. They are associated with an occurrence frequency and are analyzed with the rules corresponding to:

- Category 2 operating conditions: internal flooding, extreme weather conditions...
- Category 3 operating conditions: fire, earthquake,... The level of the earthquake corresponds to the Operating Basis Earthquake (OBE) depending on the site characteristics.
- Category 4 operating conditions: aircraft crash, external explosion, earthquake,... The level of the earthquake corresponds to the Safe Shutdown Earthquake (SSE) depending on the site characteristics.

### **A.1.2 Design extension conditions**

The design extension conditions are not defined on the basis of their occurrence frequency, but they are postulated to be bounding cases resulting from risks specific to the design or the process. Two kinds of design extension conditions are considered, the situations for which the consequences have to be demonstrated to be limited, and the severe accidents. These are beyond

design basis events (BDBEs). The goal of the safety analysis of design extension conditions is to verify that their consequences to the public are lower than the limited release targets.

#### Complex sequences and limiting events

The consequences of complex sequences and limiting events are investigated. This can lead to enhance the design in order to show that core damage is prevented, and therefore that the limiting release targets are not exceeded.

#### Severe accidents

Given the enhanced preventive safety, core damage accidents have any low occurrence frequency (the mean value of the cumulative core damage frequency is lower than the probabilistic target of  $10^{-6}$  per year) and it is not realistic to do a sensible ranking of severe accidents. Therefore, the severe accidents to consider are not classified on a probabilistic basis.

The goal of the analysis of severe accidents is to prove the effectiveness of the containment measures for limiting the consequences of core damage accidents. The radiological consequences shall be lower than the limiting release targets. This can lead to enhancements of the design in order to show that the limiting release targets are not exceeded.

### **A.1.3 Residual risk situations**

Residual risk situations are accident conditions for which the prevention is such that the analysis of their consequences is not required by the safety demonstration. The adequacy of the prevention of these accident conditions has to be demonstrated. Such a demonstration may be performed using probabilistic assessment. In this case, the goal is to show that the accident conditions where the consequences may exceed the limiting release targets have a mean frequency well below  $10^{-7}$  per year. The probabilistic safety assessment cannot be realistically used for innovative concepts with limited operating experience. It is also not easily usable during the conceptual design phase because of the lack of detailed design of system and equipment. The demonstration of adequate prevention can be performed using the lines-of-defense method.

It can be seen from this discussion that a station blackout combined with a depressurization event is a very low probability event. This is the event that the GFR NERI and I-NERI projects have been using to explore passive decay heat removal events. This is the safety boundary set by the recent work of the HTGR and PBMR communities. One possibility that should be explored which could facilitate the acceptance of the licensing case in this low probability space is combining active systems with passive systems. A semi-passive approach such as autonomous systems utilizing the reactor core decay heat or utilizing stored gas coolant inventory from the secondary side as the power source may make the design challenge less formidable.

### **A.2 RELAP5 Model Assumptions for Pebbled Bed Core Simulation**

The RELAP5/ATHENA model nodalization used for the simulation of natural convection in the 600MWt (50w/cc) pebble bed reactor design [4,5,6,7] is shown in Fig. A-1. Details of this nodalization are given below.



## Nominal Channel

The grid plate is 0.25 m thick and its porosity is the same as the pebble-bed core, 0.387. For simplicity, since the grid plate has not been designed, wherever reasonable, the grid plate hydraulic parameters will be assumed to be the same as those for the pebble bed. Thus, the hydraulic diameter, flow area, and relative roughness will be assumed to be the same as the pebble bed. The average (i.e., nominal) channel hydraulic diameter is shown below to be 0.02525 m. This was done so that the friction pressure drop in the pebble bed would agree with the Achenbach relationships. This is a good size for the grid plate holes because it is somewhat smaller than the pebble diameter (i.e., 63.1% of it), but not so small that it greatly restricts flow and requires a needlessly large number of holes. The hole diameter, of course, is the hydraulic diameter for the grid plate will be the definition of hydraulic diameter. This choice will result in the grid plate pressure drop being about two orders magnitude lower than that for a pebble bed of the same height.

The grid plate heat structure will be modeled as if the material around each hole in the grid plate were a concentric annulus. The inner surface of the annulus is assumed to be connected to the adjacent channel coolant volume and the outer radius is assumed to be insulated. The inner (hole) diameter is assumed to be 0.02525 m, as explained above. The void fraction for the grid plate will also be assumed to be the same as that for the pebble bed, 0.387. The outer diameter of this annulus must be the hole diameter divided by the square root of the pebble-bed void fraction, if the void fraction for the grid plate is to be the same as that of the pebble bed. (This is because the area of the hole divided by the area of a solid disk of the diameter of the outer diameter must equal the void fraction.) Thus, the outer diameter of the annulus, i.e., grid plate heat structure, is 0.04059 m. Thus, the left boundary for the heat structure is at  $0.02525/2 \text{ m} = 0.012625 \text{ m}$  and the right boundary is at  $0.04059/2 \text{ m} = 0.020295 \text{ m}$ .

For the heat structure representation of the grid plate 5 annular volumes were chosen with the thinner ones closer the coolant boundary condition at the center. The first 3 nodes are 1 mm thick each, the next 1 is 1 mm thick, and the last one is 2.67 mm. For the pebble bed heat structure, the radii were selected to produce 10 essentially equal volumes. The lower and upper axial reflectors are each 0.5 m thick and are made of unfueled pebbles. All of the pebbles are SiC. The pebble diameter is 4 cm = 0.040 m. The core diameter is 3.00 m. The core height for 300 MWt and 25 W/cc is  $(300/25)/(\pi \times 1.5^2) \text{ m} = 1.697652726 \text{ m} = \sim 1.698 \text{ m}$ . The same hydraulic diameter, flow area, and relative roughness are used for the grid plate as are used for the core pebble bed. The K-loss into the grid plate is 0.1 and 1.0 for reverse flow.

For the pebble bed modeling:

The void fraction for the pebble bed is 0.387.

The average channel flow area is:  $0.387 \times \pi \times 1.5^2 \text{ m}^2 = 2.736 \text{ m}^2$ .

The average channel hydraulic diameter is  $0.387/(1-0.387) \times 0.04 \text{ m} = 0.02525 \text{ m}$ .

The average channel relative roughness =  $10^{-6}$ .

Since the flow area for the grid plate is assumed to be that of the pebble-bed regions, the number of holes is the pebble-bed flow area divided by the flow area of one grid plate hole. Thus the number of holes is  $2.736/(\pi/4 \times 0.02525^2) = 5464$ . Thus, the heat transfer area for the grid plate

is  $5464 \times \pi \times 0.02525 \times 0.25 \text{ m}^2 = 108.4 \text{ m}^2$ . The area of the insulated outer diameter surface of the grid-plate heat structure is  $5464 \times \pi \times 0.04059 \times 0.25 \text{ m}^2 = 174.2 \text{ m}^2$ . (174.256  $\text{m}^2$  had to be input so that the inner/outer surfaces of the annulus have consistent surface areas.  $0.04059/0.02525 \times 108.4 \text{ m}^2 = 174.256 \text{ m}^2$  and not  $174.2 \text{ m}^2$ , which caused an error message.)

The pebble surface area is the area of one pebble times the number of pebbles. The core volume is:  $300 \text{ MWt}/(25 \text{ MWt}/\text{m}^3) = 12 \text{ m}^3$ . The volume of pebbles is  $(1 - 0.387) \times 12 \text{ m}^3$  and volume of 1 pebble is  $\pi/6 \times 0.04 \text{ m}^3$ . Thus, the number of pebbles is:  $((1 - 0.387) \times 12 \text{ m}^3)/(\pi/6 \times 0.04 \text{ m}^3) = 219,514$ . The surface area of 1 pebble is  $\pi \times 0.04^2 \text{ m}^2$ . Thus, the total surface area of the core is  $219,514 \times \pi \times 0.04^2 \text{ m}^2 = 1103.40 \text{ m}^2$ . The surface area of one of the five equal-length core volumes is  $1103.40/5 \text{ m}^2 = 220.68 \text{ m}^2$ . The core height is 1.698 m and each of the two volumes of the lower and upper axial reflectors are 0.25 m long (i.e. two 0.25m lower reflector volumes and two 0.25 m upper reflector volumes). Thus the surface area of each equal-length reflector volume is  $0.25/1.698 \times 1103.40 \text{ m}^2 = 162.46 \text{ m}^2$ .

In a heat structure a “mesh point” is actually a point. There would be one on each boundary, one at each interface between heat structure materials, and some distributed within each material layer. The number of intervals must be 1 less than the number of mesh points. For the axial power shape used the peak power was 1.32 times that average. The axial length was divided into 100 pieces and the relative power for each was provided. Based on this the axial temperature at the exit of each piece can be determined by trapezoidal integration. Then the temperature rise at over each 20% slice of the core can be obtained the fractional temperature rise, i.e., the rise for the 20% slice divided by the total temperature rise of 370° C can be obtained. The five numbers thus obtained from bottom to top are: 0.1296, 0.2292, 0.2624, 0.2292, and 0.1396 (which adds up to 1.000, as it should). These five factors were entered as the axial power factors.

For the pebble-bed regions, a fouling factor of 3.5, which increases the heat transfer because it is greater than 1, was used for the pebble region. This is based on a separate analysis that compares the RELAP5 and Achenbach Nusselt number correlations. For the grid plate no fouling factor was applied, i.e., a value of 1.0 was assumed.

The nominal channel was first developed as a stand-alone model. A time-dependent volume at the inlet connects to the channel via a time-dependent junction. The exit is connected via a regular junction to another time dependent volume. The plan is to add branches to other components around the loop and use trip logic to in effect remove the time-dependent volumes from the circuit.

Time-Dependent Volume 100 is the nominal channel source.

Time-Dependent Junction 101 connects Volumes 100 & 102.

Pipe 102 has 10 nodes and is the nominal channel including flows through the grid plate (node 1), lower axial reflector (nodes 2 and 3), core (nodes 4 through 8) and upper axial reflector (nodes 9 and 10).

Normal Junction 103 connects Volumes 102 & 104.

Time-Dependent Volume 104 is the sink for the nominal channel.

Heat structure 1021 is of cylindrical (annular) geometry and has only 1 node and is the grid plate.

Heat structure 1022 is of spherical geometry and has 9 nodes to correspond to the nine pebble-bed region nodes of the nominal channel (2 lower reflector, 5 core, and 2 upper reflector). (Note that there is a 1-node mismatch between the fluid nodes and the upper nine heat structure nodes.)

### **Emergency Heat Exchanger (HEATRIC)**

The heat exchanger design is based on the July 14, 2003 I-NERI design. Heatric heat exchangers are being considered for the emergency heat exchangers in the GFR. All of the channels are straight and parallel for both fluids. All of the channels are half circles with a diameter of 5.0 mm (millimeters!) and, of course, a radius of 2.5 mm. All of these half circles are aligned one above the other in all layers. The I-NERI project is considering a face area of 2.3 m by 2.3 m and that this corresponds to 129,491 channels per fluid. Because of the very small channel size, laminar flow is expected in the channels. For carbon dioxide as the primary coolant, the project proposes using a 0.42 m long heat exchanger and for helium on the primary side, a 1.00 m long heat exchanger is proposed.

Based on the above helium-side of the heat exchanger will consist of 129,491 parallel channels, each 1 m long and with a flow cross section of a half circle that is 2.5 mm in radius. The flow area each channel is  $\pi \times (2.5 \text{ mm})^2 / 2$  and the combined flow area is  $1.27127492 \text{ m}^2$ , or approximately  $1.27 \text{ m}^2$ . The hydraulic diameter is  $4 \times (\pi \times (2.5 \text{ mm})^2 / 2) / (\pi \times 2.5 \text{ mm} + 5.0 \text{ mm}) = 3.055077352 \text{ mm}$ , or about 0.00306 m. The cross sectional area of the steel walls in  $(2.3 \text{ m})^2 - 2 \times 129,491 \times \pi \times (2.5 \text{ mm})^2 / 2 = 2.747450161 \text{ m}^2$ , which when divided by the number of channel,  $2 \times 129,491$ , is  $1.060865296 \times 10^{-5} \text{ m}^2$  per channel. Each channel has a perimeter of  $(\pi \times 2.5 + 5) \text{ mm}$ . Therefore, the average wall thickness around each channel is 0.8253203763 mm. Thus, we can think of this heat exchange as having  $2 \times 129,491$  tube, each with a wall thickness of about 0.825 mm and all of the tubes are parallel and pressed together. Thus, the separation from a primary tube to a secondary one is two wall thickness, or about 1.65 mm. In the model the heatric emergency heat exchanger will be treated as being a series of alternating parallel plates, each of thickness 1.65 mm. The heat transfer area on each side (primary or secondary) of the plates will be the surface area of one channel times the number of channels. Thus, the surface area is  $129,491 \times (\pi \times 2.5 + 5) \text{ mm} \times 1 \text{ m} = 1664.474936 \text{ m}^2$  and since there are 5 equal axial nodes in the model, each is  $332.8949872 \text{ m}^2$ , which will be rounded off to  $333. \text{ m}^2$ .

### **Downcomer**

The downcomer annulus is assumed to be 1-foot thick. Therefore, its hydraulic diameter is 2 feet, or 0.6096 m.

### **PCU**

The volume, pressure, and temperature for the 1-node PCU volume were taken from the I-NERI design. This was done on a spreadsheet and reflects the exclusion of the electric generator volume. The volume in the RELAP5 model is  $730 \text{ m}^3$  and is rounded off from the  $731.84 \text{ m}^3$  value in the spreadsheet. Similarly, 3.513 MPa was rounded to 3.5 MPa in the model and  $447.279^\circ \text{ C}$  was rounded to  $450^\circ \text{ C}$  in the model. The spreadsheet showed that the equilibrium pressure for the plant (i.e., loss of site power without depressurization) was 45.5 MPa. The length

of this volume was taken to be  $\sqrt{2}$  m and to be angled downward at  $45^\circ$  so that it would go 1 m across and 1 m down from the outlet plenum to the down comer in the model. In order to obtain a more accurate set of volumes and pressures for the PCU nodes (2 equal nodes in the model, nodes 118 and 126) the excel spreadsheet model for the containment was adapted. The primary system volume without the PCU nodes was calculated from the RELAP output to be  $283 \text{ m}^3$  and temperature was estimated to be 940 K, and the initial pressure was estimated to 7.05 MPa. For the 4.5 MPa final pressure case, a PCU pressure of 3.5 MPa, and a temperature of 450 K, were assumed, and the spreadsheet was used to solve for a volume of  $721.65 \text{ m}^3$  which was divided in two and around off to  $361 \text{ m}^3$  per volume. For the 2.0 MPa case the pressure was arbitrarily set at 1.0 MPa in the pcu and the 450 K temperature was assumed. The spreadsheet was used to solve for a volume that yielded a final pressure of 2.0 MPa. This volume is  $1429.15 \text{ m}^3$ , which was divided into two and rounded off to  $715 \text{ m}^3$ .

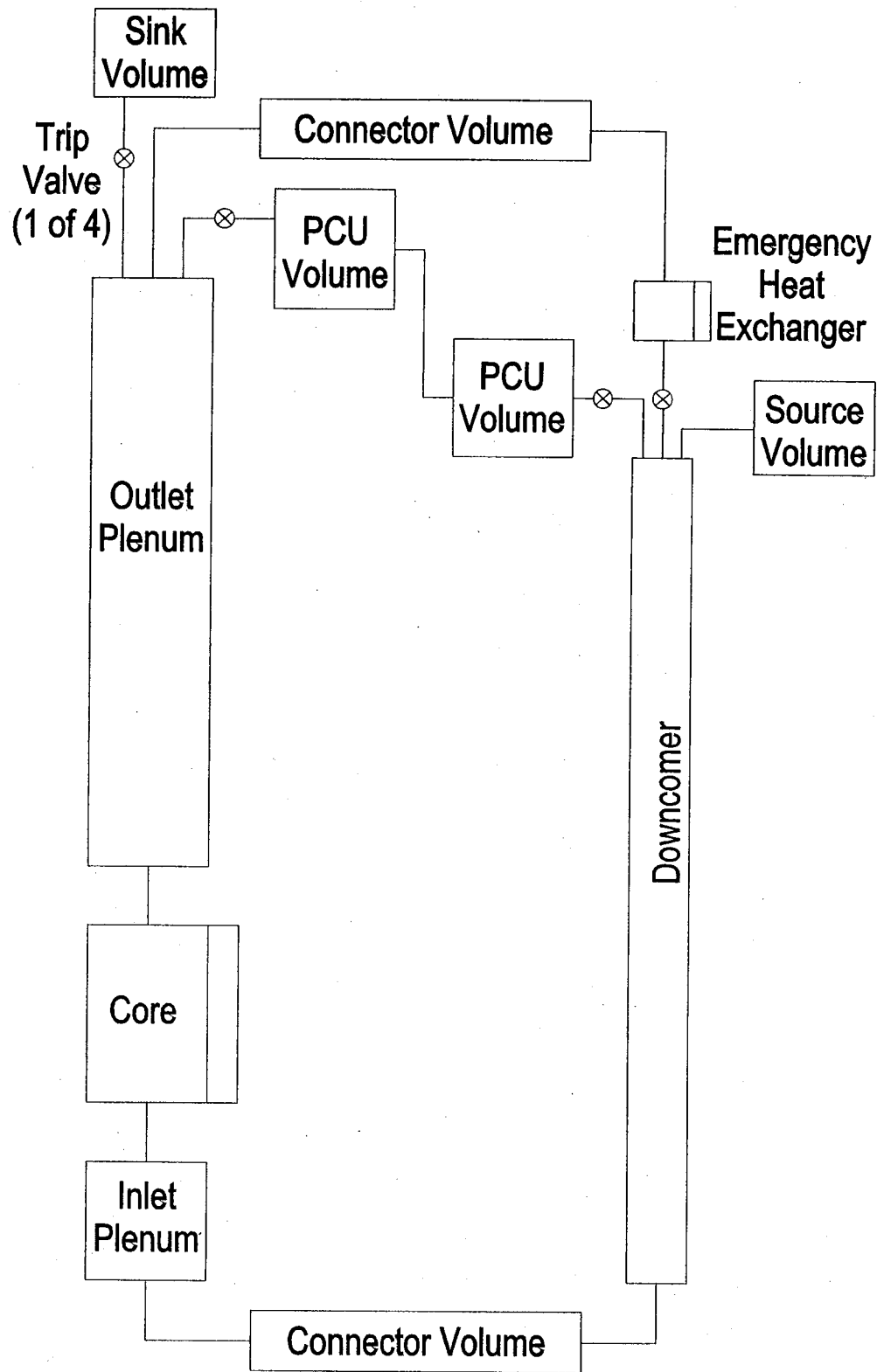


Figure A.2.1 RELAP5/ATHENA Nodalization for 600 MWt Pebble Bed Plant

### **A.3 RELAP5-3D/ATHENA Models for Block Core**

The calculations of this study were performed using the RELAP5-3D/ATHENA [18] computer code. In the RELAP model, helium (primary coolant), dry air (containment environment), and CO<sub>2</sub> (supplemental fluid) are used as the working fluids. Heat transfer in the heat structures that model the physical components of the reactor is calculated using one-dimensional radial heat conduction. Heat transfer from the heat structures to the adjacent coolant is modeled with convective heat transfer while a radiation and conduction enclosure model allows for direct thermal communication between heat structures.

In order to better capture the thermal interactions between the various reactor components, it was desired that this RELAP LOCA analysis model an essentially complete reactor system. Since the current GFR design is still in development, several assumptions about the reactor's physical characteristics were required. These characteristics are dynamic and will evolve as the reactor design progresses; however defining these characteristics allows the analysis to proceed beyond the simplistic control volume calculations.

#### **A.3.1 GFR Design Characteristics**

The RELAP analysis models the reactor vessel, reactor cavity, and the reactor cavity cooling system (RCCS). In order to derive dimensions for these components, information was required on the core design. For this purpose, the MIT GFR core design [4] (Figure A.3.1) was used. The MIT design features a prismatic fuel assembly that is comprised of “compacts”, which include the spherical fuel encapsulated in a thin SiC shell. The MIT design, refer to Table A.3.1, specifies the fuel assembly dimensions, coolant void fraction, and core arrangement.

In Figure A.3.1, three distinct regions of the core are observed: the fuel, reflector, and shield. The RELAP model depicts these three regions as five radial rings: an inner, middle, and outer fuel ring, the reflector ring, and the shield ring. The fuel region was divided into three radial rings in order to better model the fuel's thermal response during transients. Using the physical characteristics of the fuel assemblies, the radial lengths of the rings were determined as shown in Figure A.3.2. In the figure, a coolant downcomer and the reactor vessel were added to the core; the dimensions of these two structures coming from the GA Modular Helium Reactor design [19].

The five radial rings of the core provided a core radius of 2.366 m and correspondingly a core area of 17.58 m<sup>2</sup> and volume of 29.9 m<sup>3</sup>. With these dimensions, the inner diameter of the pressure vessel is 5.76 m.

The dimensions of the core height are based upon a schematic of a French GFR design, see Figure A.3.3. This design shows a concentric arrangement for the inlet and outlet coolant pipes, the reactor vessel being part of the coolant downcomer, coolant upflow through core supports, lower reflector, fuel, upper reflector, and a large gas plenum above the core to promote turbulent mixing of the hot coolant. Figure A.3.4 illustrates how the RELAP model incorporates the physical arrangement described in Figure A.3.3.

In Figure A.3.4, the inlet and outlet pipe diameters are based on the dimensions of the GA MHR. The heights of the upper and lower reflectors are based on input from INEEL GFR neutronic calculations. Lastly, the gas plenum area was derived by scaling the areas of the French design.

Having an estimate of the reactor vessel's dimensions, it was possible to estimate the containment vessel's size. The axial distribution within the containment vessel is as follows: 1) two meter height below the reactor vessel for the control rod assembly and vessel support, 2) two meter height for the inlet plenum at the bottom of the reactor vessel, 3) 0.57 m height for core support, 4) 0.15 m height for lower reflector, 5) 1.7 m height for core region {subdivided into five axial regions for better thermal modeling}, 6) 0.15 m height for upper reflector, 7) 4.5 m height for above-core gas plenum, and 8) one m height for the outlet plenum. Taking into consideration the vertical space required for overhead cranes and to initially install the reactor vessel, a height of 11.93 m above the reactor vessel is selected. Allowing a horizontal distance of 6.10 m adjacent to the reactor vessel for system support components, a containment volume of 6285 m<sup>3</sup> is calculated. A schematic of the above dimensions is presented in Figure A.3.5. Note in Figure A.3.5 that the reactor vessel is below grade.

It is important to remember that the ultimate goal of the RELAP modeling is to incorporate a majority of the standard reactor systems that will directly influence the reactor's thermal performance during a LOCA transient. To this end, it was decided to fully model the Reactor Cavity Cooling System (RCCS) specified in the GA MHTR design. The RCCS uses natural draft air and has no pumps, circulators, valves, or any active components. During normal reactor operations, GA analyses suggested that the RCCS removed 3300 kW of power.

The RCCS in this RELAP model consists of a cooling panel that attaches to cold air downcomers and hot air risers. The panel is located inside the reactor cavity and it surrounds the reactor vessel. Air is introduced to and exhausted from the panel via an inlet/outlet structure that resides on top of the containment vessel. Cold atmospheric air enters the RCCS and flows downward to the cooling panel via gravity. During this downward flow, the cold air is shielded from the reactor vessel's radiative and convective heat. At the bottom of the downcomer, the cold air enters a riser that faces the reactor vessel. The vessel's heat imparts buoyancy to the air and the air rises, collecting heat, as it moves upward towards the outlet structure to be exhausted into the atmosphere.

### **A.3.2 RELAP Model**

#### **a. Geometry**

Figure A.3.6 illustrates the complete RELAP model for the He-cooled GFR. The reactor vessel and its internals are shown in the left of the figure while the RCCS is shown on the right. The model assumes symmetry and thus portrays only the left side of the reactor. In the figure, there is the reactor vessel (#1000), the reactor head (#1001), the coolant downcomer (#120), the five radial rings that comprise the fuel, reflector, and shield (#140 - #148), the inlet plenum (#130), the core supports (#1404 - #1484), the lower reflectors (#1403 - #1483), the upper reflectors (#1402 - #1482), the gas plenum (#160), the outlet plenum (#170), the inlet pipe (#110) and the outlet pipe (#180). In the figure, the inlet and outlet pipes are drawn on different planes, but the

RELAP model is actually for two concentric pipes, see Figure A.3.7. The inlet pipe is insulated from the outlet pipe in order to prevent parasitic heating of the inlet gas stream.

The coolant heat exchangers and the turbine are not explicitly modeled. Instead, time-dependent volumes are used at the inlet and outlet. The He gas temperature in the outlet plenum is used to control the flow rate from the inlet time-dependent volume. Similarly, the He pressure in the inlet plenum is used to control the pressure in the output time-dependent volume.

The conduction enclosure model allows heat to conduct radially from the inner fuel ring out through the RCCS and to the containment vessel. Conduction can also occur from the core supports up to the reactor vessel's head. It is anticipated that the majority of the reactor's heat will be conducted radially. The model's radial mesh is very fine in the core region and a little coarser in the non-core regions. The radiation enclosure model allows heat to radiate both axially and radially from the core in a manner similar to that for the conduction enclosure model.

The containment vessel is shown in Figure A.3.6 as #900. The reactor vessel and the RCCS communicate with the containment vessel via conduction. During normal operations, the containment vessel is filled with dry air that is maintained at atmospheric temperatures and pressures. The model does not account for air leakage from the containment. The containment wall is modeled as having a stainless steel liner, one meter of concrete, a water moat adjacent to the exterior, and then soil adjacent to the water. The water moat was suggested in the MIT report as a heat sink to enhance heat removal from the containment's wall.

#### b. Neutronics

The RELAP point kinetics option is used in the model, which allowed the fuel region to have a reactor power of 600 MW and a power density of  $67 \text{ MW/m}^3$  (slightly higher power density due to smaller core size). The MIT design specifies an axial peaking factor of 1.25, however since this is a safety analysis, a more conservative peaking factor of 1.3 was used.

Doppler feedback reactivity was not included since this effect was assumed to be small for the fast spectrum of the GFR. At the onset of the LOCA, a SCRAM reactivity curve is applied. This curve is from the Seabrook plant, which is not a fast gas reactor, however, the SCRAM reactivity curve is believed to be more realistic than linearly ramping the reactivity down to zero.

#### c. Material

The materials for the GFR reactor vessel components were selected to be consistent with the latest GFR design specifications. The materials used in the RELAP model are shown in Table A.3.2. In certain cases, only one data point was available and in these cases the material properties were considered constant for the temperature range of reactor operations.

### A.3.3 Loss of Coolant Accident

The RELAP model includes provisions for simulating a LOCA scenario. The LOCA is assumed to be a double-guillotine break in the inlet/outlet pipes, which would spill He into the containment vessel. The model uses four valves to simulate the double-guillotine break. There



are divertor valves on both the inlet and outlet pipes. When the break occurs, the two valves open and He is allowed to flow into the containment vessel. Simultaneously, two valves close at the inlet/outlet time dependent volumes and the residual He in these lines also spills into the containment vessel. Figure A.3.8 shows the fluid path from the primary loop to the containment vessel. RELAP calculates the temperature and pressure responses in both the containment and the reactor vessel during the transient.

A LOCA analysis will be performed following the quality check of the RELAP model, which is in progress. Subsequent to this analysis, the model will be revised to use a flow enhancement system in which CO<sub>2</sub> flow from a reservoir turns a vane that produces circulation of the He during the LOCA.

### A.3.4 Conclusions

A RELAP model has been created for the typical GFR design. This model includes critical power plant components such as the fuel, reflector, shield, reactor vessel, and containment building. To take advantage of passive systems for removing decay heat, a draft air reactor cavity cooling system is included in the model, as well as a water moat adjacent to the containment vessel wall. The process of creating the model highlighted several design characteristics (e.g., material properties, fuel reactivity feedback) that require further definition in order to improve the modeling accuracy.

Table A.3.1. Reference GFR Parameters

Thermal power	600 MW
Average power density	55 MW/m <sup>3</sup>
Axial power peaking	1.25*
Core height	1.7 m
System pressure	7.0 MPa
Inlet coolant temperature	490 EC
Outlet coolant temperature	850 EC
Fuel	hexagonal matrix block, UPuC/SiC (50/50%)
Number of fuel assemblies	127*
Width of fuel assembly	20 cm*
Number of coolant holes	91*
Coolant void fraction	40%*

\* MIT parameter

Table A.3.2. Material Properties for GFR Reactor Components

<b>Component</b>	<b>Material</b>	<b>RELAP Model</b>
Reactor vessel	T91 (9Cr-1Mo) steel	F(t)
Reactor head	T91 (9Cr-1Mo) steel	F(t)
Fuel ring	U-SiC compact	F(t)
Upper reflector	Be	constant
Lower reflector	Be	constant
Radial reflector	Be	constant
Shield	Ti	constant
Core barrel	Incoloy alloy 800	F(t)

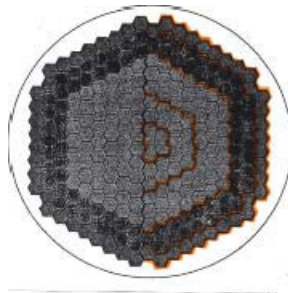


Figure A.3.1. MIT Prismatic GFR core design.

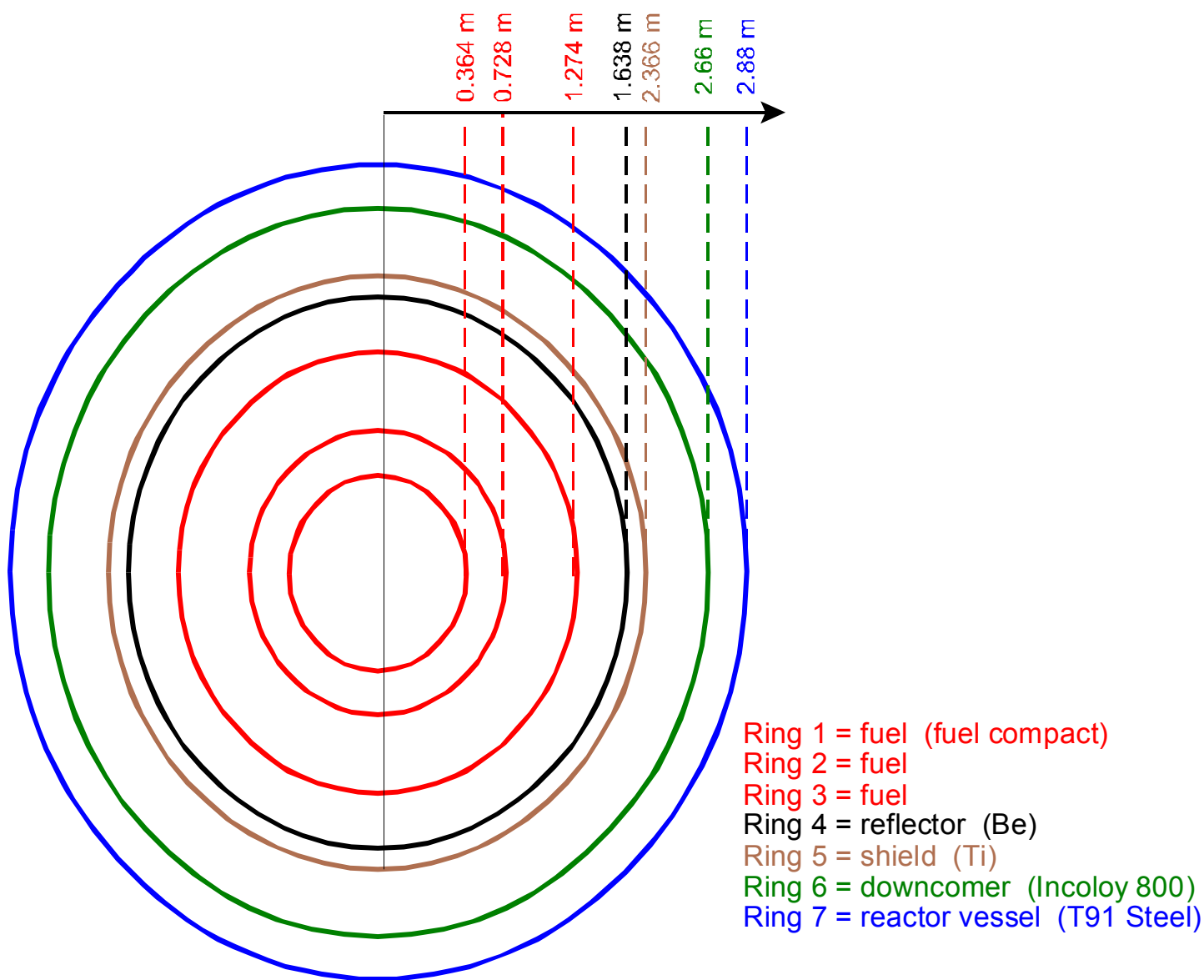


Figure A.3.2. Radial profile of the INEEL RELAP GFR core.

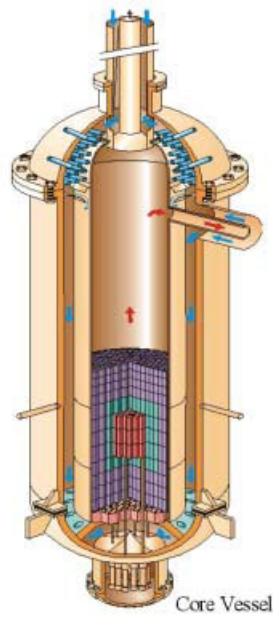


Figure A.3.3. Schematic of a French design for the GFR.

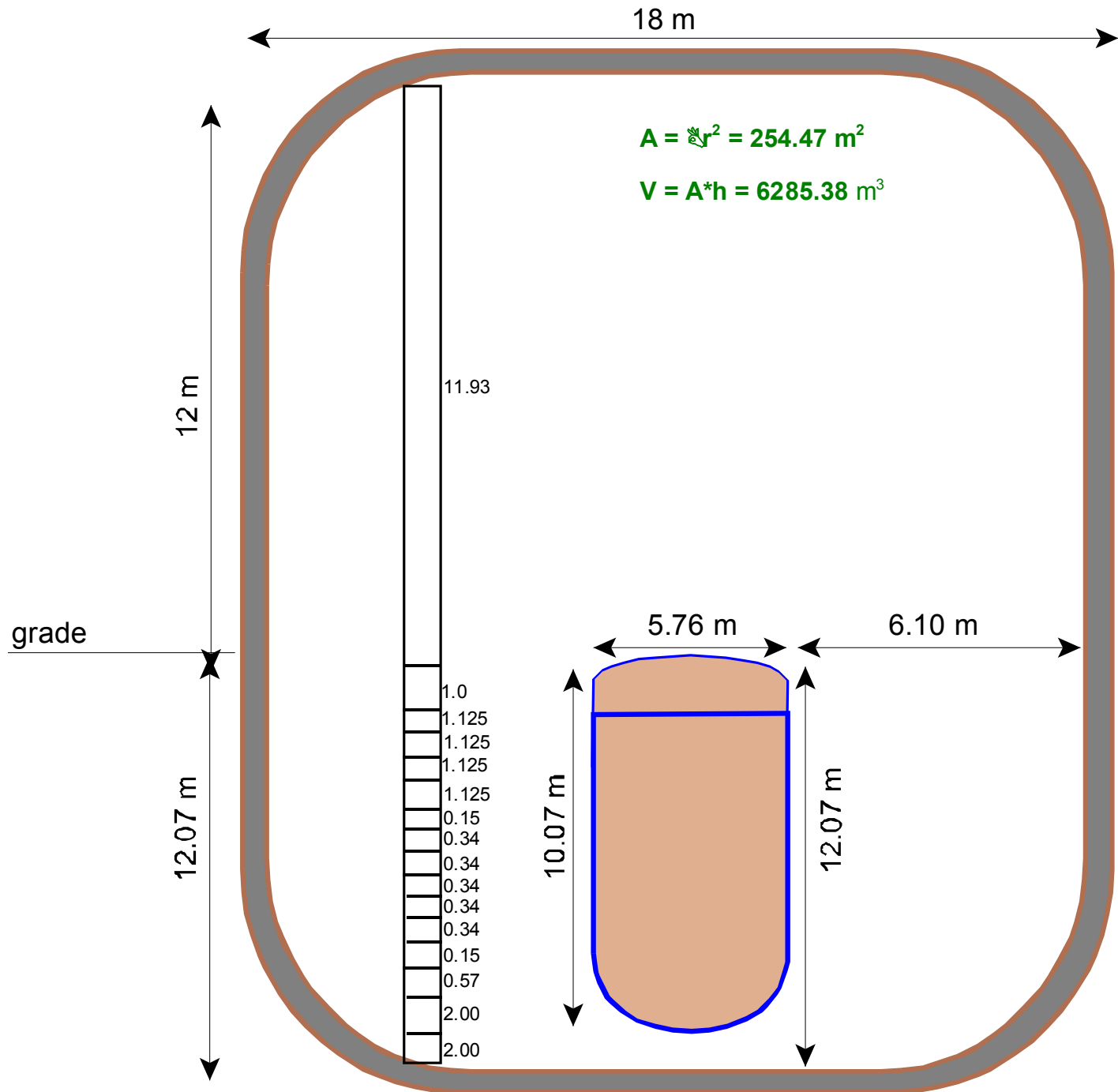


Figure A.3.5. Calculated containment vessel dimensions.

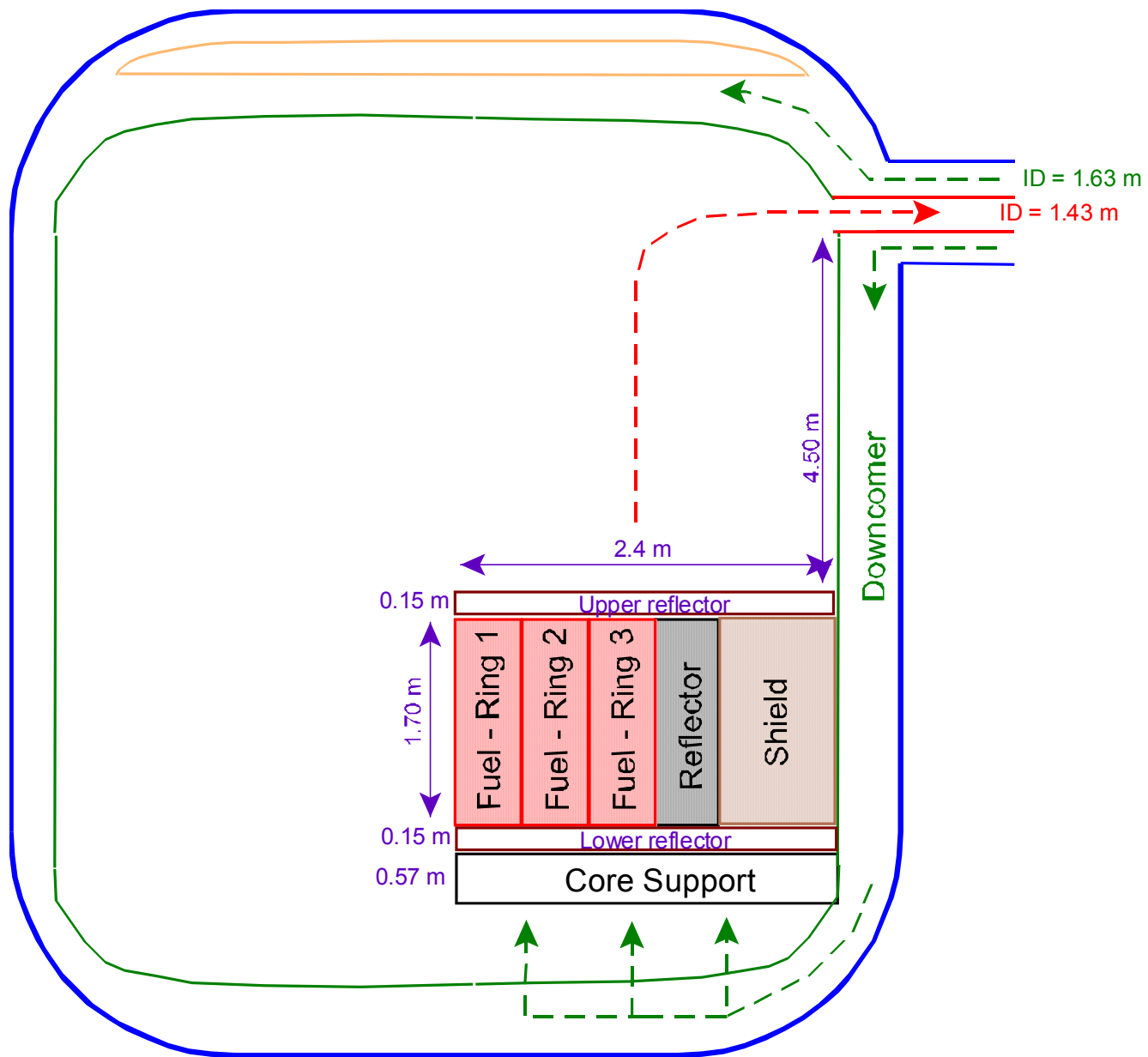


Figure A.3.4. Schematic of RELAP model of GFR reactor vessel.

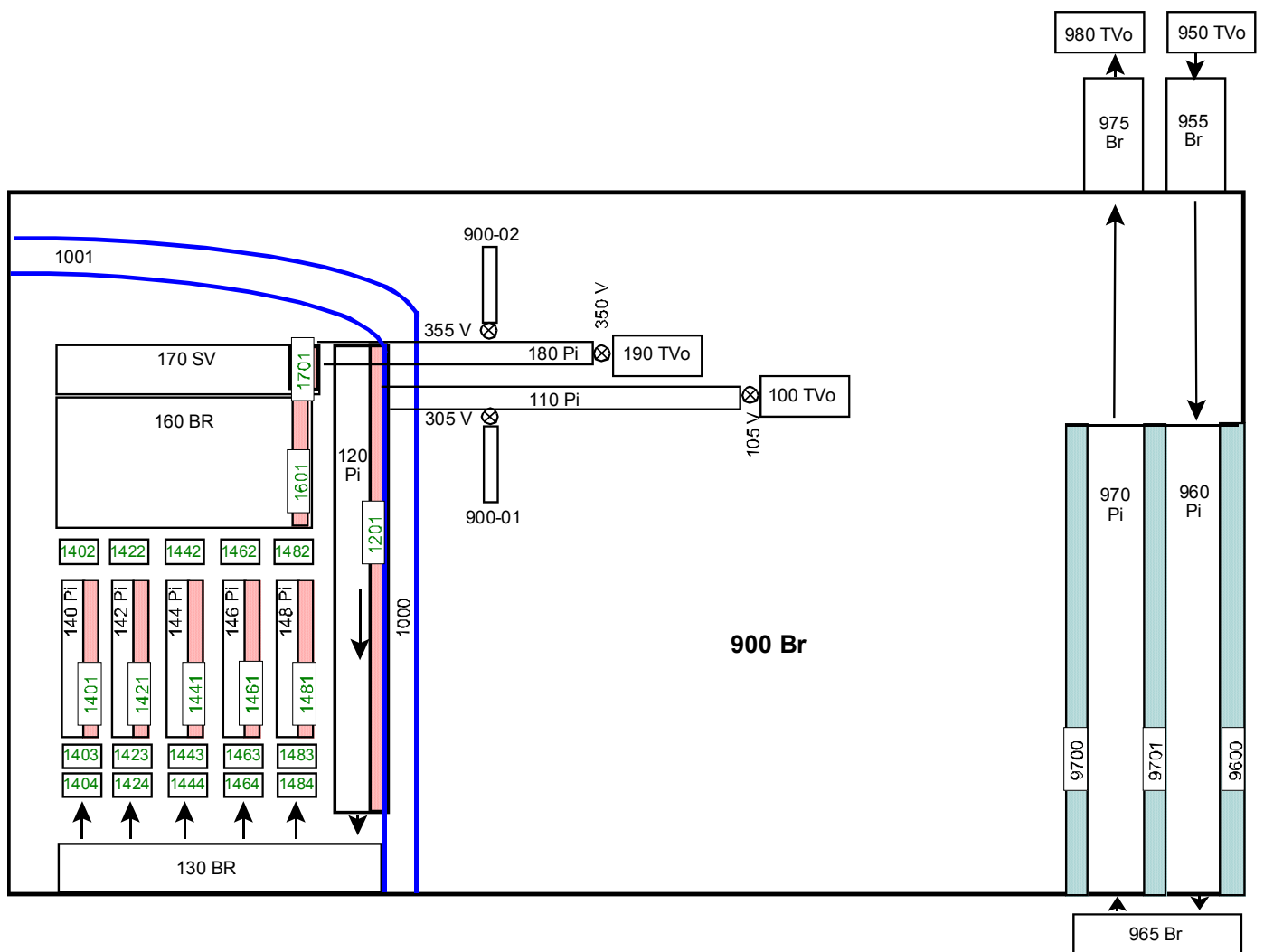


Figure A.3.6. Complete RELAP/ATHENA GFR model

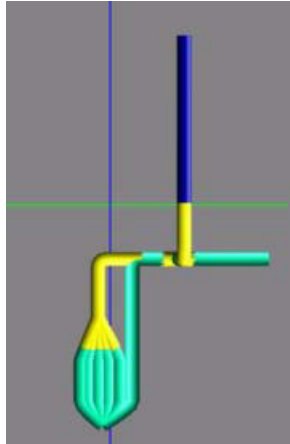


Figure A.3.7. 3D  
image of RELAP  
model for GFR  
LOCA scenario

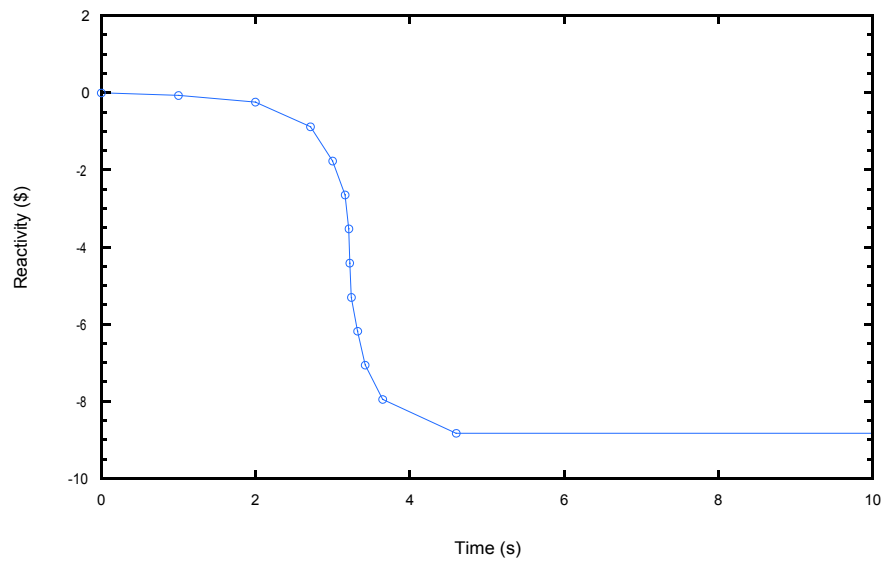


Figure A.3.8. Seabrook SCRAM reactivity curve used in GFR model



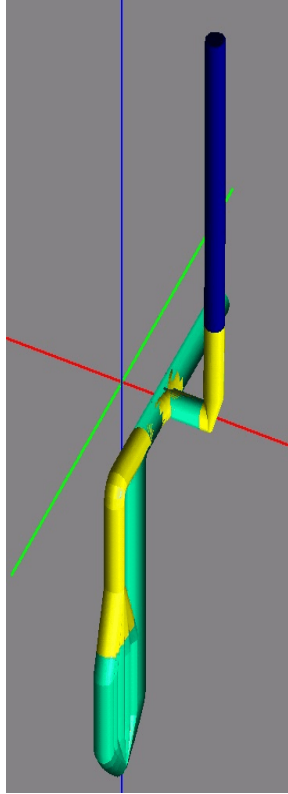


Figure A.3.9. Illustration of flow path from the primary loop to the containment vessel during a LOCA scenario

## References

- (1) B. Mathieu, J. Rouault, M. Delpéch, B. Carlucci and T. Y. C. Wei, "Gas-Cooled Fast Reactor Safety Approach General Recommendations" CEA/ANL INERI Project #20001-002-F Topical Report GFR 005, February 2003.
- (2) E. E. Feldman and T. Y. C. Wei, "Passive Decay Heat Removal in Pin-Based Cores," Argonne National Laboratory I-NERI Project #2001-002-F Topical Report GFR-006, February, 2003.
- (3) E. E. Feldman and T. Y. C. Wei, "Plant Design Concepts for a Gas-Cooled Fast Reactor," Argonne National Laboratory NERI Project #01-022 Topical Report, February, 2002
- (4) W. Williams, P. Hejzlar, M. J. Driscoll, W-S. Lee, and P. Saha, "Analysis of a Convection Loop for GFR Post-LOCA Decay Heat Removal from a Block Type Core" MIT I-NERI Project #2001-002-F, Topical Report MIT-ANP-TR-095, March, 2003
- (5) E. E. Feldman and T. Y. C. Wei, "Thermal-Hydraulic and Safety Evaluation of the PB-GCFR Core Design," Argonne National Laboratory, NERI Project #01-022 Topical Report, February, 2003
- (6) L. Y. Cheng, J. Jo, H. Ludewig and U. Rohatgi, "Passive Decay Heat Removal in Particle/Pebble Based Cores," Brookhaven National Laboratory I-NERI Project #2001-002-I Topical Report GFR-008, March, 2003
- (7) C. Poette et al, "Gas-Cooled Fast Reactor Core Designs," CEA/ANL I-NERI Project #2001-002-F Topical Report GFR-004, February, 2003
- (8) E. E. Feldman and T. Y. C. Wei, "Cold Finger In-Core Decay Heat Removal for Pebble-Bed GFR Designs," Argonne National Laboratory I-NERI Project #2001-002-F Topical Report GFR 007, February, 2003
- (9) E. E. Feldman and T. Y. C. Wei, "Core Key Mechanical Design Evaluation for a Pebble-Bed Gas-Cooled Fast Reactor," Argonne National Laboratory NERI Project #2001-022 Topical Report, February, 2003
- (10) E. E. Feldman and T. Y. C. Wei, "Design Approach for a Small Modular Pebble Bed Gas-Cooled Fast Reactor Optimized for Decay Heat Removal," Argonne National Laboratory NERI Project #01-022, August, 2003.
- (11) M.J. Driscoll, P. Hejzlar, N.E. Todreas, B. Veto, "Modern Gas-Cooled Fast Reactor Safety Assurance Considerations", MIT-ANP-TR-087, May 2003
- (12) J.M. Ravets, J.M. Tobin, "The Very High Temperature Reactor for Process Heat", Trans. Am. Nucl. Soc., Vol. 22, Nov. 1975
- (13) M.A. Pope, M.J. Driscoll, P. Hejzlar, "Reactor Physics Studies In Support of GFR Core Design", Global 2003 Proceedings, (2003)
- (14) M.J. Driscoll, M.A. Pope, P. Hejzlar, "Self-Actuated Reactivity Insertion Device for GFR Service", Trans. Am. Nucl. Soc., Vol. 89, Nov 2003
- (15) N.A. Carstens, M.J. Driscoll, "LOCA-Powered SCRAM Device for GFRs", *ibid.*
- (16) M.J. Driscoll, M.A. Pope, P. Hejzlar, "Device for Passive Reactivity Insertion During GFR LOCA", *ibid.*
- (17) P. Hejzlar, M.J. Driscoll, N.E. Todreas, "The Long-Life, Gas-Turbine Fast Reactor Matrix Core Concept," ICAPP 2002 Proceedings (2002).

- (18) The RELAP5-3D Code Development Team, RELAP5-3D Code Manual, Idaho National Engineering and Environmental Laboratory, INEEL-EXT-98-00834, Revision 2.1, April 2003.
- (19) “Gas Turbine-Modular Helium Reactor (GT-MHR) Conceptual Design Description Report,” Revision 1, Report 91720, GA Project No. 7658, General Atomics, san Diego, CA, July 1996.